بسم الله الرحمن الرحيم

Sudan University of Science &Technology

College of Graduate Studies and Scientific Research

Analysis of Magnetic Torsional Vibration Damper for Reciprocating Internal Combustion Engines

A Thesis submitted to College of Graduate Studies and Scientific Research as a partial fulfillment of the requirement for degree of Ph.D. in Mechanical Engineering.

By:

Sabir Abushousha Ahmed Abushousha

(B.Sc. & M.Sc. Mechanical Engineer)

Supervisor:

Dr. TagElsir Hussan Hussan

April 2019

جامعة السودان للعلوم والتكنولوجيا

كلية الدراسات العليا والبحث العلمي

برنامج الدكتوراة في الهندسة الميكانيكية

دراسة استخدام المخمد المغناطيسي لتخفيض الاهتزاز الالتوائي في محركات الاحتراق الداخلي الترددي

هذه الاطروحة مقدمة لكلية الدراسات العليا والبحث العلمي جامعة السودان للعلوم والتكنولوجيا كمتطلب جزئي لنيل درج دكتوارة الفلسفة في الهندسة الميكانيكية

الدارس:

صابر ابوشوشة احمد ابوشوشة

المشرف:

د. تاج السر حسن حسان

ابريل 2019 -1440

Examiners Approval Page

This thesis has been approved and accepted in partial fulfillment of the requirements for the degree of doctor of philosophy (Ph. D) in mechanical engineering

Examination Committee

External Examiner Signature

Prof.: Mohammed Eltayeb Mansour …….

Rank: Associate Professor Date: \ \ 2019

Internal Examiner Signature

Dr.: Tawfig Ahmed Gamal Eldeen …….

Rank: Associate Professor Date: \ \ 2019

Supervisor Signature

Dr.: Dr. TagElsir Hussan Hussan …….

Rank: Associate Professor Date: \ \ 2019

Declaration Of Thesis (Student)

I hereby declare that the work contained in this thesis entitled '**Analysis of Magnetic Torsional Vibration Damper for Reciprocating Internal Combustion Engines '**is work carried out by myself, the thesis has not been accepted for any previous degree and is not concurrently submitted candidature of any other degree, I have fully cited and referenced all material and results that are not original to this work. And that all sources of information have been acknowledged

Student Name: Sabir Abushousha Ahmed Abushousha

Signature: ----------

Date: 26 April 2019

Declaration Of Thesis (Supervisor)

This is to certify that the thesis entitled "**Analysis of Magnetic Torsional Vibration Damper for Reciprocating Internal Combustion Engines**" being submitted by Sabir Abushousha Ahmed Abushousha as in the Department of Mechanical Engineering, Sudan University of Science &Technology College of Graduate Studies the work carried out by him under my guidance and supervision. "I declare that I have read this thesis and in my opinion this thesis is adequate in terms of scope and quality for the purpose awarding a PhD. Degree in Mechanical Engineering.

Supervisor's Name: TagElsir Hussan Hussan
Rank: Associate Professor
Supervisor's Signature: .....
Date: .....

Sudan University of Science and Technology
College of Graduate Studies

Assigning the Copy-right to CGS

I, the signing here-under, declare that I'm the sole author of the Ph.D. thesis entitled 'Analysis of Magnetic Torsional Vibration Damper for Reciprocating Internal Combustion Engines which is an original intellectual work. Willingly, I assign the copyright of this work to the College of Graduate Studies (CGS), Sudan University of Science and Technology (SUST). Accordingly, SUST has all the rights to publish this work for scientific purposes.

Candidate's name: Sabir Abushousha Ahmed Abushousha

Candidate's signature: ----------

Date: 26 April 2019 ----------

الآية

قال تعالى:

بسم الله الرحمن الرحيم

وَإِن تَعُدُّواْ نِعْمَةَ

ٱللَّهِ لَا تُحْصُوهَآ ۗ إِنَّ ٱللَّهَ لَغَفُورٌ رَّحِيمٌ ﴿١٨﴾

سورة النحل (18)

Dedication

To my family wife and my wonderful daughters and friends who have kept me going during this Arduous task thank you.

To my mother…I cannot express how grateful I am for having this opportunity; I could not have done it without you. Your Unconditional love and support has allowed me to accomplish something I never dreamed possible.

To my father and brother Mubarak God bless you

To my brothers, sisters and colleagues thank you.

Acknowledgements

All praise and appreciation be for almighty **Allah** the most beneficent, the most merciful, by whose Grace and Mercy I have completed this work.

I would like to take this opportunity to express my gratitude to my thesis supervisors, Dr. Tag-Elsir H. Hassan, for his support, help, encouragement, and inspired guidance through my graduate studies at University.

I would like to express my gratitude to Dr. Hassan (Head of the Department) Dr. Omer Musa,Mr. Yasser and Mr. Khalid

I would also like to express my deepest gratitude to my lovely wife, for her limitless patience, understanding and encouragement during the period of my thesis preparation. Last but not the least; I am extremely appreciative of my mum and family, for their continuous and endless love and support. I should thank all of my friends who were beside me during the PhD study and wish them success and happiness in their life.

Finally, I extend my gratefulness to one and all who are directly or indirectly involved in the successful completion of this project work.

Abstract (Arabic)

المستخلص

الإهتزازات الإلتوائية في محرك الإحتراق الداخلي ظاهرة مهمة تحدث نتيجة للإثارة الناتجة من قوة الغازات المحترقة والتغير في قوة العطالة من الإجزاء المترددة أثناء تحويل الحركة من حركة ترددية إلي حركة دورانية هذا التحويل يؤدي إلي إنتاج عزم التواء علي العمود المرفقي مؤديا إلي إجهادات قد تودياإلي انكساره وتأتي أهمية الدراسة إلي أن هذه الظاهرة لا يمكن كشفها بسهولة إلي أن يحدث الفشل في المنظومة .

هنالك عدة أنواع من المخمدات تستخدم لخمد الإهتزاز الإلتوائي كالمخمد الإحتكاكي واللزج والمطاطي والديناميكي لكن معظمها تعمل علي إستهلاك نسبة من القدرة الناتجة من المحرك وتقصير عمرها الإفتراضي.

تهدف الدراسة إلي إستخدام مخمد إلكترومغناطيسي حيث تتميز عن الأنواع السابقة بقلة صرف القدرة وعدم وجود إحتكاك مباشر مع المنظومة مع سرعة الإستجابة للتغير في الإستثارة الناتجة من المحرك.

إعتمدت منهجية الدراسة علي الجانب النظري حيث تم كتابة برنامج بإستخدام ماتلاب لدراسة تأثير معامل الخمد علي علي قوة الإثارة عندحدوث ظاهرة الرنين.

وجد من الدراسة أن قيمة معامل الخمد المثالي للمحرك قيد الدراسة تساوي 0.2,0.3,0.4 وهو يتناسب مع نتائج الدراسات السابقة .

.

Abstract (English)

Torsional vibration in Internal Combustion Engines is an important phenomenon occurs due to excitation loads, cycle-to-cycle variations results from the force the burnt gases and to change in inerita forces generated by reciprocating parts during convertoin of rotary motion to the linear one . This conversion leads to twist torque on the crankshaft which, in turn, leads to high stresses causing its damage. The importance of the present study stem from the fact that this phenomenon cannot be detected till it leads eventually to system failure. There are several types of dampers to alleviate torsional vibration such as frictional, viscous, rubber and dynemic dampers but these types has the drawbacks of consumption of engine power and reduction of engine lifetime. The objective of this study is to use electromagnetic damper as this type of damper minimize power consumption, without getting in direct friction with the system in addition to quickness of response to engine excitation change. The methodology of our study is based on theortical treatement through writing a Matlab code to investigate the effect of damping coefficient on excitation during resonance condition.

It was found, through this study, that the optimal damping coefficient value is 0.2,0.3and 0.4 .in concordance with previous studies.

Table of Contents

List of Figures

List of Tables

List of Symbols And Abbreviations

Symbol	Description	Units
A	Piston cross-sectional area	[m]
B	Cylinder bore	[m]
C	Torsional damping	[kg.m^2/rad]
[C]	Damping matrix	[-]
D	Diameter	[m]
J	Rotating mass polar moment of inertia	[kg.m^2]
Jcp	Crankpin rotating inertia	[kg.m^2]
Jcr	Connecting rod rotating inertia	[kg.m^2]
Jjb	Main journal bearing rotating inertia	[kg.m^2]
Jrec	Reciprocating mass polar moment of inertia	[kg.m^2]
[J]	Inertia matrix	[-]
K	Torsional rigidity	[kg.m^2/rad]
L	Connecting rod length	[m]
L e	Effective shaft length	[m]
m	Mass	[kg]
P_g	Cylinder Pressure - Atmosphere Pressure	[Pa]
Pi_n	Inlet Pressure to Cylinder	[Pa]
s	Cylinder Displacement	[m]
s	Piston Linear Position	[m]
s	Piston Linear Velocity	[m/s]
s	Piston Linear Acceleration	[m/s^2]
T	Time	[sec]
V	Cylinder Volume	[m^3]

Mp	Reciprocating mass	[kg]
Phi	Connecting rod angle at piston pin	[rad]
Phi	Connecting rod angle at crankpin	[rad]
W	Natural frequency	[Hz]
θ	Crankshaft angle	[-]
θ	Angular velocity	[rad/s]
θ	Angular acceleration	[rad/s]

LIST OF ABREVIATIONS

BDC	Bottom dead center
ICE :	Internal Combustion Engine
ODE	Ordinary Differential Equation
TDC	Top dead center
TVD :	Torsional vibration damper
PPR	Pulses per revolution
IMEP	Indicated Mean Effective Pressure, high pressure cycle
ODE	Ordinary Differential Equations
RPM	Revolutions Per Minute
BDC	Bottom Dead Center
CA	Crank Angles

List of Appendices

List of Publications

Cylinder Pressure Variation Modeling inside a Diesel Engine

CHAPTER I INTRODUCTION

1.1 Background

Internal combustion engines are most commonly used for mobile propulsion in vehicles and portable machinery these engines have appeared in transport in almost all vehicles such as automobiles, trucks, motorcycles, boats, and in a wide variety of aircraft and locomotives (Hudson, 1997).

Crankshaft is one of the most expensive and important moving parts in the affecting engine operation and usually convert reciprocating motion of piston into rotational motion. Crankshaft vibration is one of the most important factors. The different vibrations affecting the crankshaft are lateral vibrations and torsional vibrations among which torsional vibration is usually the most important(Filipović and Aleksandar Milašinović, 2011).

Torsional vibrations problem occur in reciprocating multi-cylinder internal combustion engines is the major reason for the failures of crankshaft. The torque applied to crankshaft is not constant in time, but it varies in a complex manner as a function of crankshaft position for each cylinder. The excitation that causes torsional vibrations of crankshaft is the pressure generated during the combustion process is not constant in the engine cylinders beside the alternating torques resulting from crankshaft's slider-crank mechanism. Even if the pressure is constant, the slider-crank mechanism is incapable of producing smooth torque which is further compounded by the arrangement of the firing order of the crankshaft.

The torque impulses of the engine output are not developed smoothly but has periodic torque pulsations or torsional vibrations These torque variations in turn, produce periodic velocity variations or accelerations result in torsional vibration in the crankshaft, which as a result starts twisting back and forth at a high frequency.

These fluctuations can be very damaging to the crankshaft, putting great stress and strain on it. The speed changes associated with combustion events in an engine can cause the crankshaft to fatigue prematurely or break and leads to increased wear of the components that are being driven by it. Torsional vibration can also cause excessive wear and tear of bearings and gear parts. It can lead to broken accessory drives and the throwing/slapping of engine belts.

When the shaft is turning at such a speed that the frequency of the impulses due to the torque variation coincides with the natural frequency of the shaft system, it is at a critical speed. Under these conditions the amplitude of vibration will build up to an extent determined by certain damping factors. The stresses due to this vibration may or may not be sufficiently great to fracture

the shaft. Any elastic system may thus be set into violent vibration by applying a series of impulses at properly timed intervals.

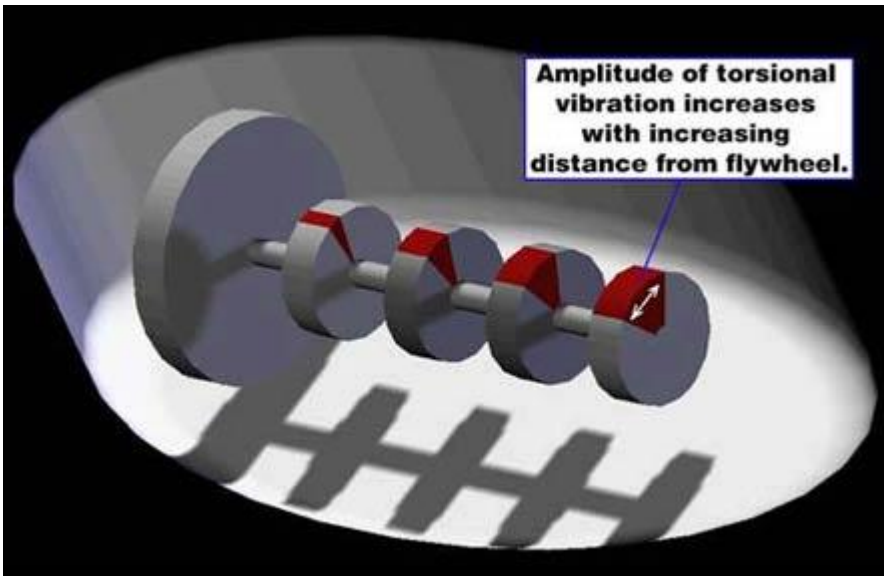

Figure 1-1amplitude of torsional vibration

Each crankshaft design has a natural torsional frequency. when frequencies get excited several times through the operating speed of engine by different components of firing pulse harmonics, called orders of an engine. The vibration amplitudes under these critical speeds of a shaft occurs when the shaft rotational speed coincides with the natural frequency of the system When this happens, the amplitude of vibration will increase and the effects can be devastating, resulting in fail of the crankshaft as well as any accessory coupled to the crankshaft(FRANK M . LEwls, 1925). These damages are usually at the front of the engine, as the flywheel's inertia cuts down motion at the rear end of the engine.

torsional vibration analyses of the shafting system to ensure that the vibratory shaft stresses are below the allowable limits(Feese, T. and Hill, 2009). This is best achieved by designing the shafting system so its natural frequencies do not coincide with the excitation frequencies

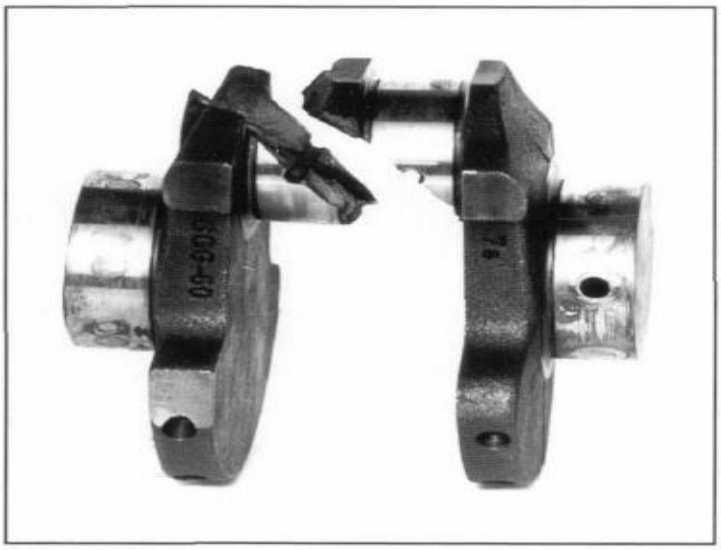

Figure 1-2 Sample failed engine crankshaft (in 45° due to torsional vibration) [12]

Figure 1-3: sample of faulire A) Motor Failure B) Damaged Coupling C) Fractured Shaft D) Melted Rubber Coupling

It is possible to modify the system inertia and hence the natural frequency by adding additional rotating mass to the engine's free end, in order to move critical speeds away from a fixed running speed. A similar modification to natural frequencies can be imposed by introducing a flexible coupling drive between the engine and the machine it is driving.

Torsional vibration is defined as inertia or rigid body oscillations about the central axis of the shaft line. or the cyclic motion corresponding to a shaft, where the shaft is twisted about its axis, alternating from one direction to the other(Lee, D.C., Lee, B.W., Park, Y.N. and Park, 1992)(Eshleman, 1988). Each power stroke tends to slightly twist the shaft. When the power stroke subsides, the crankshaft untwists.

Torsional vibrations of engine crankshaft (see Figure 1) have two parameters: frequency of vibrations and amplitude of twist angle α(see Figure2). It is desired to obtain minimal (ideally zero) twist angle α of shaft in steady-speed operation of an engine. For this purpose the engine is equipped by Torsional Vibration Damper which is installed in front part of crankshaft(George Nerubenko and Vitaliy Krupenin, 2008)

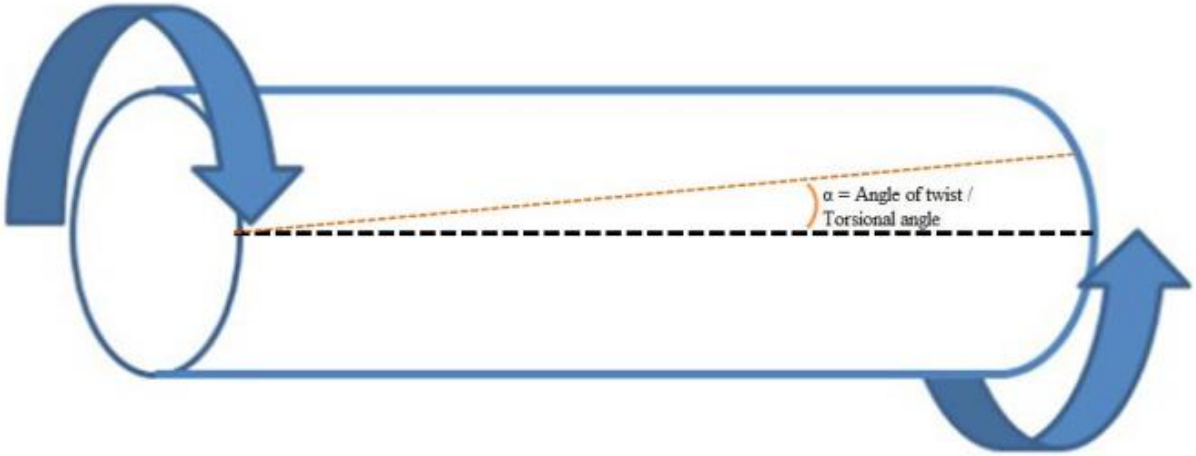

Figure 1-4: Basic principle of a twisted shaft.

1.2 Motivation

The last decade has seen a great expansion in the field of power electronics and magnetic materials that have directed to enormous enhancements in electromagnetic devices, which in turn, have led to growth of smart structures. The smart devices are now being efficiently installed as vibration dampers to enhance the ride luxury, road and safety

1.3 Problem Definition

All systems used for vibration damping are energy consuming, with short life span. They tend to dissipate energy in the form of heat necessitating cooling of these dampers in order to avoid overheating which might lead to failure. In addition, damping is not smooth.

1.4 Significance of the Research

All types of damping are continuously working which means high energy consumption beside the resolution of damping is not smooth. by using magnetic damper and control system we need to generate signal that equal the damping force.

1.5 Research Methodology

1. The mathematical model will be built upon the known equation governing vibration damping with inclusion of an expression for the proposed magnetic torsional damper.
2. To elaborate a mathematical model to monitor various parameters affecting engine performance in presence of the proposed damper system.
3. To propose a system of magnetic torsion damper to conserve engine power.

4. To find solution set of the model will be obtained using a suitable numerical technique.

5. To dedicated suitable algorism will be implemented to solve the model.

6. To validate the simulation results will be done by comparing them with the experimental work.

1.6 Limitations and Assumptions

To complete the study within the given time frame, a clear project must be defined with boundaries that are listed:

1. Only torsional vibrations will be considered.
2. The vibration analysis of power train will not be performed.
3. The engine balancing will not be analyzed in this study.
4. The study will be done mainly on numerical simulations using Matlab software.
5. Experimentation work will not be included in this study.
6. The effects of the variable inertia characteristics of reciprocating engines torsional vibration calculations will be ignored.

1.7 Research Objectives

The objectives of this thesis are:

1. To develop a method of determining individual cylinder gas torques from development of computerized method to study the effect of torsional vibration of the crankshaft of reciprocating six-cylinder diesel engine.

2. To Find a solution of the problem of vibration in internal combustion engines (ICE) by propose a system of magnetic torsion damper to conserve engine power.

3. To develop a torsional vibration model of the crankshaft including components connected to it (i.e. connecting rods, pistons, flywheels, and external loads).

4. To Validate the theoretical results will be comparing with the published work.

1.8 Thesis Organization

Thesis contains five chapters. In chapter one the importance of torsional vibration control to avoid the crankshaft failure has been discussed and the motivation for the use of eddy current damper for attenuating the vibration in reciprocating engines is presented.

In chapter two literature review about torsional vibration has been covered.

In chapter three, the approach for finding linear torsional vibration modeling of engines in the form of lumped inertia disks and shafts for different parts of the engines has been presented. The

equivalent torsional modeling has been formulated in order to extract the resonance frequencies and different mode shapes. Also, derivation of in-cylinder pressure harmonic excitation for the diesel engine using Matlab Code which uses the Fourier series to find the orders of the excitation. The final fluctuating torque due to combustion calculated.

Chapter four presents and describes results acquired through simulations made with the model.

Chapter five covers conclusions drawn from the results described in the previous chapter And Finally some topics for future improvements research and possible extensions to the model are suggested for controlling the torsional vibration.

CHAPTER II LITERATURE REVIEW

2.1 Introduction

Vibration an everyday life phenomenon which can be defined as oscillations of a system about an equilbrium position. All vibratory system in general containing three basic components, include a means for storing potential energy (spring or elasticity), a means for storing kinetic energy (mass or inertia), and a means by which energy is gradually lost (damping or resistance)(Rao, 2004). vibration is defined as oscillatory motions of bodies and the forces associated with them in vibration analysis, it is important to understand that the location of a vibrating body's surface varies with time. This motion of the body's surface is called a vibration or oscillation(Weaver Jr, William and Timoshenko, Stephen P and Young, no date).

Vibration can be classified Free or Forced vibration depending on the type of(Drápal and Novotný, 2017).Free vibration is a condition with no external forces on the system,when a system is initially disturbed by a displacement, velocity or acceleration, the system starts to vibrate with a constant amplitude and frequency depend on its stiffness and mass. This frequency is called as natural frequency, and the form of the vibration is called as mode shapes.

2.2 Crankshaft Vibrations Classification

Crankshaft is the most significant part of the I.C. engine which converts linear motion into rotational motion. Any defect or failure in the crankshaft will lead to the failure of the I.C. engine. Periodic changes in gas pressure and inertial forces generate the following major three types of the crankshaft vibration such as buckling (flexural) bending, longitudinal (axial) and Torsional vibrations(Homik and Ph, 2011).The most types of vibration are shown in figure 2.1

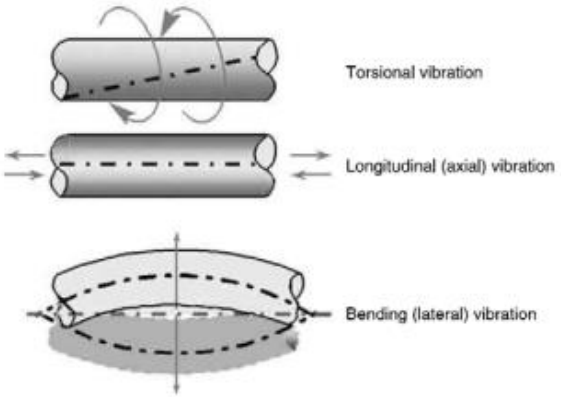

Figure 2-1 types of torsional vibration

2.2.1 **Bending Vibration**

This vibration occurs due to cyclic forces employed by connecting rod at crankpin acting perpendicular to the axis of crankshaft rotation. Currently, every engine is built with main crank pin bearing after each crank throw. Therefore, distance between two adjacent journals is quite short resulting in high natural frequencies of bending vibration which do not interfere with operational revolutions of the engine. However, bending vibration is an issue by engines with a small number of cylinders, where mass of flywheel needs to be very high due to speed non-uniformity(POLÁČEK, 2011).

2.2.2 **Axial Vibration**

The torsional vibrations can cause axial vibration in the twisting and untwisting motion. Also radial forces at crankpin cause some axial movement of crank throw(Desavale and Patil, 2013).

2.2.3 **Coupled Vibrations**

In general, however the various modes of vibration are usually appearing in a coupling of the torsional, bending and longitudinal vibrations. These are not troublesome if there is considerable spread between the natural frequencies of the modes of vibration involved; i.e. the modes get weakly coupled. The vibrations in a real crankshaft system are much more complicated (Okamura H, 1983).

2.2.4 **Torsional Vibration**

The most dangerous type of vibration occurring in multi-cylinder engine crankshafts. The fluctuating torque at the crankpin causes the twisting and untwisting periodically. Hence the torsional vibrations are induced.

Torsional vibrations of engines arise due to application of periodic combustion forces in the cylinder and associated inertial forces. the crankshaft torsional vibration occurs by expanding gases in cylinders at each power stroke which tends to twist the crank shaft throws. When the power stroke subsides, the crankshaft untwists. This rapid twisting of the crank throws is transmitted to main crank journals and causes non-uniformity in engine speed. One would think that something like crankshaft would not twist significantly, but any piece of metal always deflects a bit when force is applied, and in case of IC engines, where large amount of power is generated, these forces can become huge indeed(Montazersadgh. F. H., 2008)(Amitpal Singh Punewale, Tushar Khobragade, Amit Chaudhari, 2015).

When a natural frequency coincides with an excitation frequency, a resonance occurs followed by increased noise and engine vibration. This is called a critical speed of crankshaft. If the

excitation forces are applied with this frequency, the amplitude of vibration increases until it can lead to destroys the crankshaft by a fatigue failure, or until speed moves away from its critical value(Eshleman, no date).

Excessive torsional vibrations do not affect only crankshaft but can also can result in gear wear, gear tooth failures, key failures, shrink fit slippage, a valve timing mechanism and broken shafts in many cases(J.C. (Buddy) Wachel, 1993).

Due to a wide speed range in which the engine needs to run, it is not possible to keep the system natural frequency from the range of critical speeds. This condition, known as resonance, is to be avoided to prevent failure of the system by increasing the shaft stiffness or reliving of oscillating parts(Rao, 2004).

The phenomena can be explained by Observing the Figure [1]: RPM vs time curve of a 4-cylinder engine run-up. We see While the overall rpm rises from 1000 RPM to 3500 RPM, it does not increase steadily. There is a fluctuation in the rotating speed within each rotational cycle (see zoomed image in Figure 2: There is a 100 RPM variation in rotating speed.

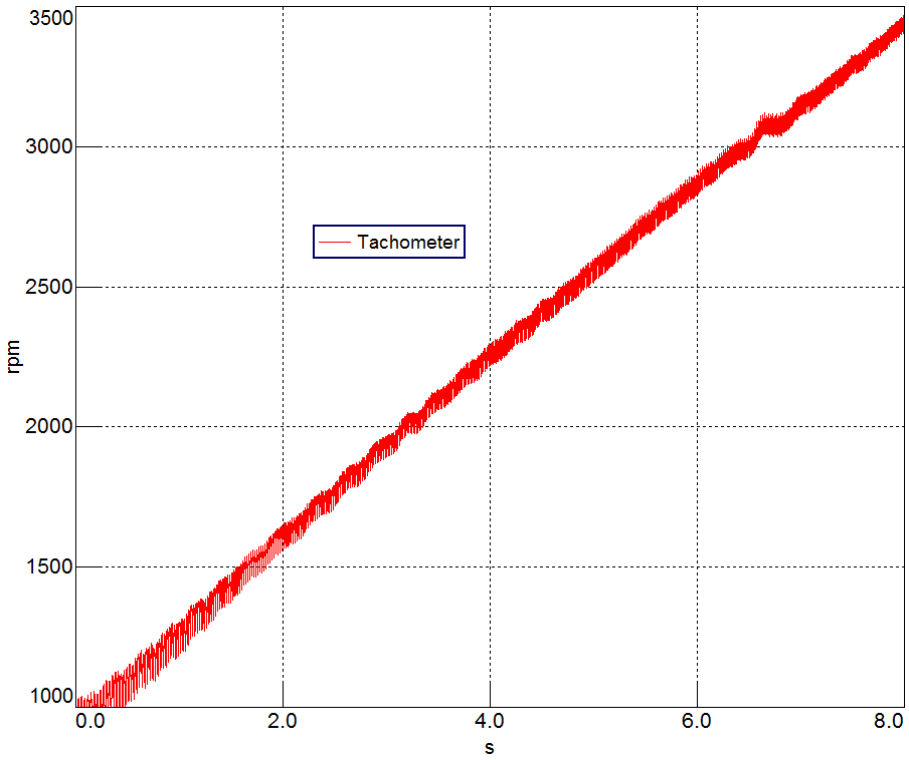

Figure 2-2 rpm vs time curve of a 4- cylinder engine run-up.

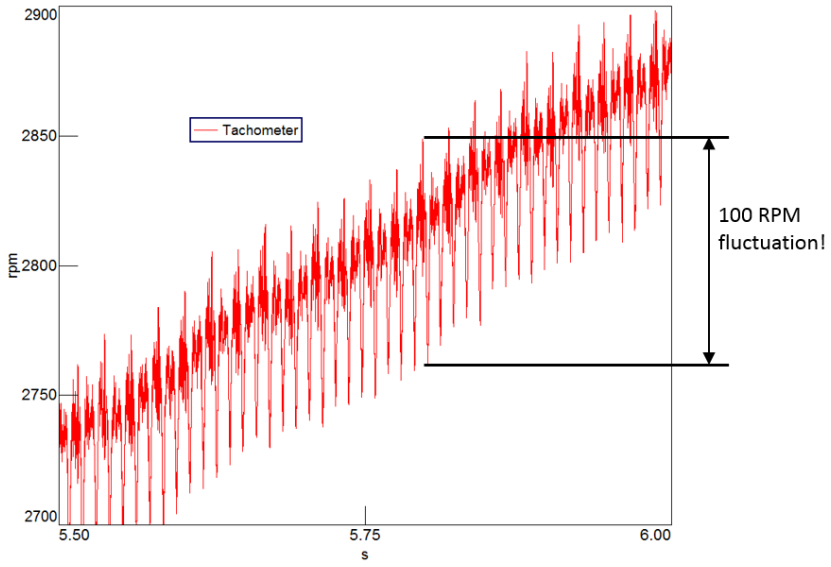

Figure 2-3 : A 100 RPM fluctuation in rotational speed

2.2.4.1 Torsional Vibration Definition

Torsion in solid mechanics defined as the twisting of an object as a result of applied torque. Torsional vibration can be broadly described as the angular vibration of any object. It can be defined specifically as the periodic motion corresponding to a shaft, where the shaft is twisted about its axis, alternating from one direction to the other. Or the fluctuation in the rotational velocity of a rotating component. These fluctuations are superimposed on the steady running speed. These unsteady variations speed changes are called torsional vibration

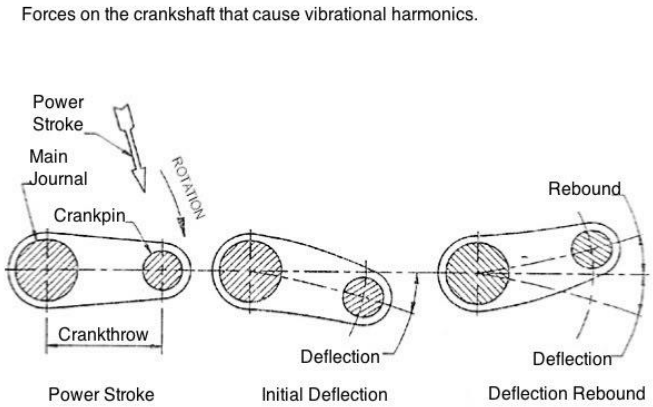

Figure 2-4:Forces on the crank shaft causes torsional vibration

2.2.4.2 Torsional Vibration Measuring

The most common way to calculate torsional vibration is by using equidistant pulses over a single shaft revolution. Shaft encoders or gear tooth pick up transducers dedicated for this task generate these pulses. The resultant pulse train is converted into either a digital rpm reading or a voltage proportional to the rpm. Dual beam lasers are also used, this method calculates the difference in reflection frequency between two perfectly aligned beams pointing at different points of a shaft. The lower Pulses per revolution [PPR] rate (black) did not capture the torsional vibration. The highPPR (red) captured the fluctuation of rotational speed within the rotation cycle as shown in figure 2.5.

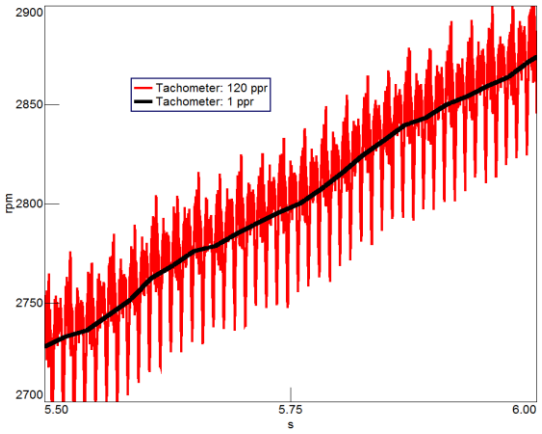

Figure 2-5: The pulses per revolution [PPR] for capturing the fluctuation of rotational speed

2.3 Internal Combustion Engines Torsional Vibration Theory

An internal combustion engine produces power using the very rapid pressure pulse of burning air fuel mixture above the piston. These powerful pulses of energy cause the engine to vibrate in response. These forces cannot be canceled out to minimize or eliminate all vibrations in an engine. The perfect engine tends to produce a characteristic vibration spectrum signature. Vibration analysis of IC engines then must focus on variations from the normal vibration signature.Torsional vibration is common to internal combustion engine crankshafts for many reasons:

1. The crankshaft's slider-crank mechanism that connects the rod and piston results in alternating torques.
2. The cylinder pressure generated during the combustion stroke is not constant throughout the internal combustion process. Even if the pressure is constant, the slider-crank mechanism is incapable of producing smooth torque.

Furthermore, engines that incorporate multiple cylinders usually have very flexible crankshafts because of their long length.

2.4 Engine Firing Order

The crankshaft is driven by cylinders that fire within each rotation of the crankshaft. Each time the cylinder fires, the crankshaft speeds up a little.

The slower the engine is firing and the less cylinders an engine has the longer the time between combustion events, and the more the crankshaft slows between combustion events. Therefore, the lower the RPM, the greater the torsional vibration.

The firing order is shown by the sequence of the number of cylinders in which cylinders generate power stroke. Each combustion pulse acts as a hammer blow, hitting the engine with an impulse of energy. is selected as part of engine design to obtain best engine performance (Nestorides, 1958), (Challen, 1999).The vibration spectrum of these pulses are a sequence of vibration spectral lines. These spectral lines will be at integer multiples of the firing order of each piston. for a 4-stroke the engine fires every tow rotation, therefore the

fundamental order will be at halve the engine RPM, often called the 0.5 order vibration. The result will be a vibration signature that has spectral lines at the 1/2 order, 1P, 1-1/2P, 2P, 2-1/2P, 3P ... etc. If the engine is a two-stroke, there will be one power pulse per revolution in each of its n cylinders(Norton and Worcester, 1999).

2.4.1 Major Order

The engine excitation curve can be divided in to number of sinusoidal curves of different frequencies. These frequencies are multiples or submultiples of the engine speed. These multiples and submultiples define the order of the engine. A major order is the one which causes the largest excitation and the torsional oscillations can be induced at this order. In case of the engine, the major order is mostly the firing order which is obtained from following formulae [Martyr et.al, 2007].

Nc= (Number of cylinders)/2, 4- four stroke engine.

Nc= Number of cylinders, for a 2- stroke engine.

Nc= (Number of cylinders)/4, for a Vee engine 4-stroke engine.

It has been proved that, the major order resonance is of highest importance as compared to other orders. For example, an even-firing 8-cylinder, 4-stroke engine produces four torque pulses per revolution (a fourth order excitation). If an engine operating at 6000 RPM, then the frequency of

the 4th excitation is 4x6000/60 = 400 Hz. To get the first order of the engine in Hz you divide the running speed of the engine by 60, so for an engine running at 720 rpm the first order is 720/60 = 12Hz. So if there is a peak at 24Hz (2x12 Hz), it is at the engine's 2nd order.

2.4.2 Minor orders

The torque impulses are being applied at various points of the crankshaft, and in a specific order based on the engine's firing sequence. As a result, some harmonic orders partially cancel one another and are termed.

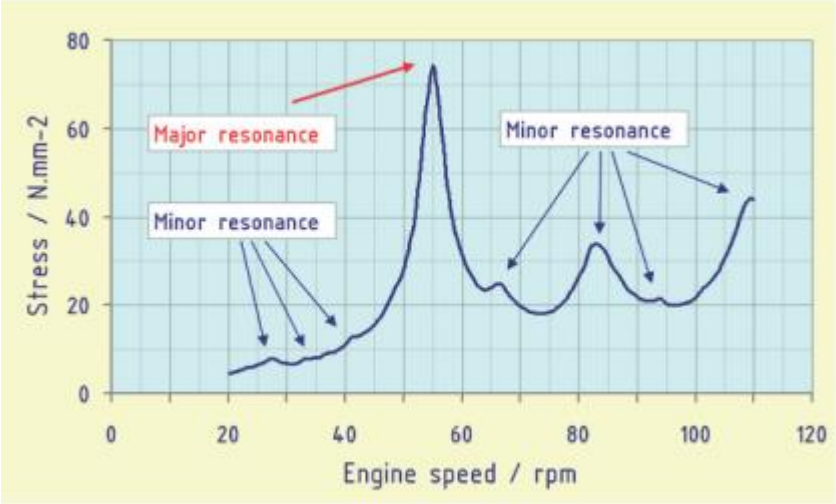

Figure 2-6: Peaks on a diagram correspond to system resonances. (Magazinović, 1998)

2.5 Phase And Resonance

The phase relationship between the driving oscillation and the oscillation of the object being driven is different at different frequencies. Below resonance they are in phase with each other. At resonance the phase relationship is 90^{o} or $\pi/2$ rad. Above resonance the phase relationship is 180^{o} or π rad.

2.6 Influence of Crankshaft Torsional Vibrations

Unrestricted torsional vibrations cause the angular velocities of all the cranks to vary but in different magnitude. stresses of fluctuating intensity nature are produced in whole length of the crankshaft causing cracking, failure fatigue of crankshaft, reducing its life, or parts that the crankshaft drives. The stresses induced are dangerous at fillet or oil-hole locations.

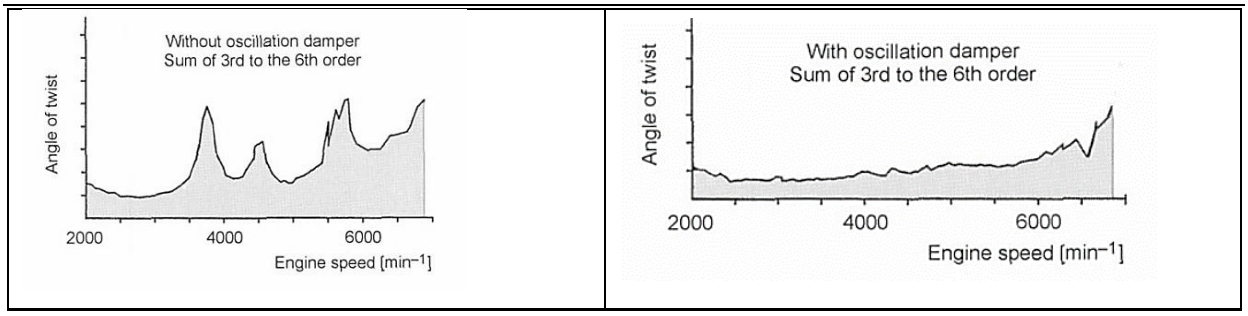

Figure 2-7 Torsional Vibration with or without damper(Basshuysen and , Schäfer, 2004)

2.7 Torsional Vibration Control

In many practical situations, it is possible to reduce but not eliminate the dynamic forces that cause vibrations. damping may be introduced in a variety of ways are used to control vibrations. Among them, the following are important:

Shifting the critical resonant vibrations regimes outside the ICE engine operating range(Piotr Deuszkiewicz, 2015). Introducing energy- dissipating devices to reduce the vibration amplitude in the resonant regimes. Modification the response of the system by the addition of an auxiliary mass neutralizer or vibration absorber (Rao, 2004).

The first three solutions may be impossible to implement from point of view of construction requires increasing the crankshaft stiffness while reducing the moment of inertia of all masses of the entire piston and connecting rod assembly. Using various types of torsional dampers can move the critical speeds from the operational range.

Torsional vibration dampers and absorbers are usually mounted on a crankshaft's free end where highest angular deviations occur. They reduce vibration amplitudes by moving the critical speeds from the resonant frequency operational range thus limiting vibration stress, act to reduce wear and improve comfort(Klaus Mollenhauer and Helmut Tschoeke, 2010).The majority of the torsional dampers work on a principle of consuming and dissipating vibratory energy to heat(Klaus Mollenhauer and Helmut Tschoeke, 2010). Typically, it is not possible to remove all of the crankshaft's undesirable critical speeds from the engine's operating range. Thus, a vibration damper is needed to reduce the amplitudes of these resonances to acceptable levels.

Torsional vibration dampers used in ICE engines differ in structure and working principles (Filipović, 2007) (Wilson, 1968). For road motor vehicles, viscous and rubber dampers were irreplaceable for a long period of time. They are more suitable because of their simplicity, cost and easier maintenance.

Recently, there has been a trend of replacing the TVD as a separate unit with different variants of the dynamic absorber built in into the existing engine parts. So, torsional vibration absorbers are today already extensively developed and used as incorporated into the engine flywheel or the crankshaft balance weights(Gerhardt *et al.*, 2002)(Bibić and Pecar, 2012) (Lee, D.C., Lee, B.W., Park, Y.N. and Park, 1992)(Kroll, Kooy and Seebacher, 2010).

There are two types of damping external and internal. External damping is energy dissipation that is dependent on the absolute velocity of a particular inertia and modelled as a dashpot between the inertia and ground which associated with disk element. internal damping is modelled as a dashpot in parallel with the torsional spring representing the appropriate shaft element. Shaft material hysteresis and damping in couplings are modelled as internal dampers. Both external and internal damping elements are modelled as linear dashpots, as is illustrated in Figure 2.8.

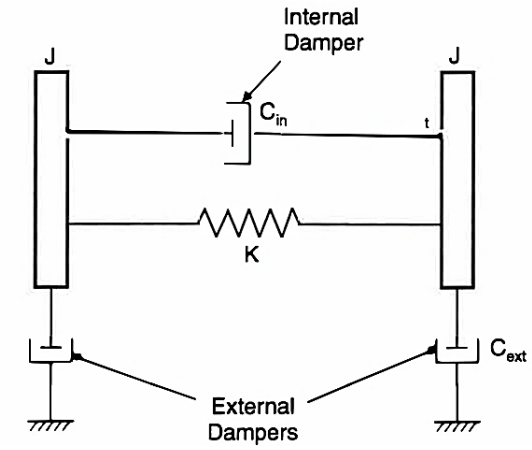

Figure 2-8 Types of external and internal damping

2.7.1 Vibration damper

Often, the vibration attenuating devices on the free end of an engine crankshaft are incorrectly referred to as "dampers". in most cases, they are absorbers. A damper is a device which dissipates energy, mainly in the form of heat. an absorber is a device which is designed to oscillate in direct opposition to a vibration at either a specific frequency or a specific order, depending on the design. Vibration dampers or absorbers can be classified du to operation in to tuned or untuned absorbers

Two types of dampers exist: tuned and untuned. A tuned damper is designed to a specific frequency or engine speed.

.

2.7.1.1 Tuned Dampers

Tuned Dampers. The tuned damper is essentially a single degree-of-freedom mass-spring system having its resonance frequency close to the selected resonance frequency of the system to be damped, i.e., tuned. As the structure vibrates, the damper elastomeric element vibrates with much greater amplitude than the structure at the point of attachment and dissipates significant amounts of energy per cycle, thereby introducing large damping forces back to the structure which tend to reduce the amplitude. The system also adds another degree of freedom, so two peaks arise in place of the single original resonance. Proper tuning is required to ensure that the two new peaks are both lower in amplitude than the original single peak. The damper mass should be as large as practicable in order to maximize the damper effectiveness, up to perhaps 5 or 10 percent of the weight of the structure at most, and the damping capability of the resilient element should be as high as possible. The weight increase needed to add significant damping in a single mode is usually smaller than for a layered treatment, perhaps 5 percent or less. This type of dampener is referred to as untuned because it will dampen the vibration regardless of frequency, as can be seen in the plot of Figure 2.5(Dondlinge, 2015).

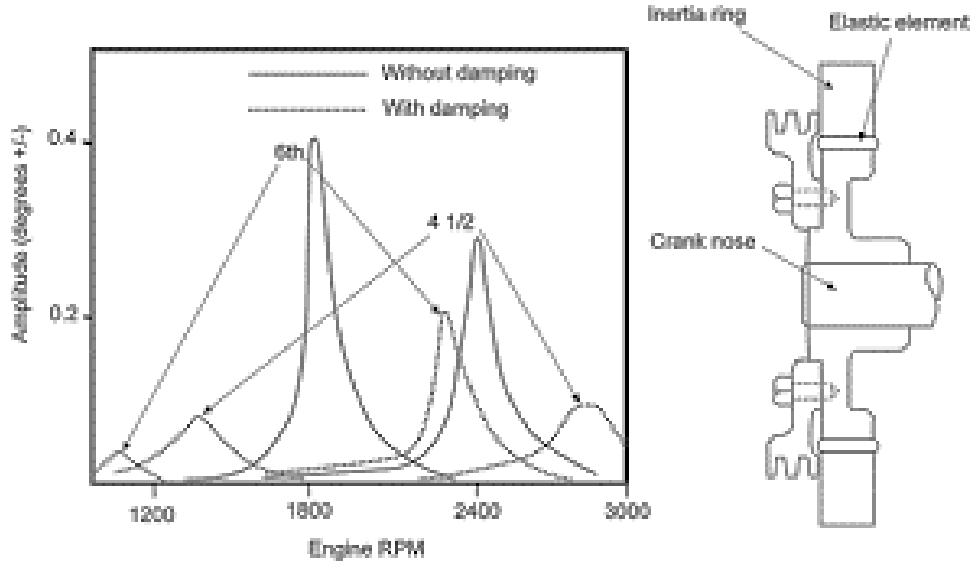

Figure 2-9: tuned vibration damper

A tuned mass damper (TMD) is a device consisting of a mass, a spring, and a damper that is attached to a system in order to reduce the dynamic response of the system. As the system vibrates, the damper element vibrates by amplitude greater than the system at the attachment point lead to disperses substantial quantities of energy, thereby introducing large damping forces back to the system which tend to reduce the amplitude. The system also adds additional degree of freedom, so two crests arise in place of the single original resonance. Proper tuning is required

to ensure that the two new peaks are both lower in amplitude than the original single peak. The frequency of the damper is tuned to a particular structural frequency so that when that frequency is excited, the damper will resonate out of phase with the structural motion. Energy is dissipated by the damper inertia force acting on the structure. The TMD concept was first applied by Frahm (Frahm, 1911)to reduce the rolling motion of ships as well as ship hull vibrations.it should be pointed out that coulomb friction, which is independent of angular velocity, does not provide damping of torsional vibration(Corbo and Melanoski, 1996).

2.7.1.2 Untuned Dampers

More commonly used in automobiles is the tuned harmonic dampener shown in Figure 2.7. In this design the dampener hub is again rigidly mounted to the crankshaft nose, and a seismic mass is then mounted around the hub through a rubber isolator. The combination of the mass and the stiffness of the rubber isolator is tuned to dampen out vibration at a particular frequency, as shown in the figure. It should be noted that each order now has two resonant frequencies because the coupled mass acts as a second torsional system linked through the rubber isolator(Dondlinge, 2015).

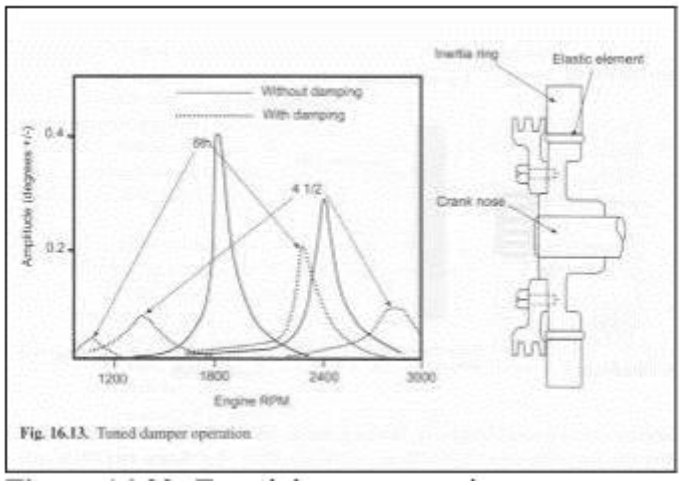

Figure 2-10:Untuned vibration damper

2.8 Dynamic Vibration Absorber (Tuned Damper)

A dynamic vibration absorber is an auxiliary mass-spring system which tends to neutralize vibration of a structure to which it is attached. The basic principle of operation is vibration out-of-phase with the vibration of such structure, thereby applying a counteracting force.

2.9 Vibration Absorbers

An effective means of alleviating some torsional vibration problems involves the use of a vibration absorber or damper. One category of such devices is composed of an auxiliary mass,

referred as the seismic mass, that is coupled to the main system by some elastic and/or viscous medium as depicted in Figure 2.10(a). Such devices can include tuned and untuned absorbers as well as viscous damping devices sometimes referred to as Houdaille dampers. Tuned absorbers which have negligible damping are sometimes employed to shift the system's natural frequencies or to provide an anti- resonance at a particular frequency. Untuned absorbers which have a significant amount of damping are often used to reduce amplitude levels over a wider range of frequencies than tuned absorbers. Houdaille dampers serve as devices for dissipating vibratory energy(Griffin, 1998).

2.10 Frictional Dampers

Convert vibratory energy in form of friction torque and dissipate it as a heat when relative motion takes place between adjacent members These forces are independent of amplitude and frequency; they always oppose the motion and their magnitude may. There are two types of the frictional or Coulomb (dry friction) dampers known as Lanchester damper In general, it is less effective than tuned vibration absorbers(Harris, 2002). a viscous type, where the friction occurs in fluid, silicone oil, captured between a light sheet cover mounted on the crankshaft and a heavy inertia mass disc. The second is a solid type, which basically acts as a dry clutch, where the dry friction originates between inertia discs pressed together by springs. Their disadvantage is a relatively low damping.

2.10.1 **Viscous Dampers**

A simple type of dissipation mechanism typically considered in vibrations damping (William J. Bottega, 2011).A viscous damper has a sealed outer housing with a precision machined hub. Inside of the housing is an inertia ring with a viscous fluid (Fluidampr uses specialized silicone) filling the cavity. It is used to limit vibrations and crankshaft stresses and protect the engine and not necessarily the driven machinery. usually located near the front end of the engine(Spångberg, 2012). The viscous damping force is proportional to the first power of the velocity across the damper, and it always opposes the motion, so that the damping force is a linear continuous function of the velocity. Because of the mathematical treatment simplicity they used to approximate more complex types of damping approximated as the viscous type(C. E Beards, 1983). it consists of a flywheel that rotates inside the housing, which consists of a fluid with high viscosity. A principal sketch of a viscous damper is seen in Figure 2.10.

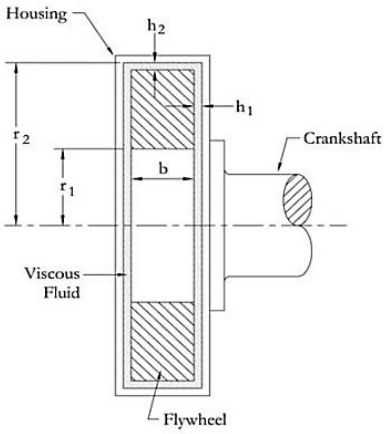

Figure 2-11:Principal sketch of a viscous damper.

2.11 Untuned Viscous Damper (Houdaille Damper) :

This type of damper is similar in principle to the Lanchester Damper except that instead of using friction plates for dry friction damping, this system uses friction damping. It consists of a freely rotating disc enclosed in the close-fitting case which is keyed to the shaft. Normally the disc rotates at the shaft speed owing to the viscous drag of the oil between the disc and the case. However, if the shaft vibrates torsionally, viscous action of the oil between the disc and casing gives a damping action.

2.12 Dynamic Torsional Damper

They sometimes called eliminator, or converter. It does not consume vibratory energy. The pendulum is linked to an oscillating shaft in means that a natural frequency of the pendulum matches a natural frequency of the torsional system. the benefit of these dampers acceleration from centrifugal force is much bigger than the gravity acceleration, so, only low inertia mass is favorite to compensate torsional vibration of the entire engine. An inaccuracy of the dynamic damper tuning can be a drawback.

2.13 Resonant Dampers (Rubber)

Also called tuned rubber torsional dampers. They consist of two parts, a flange, bolted to a pulley on front end of crankshaft, and a heavy inertia ring bonded together with the flange by a compound rubber band such as shown in figure 2.12. If the front end is accelerated, the mass ring tends to delay behind generating shear stress in the rubber band. The movement is damped by elastic hysteresis losses in the rubber and heat rejection to the surroundings. If needed an extra inertia ring can be added – dual mass torsional damper.

Rubber torsional dampers are efficient and simple to fabricate but their characteristics depends on temperature and life time of the rubber.

Rubber stiffness decreases with high deformation while its damping ability remains constant or even decreases. Likewise, heat reduces both the stiffness and the damping ability. Rubber has the capacity to store huge amounts of energy and can release a large amount of this energy on retraction. The most important difference between a rubber and a viscous damper , viscous damper is untuned but is capable of dropping the amplitude and smoothing out main critical orders. as a result, the rubber damper has its own natural frequency, the value of which is chosen to detune major critical orders so that their vibrations occur at different speeds with much reduced amplitude.

Figure 2-12:Rubber torsional damper bolt

Most commonly used conventional dampers for engines for road vehicles are named viscoelastic dampers (dampers plus rubber), who have a number of merits (efficiency, durability, storage space, etc.). Method to define the basic features of damping and a way of modeling these dampers is given in(FILIPOVIC, DOLECEK and BIBIC, 2005) (Blažević *et al.*, 2016). Rubber dampers are typically effective for engines with a total engine displacement of less than 7 liters (427 cubic inches). They are limited by their capacity to dissipate heat and rubber stress(V.R.Navale, 2015). It is the most weight-efficient design and the most economical to build beside it is effective, reliable, Properly designed, and long-lived. The biggest difference is that the inertia ring does not go resonant at any frequency and is thus not "tuned" like the rubber damper.

2.14 Eddy current damping

If a non-ferrous conducting object moves in a direction perpendicular lines of magnetic flux is produced by current is induced in the object. And proportional to velocity of the object. The current induced is called eddy current which set up its own magnetic field opposite to original magnetic field that has induced it. This provides resistance to motion object It forms magnetic field. This type of damping produced by eddy currents is called eddy current damping. it is used in vibrometers and in some vibration control systems.

2.15 Magnetic Damper

The first design considered was the magnetic damper system. The basic idea behind the device was to have input and output shafts completely unconnected from one another with a transfer of the rotational movement through magnetic fields. The advantage of this design was the small amount of losses because there are no physical contact points where frictional losses could occur. Further, magnets, as opposed to springs, have a nearly infinite life where as springs exhibit fatigue over time and lose their strength.

2.16 Combined Viscous And Coulomb Damping

The free vibration of dynamic structures with viscous damping is characterized by an exponential decay of the oscillation, whereas structures with Coulomb damping possess a linear decay of oscillation. Many real structures have both forms of damping, so that their vibration decay is a combination of exponential and linear functions.

2.17 Hysteretic Damping

Experiments on the damping that occurs in solid materials and structures that have been subjected to cyclic stressing have shown the damping force to be independent of frequency. This internal, or material, damping is referred to as hysteretic damping. Since the viscous damping force is dependent upon the frequency of oscillation, it is not a suitable way of modelling the internal damping of solids and structures. The analysis of systems and structures with this form of damping therefore requires the damping force to be divided by the frequency of oscillation.

2.18 Centrifugal Pendulum Vibration Absorber (CPVA)

are a long-known device to reduce torsional vibration in rotating systems. They are used successfully in aircraft since the late thirties. To implement these devices into combustion engines of passenger cars, the design space and weight to effectiveness ratio have to be Optimized. There are different principal designs of CPVA patented by Kutzbach, Carter, Salomon and Sarazin (Mathias Pfabe and Christoph Woernle, 2009).

Figure 2-13 Centrifugal Pendulum Vibration Absorber (CPVA)

2.19 Damper Problems

A damper which is in poor condition or which is not operating will increase the torsional vibration, resulting in an increase in material stresses and can lead to undue strain on the crankshaft and transmission components. The lifetime of a damper depends on its thermal load and on the running conditions. The effective operation of the damper may reduce after some period.

2.20 Literature Review

(Ivan Filipoviæ, 51(2005)12,) in heavy-duty diesel engines multi-cylinder, in-line**,** the conformity between calculated and experimental outcomes implies that the suggested procedure for parameters modeling and calculating of corresponding torsional systems can be manipulated in reality.

(homik, 2011) show In practice the detrimental phenomenon makes that the damper, instead to damp vibrations, starts to excite them.

The damper, if correctly designed, should operate reliably for 20000 - 30000 h in negative temperatures and first of all higher temperatures even as high as 120°C. Laboratory tests performed on viscous torsional vibration dampers demonstrated that events of seizing the dampers occurred when their working temperature values exceeded by 60°C the temperature for which they were designed. Satisfactory effects of damper operation are reached when it operates within the temperature range from 75° ÷ 90°C in continuous cycle of work.

(Wilson, 1956)established a torsional vibration model of a crankshaft with reciprocating mechanisms. his techniques were used to determine the inertia, stiffness, and damping between cylinder crank throws and the rest of the shaft. His methods are now used by industry to develop torsional vibration models of crankshafts.

(Kabele, 1984) developed a torsional vibration model of a V-8 diesel engine crankshaft which included piston and ring friction, connecting rod, hysteretic damping in the crankshaft, and cylinder pressure as a forcing function. The model was resulting from Newtonian Mechanics and the governing differential equations were non-linear making a mathematical solution necessary. As soon as his model was developed, he compared measured and model anticipated vibration amplitudes for numerous harmonic orders and concluded that relationship between the two was outstanding.

(Citron S. J., O'Higgins J. E., Chen L. Y., no date) prepared a computer model and created cylinder pressure torque by means of an flexible model of an engine, drivetrain system, and measured speed fluctuations. These speed variation data were delivered back through the model

to define the fluctuation waveform of both the entire engine torque being developed and the cylinder pressure waveform which gave rise to it.

(Rizzoni, 1989)proposed passing crankshaft speed fluctuations through an equivalent electronic circuit representing engine dynamics to forecast cylinder misfires. He piloted investigational work on production spark ignited vehicles and confirmed that it is possible to apply this method with minimal hardware and computational overhead.

(Sobel J. R., Jeremiasson J., 1AD) described a technique for measuring immediate crankshaft torque utilizing a non-contact ferromagnetic material to predict torsional stress in the crankshaft. The instantaneous torque of an internal combustion, four-cylinder engine was measured at the flywheel and compared with pressure signals during workbench experiments. Excellent correlation between this non-contact measured torque and values of the mean effective pressure for each cylinder were obtained.

(Brown T. S., 1992)presented a non- contact method for determining simultaneously the pressure in individual cylinder by using a pattern recognition method to compare crankshaft speed fluctuations to reference patterns in a knowledge base. The non-contact method utilized was an interval timer and a magnetic measuring device which timed the flywheel gear teeth as they passed. The experiment was conducted on a Detroit Diesel 6V-92TA engine. The investigational outcomes show that the method estimates the cylinder pressures with an RMS error not more than 6%. But this needs widespread data bases for each situation.

(Bell, 1996)concluded, employing the same Detroit Diesel 3-53 engine used in this study, that the deviation of shaft speed held information which could be used to guess cylinder firing pressures. He also recommended the improvement of a torsional vibration model of the engine and flywheel system along with a more rigid optical encoder mounting for further precise time resolved measurement.

(Draminski, 1965)prove that certain systems undergo excessive torsional oscillations at specific engine speeds .

Recently (Hestermann, D. C. and Stone, 1994) study the effect variation of inertia due the crank mechanism was shown to the cause unexpected large angular displacements. These secondary effects were verified and checked and were found to be responsible for many structural failures of crankshafts.

The aforementioned secondary effects were inserted by (Pasricha, 2001) in earlier reported calculation. He concluded that, in at least some instances, they can lead to detrimental effects on crankshaft

(Johnston, P. R. and Shusto, 1987)used the modal superimposing method to develop and apply a method to predict the torsional performance in ICEs in transient and steady-state. The computed values of this modeling were validated with respect to the actual values in the usual manner (Brusa, Delprete and Genta, 1997)studied the introduction of functions taking into account the variation of inertia in the crankshaft's angular position and the coupling of axial /flexural vibrations. These considerations substantially increased the number of equations to be solved and the computational cost, but the final results were more accurate for the cases reported in their article.

(Song *et al.*, 1991) The combined effect of torsional and axial vibration in the crankshaft was analyzed by Song and co-workers. They showed that when both the natural axial and torsional frequencies are equal, large displacements are ensued

(Den Hartog, 1985)and (Wilson, 1956)erroneously estimated torsional damping coefficients of ICEs based on empirical determinations. Their estimation introduced-in most cases- considerable variation in the dynamic response in the studied systems.

coefficients were proposed by (Iwamoto, S. and Wakabayashi, 1985), who considered analytical relations between the damping and other measurable engine parameters.

(Wang, Y. and Lim, 2000)–used a single cylinder powered by an electric motor to estimate absolute damping correctly. They only considered the first two modes of the system to arrive at the absolute damping coefficient as a function of the crank angle.

(Honda, Y. and Saito, 1987)used the transition state matrix methodology to analyze the torsional vibration of six-cylinder diesel engine. They use a rubber TVD to found that the torsional rigidity of the rubber has a dominant influence in the system's characteristics than the engine's internal damping and even TVD damping.

(Maragonis, 1992)The excitation torque is usually considered constant and equal in all cylinders. This holds true only for new engines and considerable variations in the shape of the cylinder's internal pressure curves can be expected during the engine's operational life.

(Boysal and Rahnejat, 1997) shown that crankshaft experiences large number of load cycles subsequent from gas combustion and inertia forces, through its life time. These apply forces on the crankshaft resulting two kinds of cyclic loads on the crankshaft structure i.e. torsional and bending loads. Some systems can existing extreme torsional vibrations at specific engine speeds.

(Kushwaha *et al.*, 2002).Non linearity within the engine arises from multitude of sources which could be traced down to crankshaft elasticity, assembly constraints, journal bearing hydrodynamics and combustion processes.

(Tomoanki Kodama, Katsuhiko Wakabayashi and Yasuhiro Honda, 2001) have made test to find the dynamic characteristics of the viscous friction damper by the method by adopting instantaneous vibration measurement method at two points. The experiment, the vibration shifts of the damper casing and the inertia ring can be simultaneously measured in this method he concluded the dynamic properties of the silicone fluid can be found by changing the clearances between the viscosities of fluid. The torsional vibration amplitudes at damper casing and the Inertia ring are calculated by using the pulse tapes & acrylic casing. Damper optimum internal clearance are decided by experimentation

(Nestorides, 1958) gives the number of formulae to calculate the crankshaft stiffness for different configurations of crankshaft. The various damper design criteria's for moment of inertia of seismic mass, m.i of casing and outward area for heat dissipation are suggested.

(Wilson, 1956) has proposed the methods for calculation of the natural frequency of rotating multiple inertia system. he also gives the phase angle drawing and phase angle vector summation for several arrangements of the engines.

(Wojciech Homik, 2011) described the causes of torsional vibrations in the engine crankshaft. Also proposed the method for damper design for specific application. also proposed that the maximum working temperature of viscous damper is 120 degree C.But the seizing of the viscous damper will happen when the damper surface temperature exceed by 60 deg. C from damper design temperature.

(Malanoski, no date) proposed the method for encounter the torsional vibration problems in practical. He had proposed the method for obtaining the natural frequency in practical circumstance also stated stages to be taken once the natural frequencies are calculated to avoid the resonance condition also The Torsional vibration problem related to the startup motor is discussed.

(Meirelles, 2007).The scope of this paper is the study of the crankshaft torsional vibration phenomenon in internal combustion engines. The analysis formulation, based on state equation solution with system steady state response calculation performed by transition state matrix and the convolution integral. The analysis considers a rubber and a viscous damper assembled to the crankshaft front-end. From the torsional vibrations analysis, it is possible to obtain the dynamic loading on each crankshaft section and these loads can be applied as boundary conditions in a finite element model to predict the safety factor of the component and compare the system behavior with rubber and viscous damping options. By this way, it is possible to emphasize the importance of the torsional vibration's analysis on the structural dimensioning of the crankshafts.

(P. S. Meirelles, D. E. Zampieri, 2007) their study formulation, based on state equation solution with system steady state response calculation completed by transition state matrix and the convolution integral, will be applied to a six-cylinder Diesel engine. The analysis considers a rubber and a viscous damper bring together to the crankshaft front-end. From analysis, it is possible to obtain the dynamic loading on each crankshaft section and these loads can be applied as boundary conditions in a finite element model to predict the safety factor of the component and compare the system behavior with rubber and viscous damping options.

(Meirelles, 2007)Authors has proposed the formulation for torsional vibration analysis of six cylinder diesel engine. Analysis consist of the comparison of outcomes of engine by means of the rubber and viscous damper. Vibration amplitude results compared with measured values for experimental validation.

(Homik W., 2012)presented the sources of several forms of vibrations in multi cylinder engine, particular consideration was focused on torsional oscillation which is severe threat to engine crankshaft. Also presented damping technique, problems of damping efficiency, modification of viscosity, amplitude-frequency characteristics of numerous viscotic dampers

(WLADYSLAW MITIANIEC, no date) author studied torsional vibration analysis of crankshaft in six cylinder inline heavy duty engine taking benefit of the crank train reduction to multi mass model. The outcomes Results of multi mass model compared with FEM results. The error between two methods is not important hence the multi mass model reflects the reality.

CHPTER III

METHODOLOGY

3.1 Introduction

The aim of a torsional analysis is to predict the vibration behavior of the system.so that harmful vibrations do not appear under any operational conditions. A multi-cylinder reciprocating engine contains many reciprocating and rotating parts such as pistons, connecting rod, crankshaft, flywheel, damper and auxiliary drives. The system is so complex that it is difficult to do an exact analysis**.** Crankshaft plays the role of changing the reciprocating mechanism to rotational motion or vice versa Regardless of the number of cylinders in a reciprocating engine, we have 2-stroke and 4- stroke combustion mechanism for firing, which relates the firing torque cycle and rotational speed (ω).It can be modeled as a rotating shaft connected to the inertia disks.

3.2 Engine Crankshaft Modeling Methods

Crankshaft is the main component of internal combustion engine and shaft vibration is the most important factors affecting engine operation. So, crankshaft modeling is the base of crankshaft torsional vibration analysis. There are many shaft models used in modeling torsional vibration:

1. Simple mass - spring model.
2. Continuous mass model.
3. Multi-segment concentrated mass model.
4. Continuous mass model
5. Multisegment concentrated mass model.
6. Soft body dynamics model.

3.2.1 Simple Mass - Spring Model

The simple mass - spring or lumped parameter model is the earliest mechanics model to analysis shaft vibration(Xingyu *et al.*, 2011).

3.3 Equivalent Crankshaft System

number of variables influencing the oscillating torsional system, it is appropriate to replace the real system with a substitutional torsional system – the equivalent system consisting of inertia discs connected by straight shafts. By the reduction it is presumed that [2].Diameter of the substitution connecting shafts is usually set equal to diameter of the main crank journal. Thus, the equivalent crankshaft system should be energetically equal to the original torsional

system.The actual system is characterized by the presence of unpredictable effects such as variable inertia, internal damping, misalignment in the transmission units, uneven firing intervals . The system can then be reduced to a simple system with a series of rigid rotor (representing the inertias) connected by the massless flexible shafts. Simple procedures will be described to reduce reciprocating inertias to equivalent rotating inertias. Simple spring mass model schematic diagram as shown in Figure. 3.1.

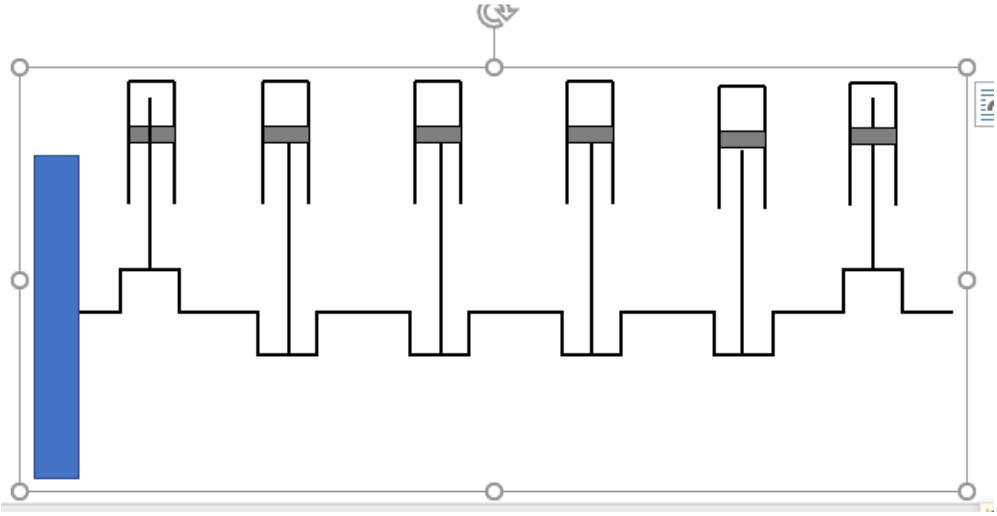

Figure 3-1:A typical reciprocating engine

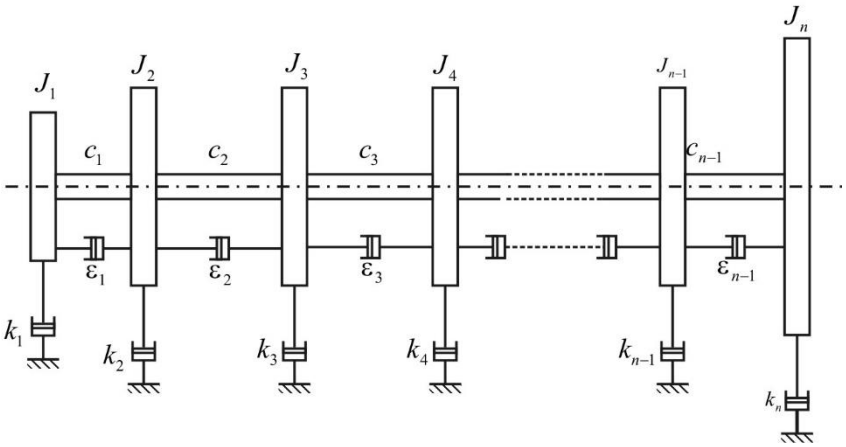

Figure 3-2:An equivalent rotor model with N-disc

3.4 Engine Torsional Modeling

The first step in determining the torsional response is to calculate the natural frequencies of the system, this requires the stiffness and mass inertia of the shaft and components.

3.4.1 **Torsional Stiffness**

Many equations are given in (Wilson, 1968) and (Nestorides, 1958) for calculating the torsional stiffness of a crankshaft. The basic dimensions of the journals, webs, and crankpins are needed, as well as the shear modulus of the shaft material.

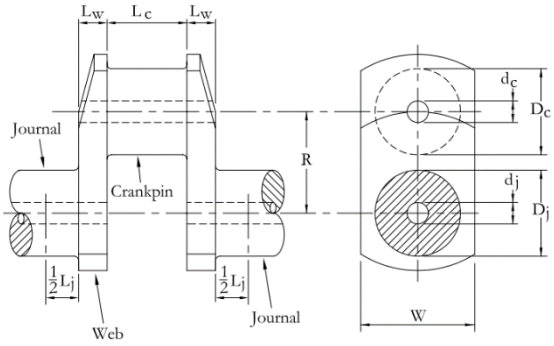

Figure 3-3: Typical Crankshaft Throw

1.Carter's Formula

$$k_t = \frac{G\pi}{32\left[\frac{L_j + 0.8L_w}{D_j^4 - d_j^4} + \frac{L_c}{D_c^4 - d_c^4} + \frac{L_j}{L_w W^3}\right]} \quad 3\text{-}1$$

2.Ker Wilson's Formula

$$k_t = \frac{G\pi}{32\left[\frac{L_j + 0.4L_w}{D_j^4 - d_j^4} + \frac{L_c + 0.4D_c}{D_c^4 - d_c^4} + \frac{R - 0.2(D_j + D_c)_c}{L_w W^3}\right]} \quad \text{.....(3-2)}$$

3.4.2 **Polar Moment Of Inertia Of The Connecting Rod**

The moment of inertia at each crankshaft throw depends on the rotating inertia which is constant, but the inertia of the reciprocating parts varies with crankshaft rotation. The equivalent inertia, J_{eqv}, can be approximated by the relation. Thus, the inertia moment of the masses assumed to be constant i.e. independent of rotation angle. This assumption leads to satisfactory results for small reciprocated machines but it is also still used in conventional TVA calculations of large marine two stroke diesel engines too. A piston-conrod-crank mechanism of the engine Fig.3.4 usually is modelled by an equivalent lumped mass which is assumed to excite the same torsional vibration as the actual complicated crank mechanism.The simplest formula for crank inertia moment I is as follows (Den Hartog, 1985):

$$J_{eqvt} = J_{rot} + 0.5M_{rec}R^2 \quad \text{.....} \quad 3\text{-}3$$

$J_{rot} \equiv$ the moment of inertia of purely rotating parts

$M_{rec} \equiv$ the sum of the mass of the piston and of a part of the connecting rod

R≡crankshaft throw radius

The connecting rod is heavier at the crankpin end and lighter at the reciprocating end. If the weight distribution of the connecting rod is unknown, assume 2/3 of the weight is rotating and 1/3 is reciprocating(Nestorides, 1958). The rotating mass of the connecting rod is multiplied by the throw radius squared and added to the crankshaft rotating inertia to obtain equivalent inertia, Irot. Ieqv,

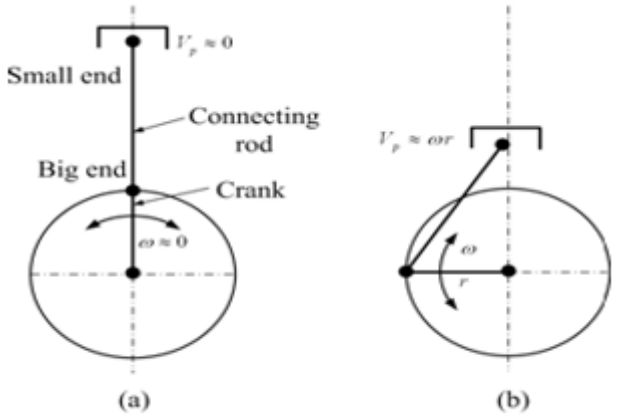

Figure 3-4: (a and b) An equivalent polar moment of inertia of the piston at two positions

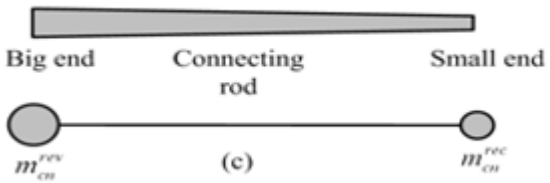

Figure 3-5 dynamically equivalent two-mass system of the connecting rod

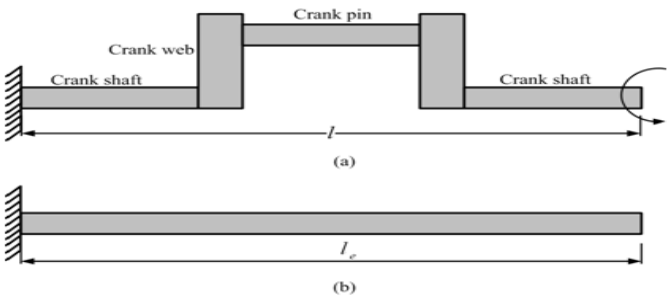

Figure 3-6 (a) Actual crank shaft (b) The equivalent length of the crank shaft

The inertia of connecting rod can be obtained by considering a two-mass equivalent dynamic system with mass one at piston, **mcn rec** and other mass at crank pin, **mcn rev**. With some approximation the mass of the connecting rod ***mcn*** can be considered as two mass one at the piston. From figure 3.6 we can find the total length of the connecting rod.

L = a + c.....(3-4)

$$mcn_{rec} = mcn * {}^{c}\!/_{L} \quad \text{.....(3-5)}$$

$$mcn_{rev} = mcn * {}^{a}\!/_{L} \quad \text{.....(3-6)}$$

where $L \equiv$ Length of the connecting rod[m].

c ≡Distance from the piston pin to the center of gravity of the connecting rod[m].

a ≡Distance from the crank pin to the center of gravity of the connecting rod[m].

$m_{cn} \equiv$ connecting rod total mass [kg].

$m_{rev} \equiv$ mass of revolving part of the connecting rod at crank pin[kg].

mcn $_{rec} \equiv$ connecting rod oscillating mass *at piston pin* [kg].

igure 3-7: Dimensions considered for the division of con rod masses(Akbulut, 2018)

The total connecting rod mass is

$$m_{cn} = mcn_{rec} + m_{rev} \qquad 3\text{-}7$$

The total revolving parts mass

$$M_{rev} = M_{cr} + mcn_{rev} \qquad 3\text{-}8$$

$M_{rev} \equiv$The total revolving parts mass.

$M_{cr} =$ the mass of crank web

$$M_{rec} = M_p + mcn_{rec} \quad 3\text{-}9$$

M_{rec} ≡total oscillating masses [kg]

Mp ≡Piston and pin masses [kg].

$$J_{eqvt} = M_{rev} + 0.5M_{cr}r^2 \quad 3\text{-}10$$

3.4.3 Flywheel Polar Moment of Inertia

The flywheel is a rotating mechanical device that is used to store rotational energy. It has large inertia so that it can help to reduce vibration by smoothing out the power stroke as each cylinder fires. It also can control the speed constant or stay in smooth rate. The flywheel inertia is usually lager than the crank shaft, by comparing different data from different type of engines we assume that it is about 5 times larger than the crankshaft. The most common types of flywheels used in commercial applications are single-mass flywheels, dual-mass flywheels. The following formula used to calculate the moment of inertia of the flywheel.

$$J_f = M_f R^2 \quad 3\text{-}11$$

M_f ≡ the mass of the flywheel is (kg)

R ≡ the radius of gyration (m).

3.5 Torsional Vibration Calculations

for torsional vibration calculation of n-degree-of-freedom system. Let we consider the model on the Fig.1. The equations of motion are possible to obtain by using of Newton equations. In such simple models it is possible to write directly for each mass as shown in equation (12).

3.5.1 Seven Degree Of Freedom System

The method of generalized coordinates system is demonstrated in Figure 3.7.

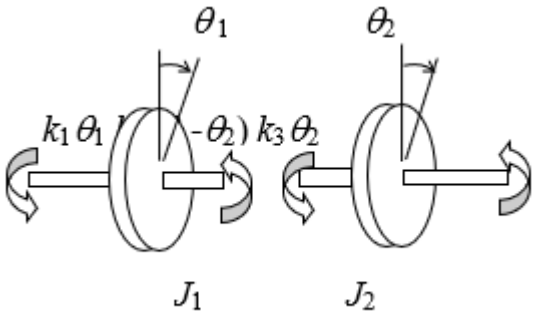

Figure 3-8: A free-body diagram

3.5.2 Equation Of Motion of 8 Degree Of Freedom Derivation

On the basis of the equivalent system, it is possible to create a mathematical model describing the movement of the crankshaft. In order to achieve matching between the dynamic models of the real system and equivalent system, it is necessary to define the parameters of the equivalent system precisely [3]. The mathematical model of the crankshaft motion as a rigid body is given by equation

$$J\ddot{\alpha} = T_g + T_i + T_t + T_k (3$$

where is *J* the reduced mass moment of inertia of the crankshaft, T_g the gas torque, T_i the inertial torque being a result of the crank slider mechanism motion, T_t the friction torque and T_k the load torque .

As you can see, equations involving the non-singular matrix have one and only one solution, but equation involving a singular matrix are more complicated We obtained *n* simultaneous differential equations of second order with constant coefficients.

$$\begin{aligned}
&J_1\ddot{\theta}_1 + k_2(\theta_1 - \theta_2) + C_2(\dot{\theta}_1 - \dot{\theta}_2) = M_1(t)\\
&J_2\ddot{\theta}_2 + k_2(\theta_2 - \theta_3) + k_1(\theta_2 - \theta_1) + C_2(\dot{\theta}_2 - \dot{\theta}_3) + C_1(\dot{\theta}_2 - \dot{\theta}_1) = M_2(t)\\
&J_3\ddot{\theta}_3 + k_3(\theta_3 - \theta_4) + k_2(\theta_3 - \theta_2) + C_3(\dot{\theta}_3 - \dot{\theta}_4) + C_2(\dot{\theta}_3 - \dot{\theta}_2) = M_3(t)\\
&J_4\ddot{\theta}_4 + k_4(\theta_4 - \theta_5) + k_3(\theta_4 - \theta_3) + C_4(\dot{\theta}_4 - \dot{\theta}_5) + C_3(\dot{\theta}_4 - \dot{\theta}_3) = M_4(t)\\
&J_5\ddot{\theta}_5 + k_5(\theta_5 - \theta_6) + k_4(\theta_5 - \theta_4) + C_5(\dot{\theta}_5 - \dot{\theta}_6) + C_4(\dot{\theta}_5 - \dot{\theta}_4) = M_5(t)\\
&J_6\ddot{\theta}_6 + k_6(\theta_6 - \theta_7) + k_5(\theta_6 - \theta_5) + C_6(\dot{\theta}_6 - \dot{\theta}_7) + C_6(\dot{\theta}_6 - \dot{\theta}_5) = M_6(t)\\
&J_7\ddot{\theta}_7 + k_7(\theta_7 - \theta_8) + k_6(\theta_7 - \theta_6) + C_7(\dot{\theta}_7 - \dot{\theta}_8) + C_6(\dot{\theta}_7 - \dot{\theta}_6) = M_7(t)\\
&J_8\ddot{\theta}_8 + k_7(\theta_8 - \theta_7) + C_7(\dot{\theta}_8 - \dot{\theta}_7) = 0
\end{aligned} \qquad 3\text{-}12$$

For simplicity, the eight equations can be combined into one matrix equation form:

$$\text{Mass Matrix}\begin{bmatrix} J_1 & 0 & 0 & \cdot & 0 \\ 0 & J_2 & 0 & \cdot & 0 \\ 0 & 0 & J_3 & \cdot & 0 \\ \cdot & \cdot & \cdot & \cdot & \cdot \\ 0 & 0 & 0 & \cdot & J_n \end{bmatrix} \text{Spring Matrix}\begin{bmatrix} K_1 & -K_2 & 0 & 0 & 0 & 0 \\ -K_2 & K_2+K_3 & -K_3 & 0 & 0 & 0 \\ 0 & -K_3 & K_3+K_4 & -K_4 & 0 & 0 \\ 0 & 0 & -K_4 & K_4+K_5 & -K_5 & 0 \\ 0 & 0 & 0 & -K_5 & K_5+K_6 & K_6 \\ 0 & 0 & 0 & 0 & -K_n & K_n \end{bmatrix}$$

$$\text{Damping Matrix}\begin{bmatrix} C_1 & -C_2 & 0 & 0 & 0 & 0 \\ -C_2 & C_2+C_3 & -C_3 & 0 & 0 & 0 \\ 0 & -C_3 & C_3+C_4 & -C_4 & 0 & 0 \\ 0 & 0 & -C_4 & C_4+C_5 & -C_5 & 0 \\ 0 & 0 & 0 & -C_5 & C_5+C_6 & C_6 \\ 0 & 0 & 0 & 0 & -C_n & C_n \end{bmatrix} = \begin{bmatrix} M_1 \\ M_2 \\ M_3 \\ M_4 \\ M_{N-1} \\ M_N \end{bmatrix} \quad \text{.....(3-13)}$$

When the number of degrees increases the solution is difficult and not providing an easy survey. Therefore we write the set of equation of motion in matrix

$$J\ddot{\theta} + C\ddot{\theta} + K\theta = Mt \qquad (3\text{-}14)$$

where $\ddot{\theta}, \dot{\theta}, \theta$ displacement, velocity, acceleration, respectively. They are expressed by a column matrix $\theta^T = [\theta_1, \theta_2, ..., \theta_n]$. $M^T(t) = [M_1, M_2, ..., M_n]$ is the vector of time depending exciting forces.

[J] represents a diagonal mass matrix

[K] a diagonal stiffness matrix.

[C] a diagonal damping matrix.

3.5.3 Free Vibrations Of MDOF undamped System

Consider the homogeneous form of equation (14) by assuming the Mn = 0 and C= in equation (13) we find

$$J\ddot{\theta} + K\theta = 0 \qquad (3\text{-}15)$$

Seek a solution of the form(we assume the complex harmonic response)

$$\theta = \bar{q}\exp(j\omega t) \qquad (3\text{-}16)$$

The q vector is the generalized coordinate vector.

Note that

$$\dot{\theta} = j\omega\bar{q}\exp(j\omega t) \qquad (3\text{-}17)$$

$$\ddot{\theta} = -\omega^2\bar{q}\exp(j\omega t) \qquad (3\text{-}18)$$

Substitute equations (3.18) and (3.16) into equation (3.15).

$$-\omega^2 J\bar{q}\exp(j\omega t) + K\bar{q}\exp(j\omega t) = 0 \qquad (3\text{-}19)$$

$$\left\{-\omega^2 J q + K q\right\}\exp(j\omega t) = 0 \qquad (3\text{-}20)$$

$$-\omega^2 J q + K q = 0 \qquad (3\text{-}21)$$

$$\left\{ -\omega^2 J + K \right\} q = 0 \qquad (3\text{-}22)$$

$$\left\{ K - \omega^2 J \right\} q = 0 \qquad (3\text{-}23)$$

Equation (23) is an example of a generalized eigenvalue problem. The eigenvalues can be found by setting the determinant equal to zero.

$$\det\left\{ K - \omega^2 J \right\} = \bar{0} \qquad (3\text{-}24)$$

let $\lambda = \omega^2$

$$\det\left\{ K - \lambda J \right\} = 0 \qquad (3\text{-}25)$$

The expansion of the above equation will lead to a polynomial of λ of order *N*. This polynomial equation will have *N* roots, $\lambda_1, \lambda_2, \ldots, \lambda_N$, called *eigenvalues*, which relate to the *natural frequency* of the system by Eq. (3.23).

The natural frequency is a very important characteristic of the systems carrying dynamic loads. It has been found that if a system is excited by a load with a frequency of one of the systems' natural frequencies, the systems can undergo extremely violent vibration, which often leads to catastrophic failure of the structural system. Such a phenomenon is called *resonance*. Therefore, an eigenvalue analysis has to be performed in designing a system that is to be subjected to dynamic loadings.

By substituting an eigenvalue λi back into the eigenvalue equation (23), we have

$$\left\{ K - \lambda J \right\} q = 0 \qquad (3\text{-}26)$$

which is a set of algebraic equations. Solving the above equation for $\boldsymbol{\varphi}$, a vector denoted by q_i can then be obtained. This vector corresponding to the *i*th eigenvalue λ_i is called the *i*-th *eigenvector* that satisfies the following equation:

$$\left\{ K - \lambda_i J \right\} q_i = 0 \qquad (3\text{-}27)$$

An eigenvector q_i corresponds to a *vibration mode* that gives the shape of the vibrating systems of the *i*-th mode. Therefore, analysis of the eigenvalue equation also gives very important information on possible vibration modes experienced by the systems when it undergoes a vibration. Vibration modes of a systems are therefore another important characteristic of the systems. Mathematically, the eigenvectors can be used to construct the displacement fields. It has been found that using a few of the lowest modes can obtain very accurate results for many engineering problems. Modal analysis techniques have been developed to take advantage of these properties.

w=the eigenvalue, is the natural frequency of the system. ,

q=the eigenvector, is the mode shape of the system. also known as modal vectors,

w, tells the frequency of oscillation while q dictates the displacement configuration.

3.6 Campbell diagrams

Provide an excellent overview of the system's torsional vibration situation, analogous to the function provided by critical speed maps in lateral systems. A Campbell diagram should always be generated as soon as the undamped analysis is completed. A representative diagram for a ungeared system is depicted in Figure 3.9. The natural frequencies are plotted as horizontal lines and the operating speed range is designated by vertical lines.

3.7 Forced Vibrations of MDOF Damped System

When we need only one natural frequency, we construct a mechanical simple model like in the Fig.6.1. which represents the properties with enough accuracy. Simpler model enables more easy mathematical calculation and many times gives a sufficient accuracy. If we need to know also the higher natural frequencies, the model must be more complicated.

Usually we design more complicated mechanical model – so called *linear discrete model*. We obtain as many natural frequencies, and as many natural modes as they are degrees of freedom.Computational model for *n*-DOF system.Therefore we write the set of equation of motion in matrix notation

$$J\ddot{\theta}+C\ddot{\theta}+K\theta=Mt \qquad (3\text{-}28)$$

3.8 Torque Variations In A Reciprocating Machinery

There are 3 methods to find the engine torque, needed to obtain the responses of the systems.

1. Measure the torque on an engine by adding a torque sensor at the crankshaft.
2. Obtain the torque data form literature.
3. Use an algorithm to create torque curve.

Measuring the engine torque requires test facilities and an engine which can deactivated cylinders. Measuring torque data for the entire speed and load range is time consuming. Data is also only applicable for similar engines, as the one used during the measurements. Torque data from literature is often not sufficient enough to model the entire engine operating range. Using algorithms makes it possible to change the shape of the torque curve rather easily and is therefore preferred. It also is an easy method to transform into a model. The engine torque is a combination of the gas pressure torque and inertia torque

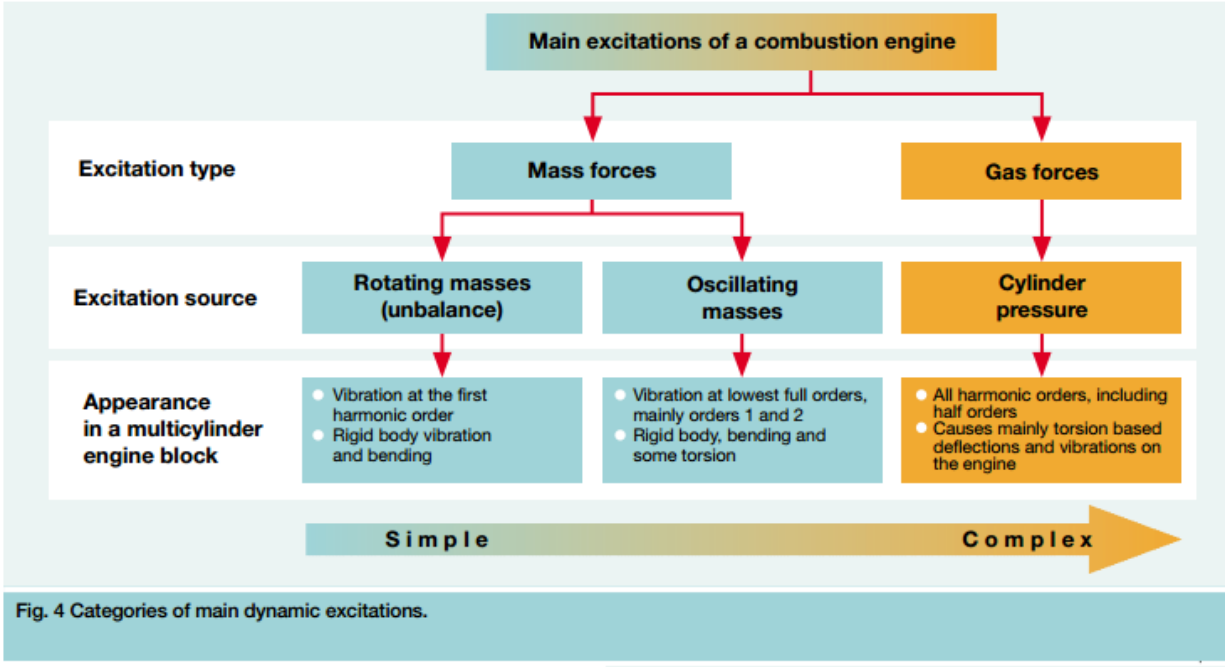

Figure 3-9: Categories of main excitations

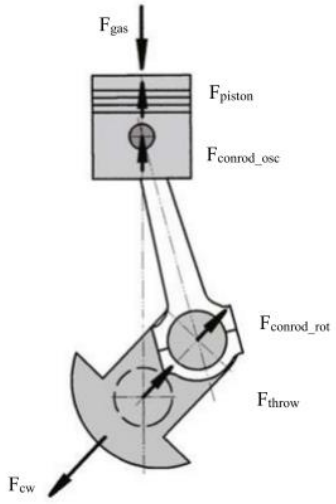

Figure 3-10: Forces acting on crankshaft

3.8.1 Gas Pressure Force

The gas pressure torque is a result of the gas pressure working on top of the piston, incorporating the combustion pressure, compression and gas exchange pressures.

The gas force can be obtained by the equation

$$F_g = \pi \frac{d^2}{4} p \qquad (3\text{-}29)$$

Where

F_g ≡gas force [N]

d ≡ is the piston diameter [m]

p ≡the cylinder pressure [bar]

The gas pressure torque can be modeled by a Fourier algorithm, equation below)

If multiple cylinders are being used equation B.7 can be changed into equation B.8, with αj being the firing distance. For a 4-cylinder 4 stroke engine the firing distance is evenly spaced with an interval of π and a firing order of 1342.

3.8.1.1 *Prediction Of Pressure Inside The Engine Cylinder*

There are many works concerned mainly with prediction of pressure inside the engine cylinder. But the pressure and volume are influenced by engine specifications during variation of crank angle. The pressure and displacement volume are needed to convert as functions of crank angle. (KUO., 1996) and (Colin.R.Ferguson, 2001) proposed the method that can calculate the pressure and volume at any crank angle. The calculations for this subchapter were done with Matlab code. The program code is shown in Appendix A.

3.8.2 Tangential Gas Force

The tangential gas force is computed as

$$F_{tg} = F_g \frac{\sin(\alpha + \beta)}{\cos(\beta)} \qquad (3\text{-}30)$$

sin β = λ sin α

α ≡crankshaft angle (degrees)

β ≡connecting rod angle (degrees)

3.8.3 Inertial Force

The reciprocating parts in an internal combustion engine generate a torque due to constantly acceleration and deceleration of the reciprocating engine masses. The reciprocating engine mass m_{rec} consist of the piston mass *m piston* and roughly one third of the c_{onrod} mass m_{conrod}. Because of the crank c_{onrod} mechanism, the reciprocating masses undergo both a primary and secondary motion, resulting in a odd looking sine wave, see figure B.1.

$$\text{mrec} = \text{m}_{piston} + (1/3)\ \text{m}_{conrod} \qquad (3\text{-}31)$$

The inertia torque *Ti* can be modeled with the Fourier algorithm A periodic function is broken down and expressed in terms of sine and cosine terms. ([4], [22] and [10]) from equation B.2, where R_{crank} represents the crank radius.

The inertial force can be determined as follows

$$F_{ia} = m_a r\omega^2(\cos\alpha + \lambda\cos 2\alpha + \frac{\lambda^3}{4}\cos 4\alpha + \frac{9\lambda^5}{128}\cos 6\alpha\, p \qquad (3\text{-}32)$$

λ = R/L connecting rod to crank radius ratio

3.8.4 Tangential Inertial Force

The tangential inertial force is

$$F_{ta} = F_{ia}\frac{\sin(\alpha+\beta)}{\cos(\beta)} \qquad (3\text{-}33)$$

F_{ta} ≡ tangential oscillating force (N)

F_{ia} oscillating inertial force (N)

3.8.5 Total Tangential Force

$$F_t = F_{tg} + F_{ta} \qquad (3\text{-}34)$$

Where F_t ≡ total tangential force (N)

F_{tg} ≡ tangential gas force(N)

3.8.6 Total torque

$$M_t = F_t.r \qquad (3\text{-}35)$$

M_t ≡ torque (Nm)

Inertia torque for multi cylinder engine with phase angle

$$\det\{K - \lambda J\} = 0 \qquad (3\text{-}36)$$

$$Ti = \frac{1}{2}.M_B R^2\omega^2 \sum_{n=1}^{\infty}\left(\frac{1}{2}.a.\sin(wt-\varphi) - \sin 2(wt-\varphi) - \frac{3}{2}.a.\sin.3(wt-\varphi)\right) \qquad 3\text{-}37$$

Gas torque for multi cylinder engine with phase angle

$$\det\{K - \lambda J\} = 0 \qquad (3\text{-}38)$$

$$Tg = F_g.R\sum_{i=1}^{k}\sin(wt-\varphi)(1 + a.\cos(wt-\varphi) \qquad 3\text{-}39$$

Fourier series

$$T(t) = a_0 + \sum_{k=1}^{\infty} a_k \cos(kwt) + b_k \sin(kwt) \qquad (3\text{-}40)$$

The unknown Fourier coefficients a_0, a_k and b_k can be computed as

$$a_0 = \left(\frac{1}{T}\right)\int_0^T T(t)d\theta \qquad (3\text{-}41)$$

$$a_k = \left(\frac{2}{T}\right)\int_0^T Tt\cos(kwt)d\theta \qquad (3\text{-}42)$$

$$b_k = \left(\frac{2}{T}\right)\int_0^T Tt\sin(kwt)d\theta \qquad (3\text{-}43)$$

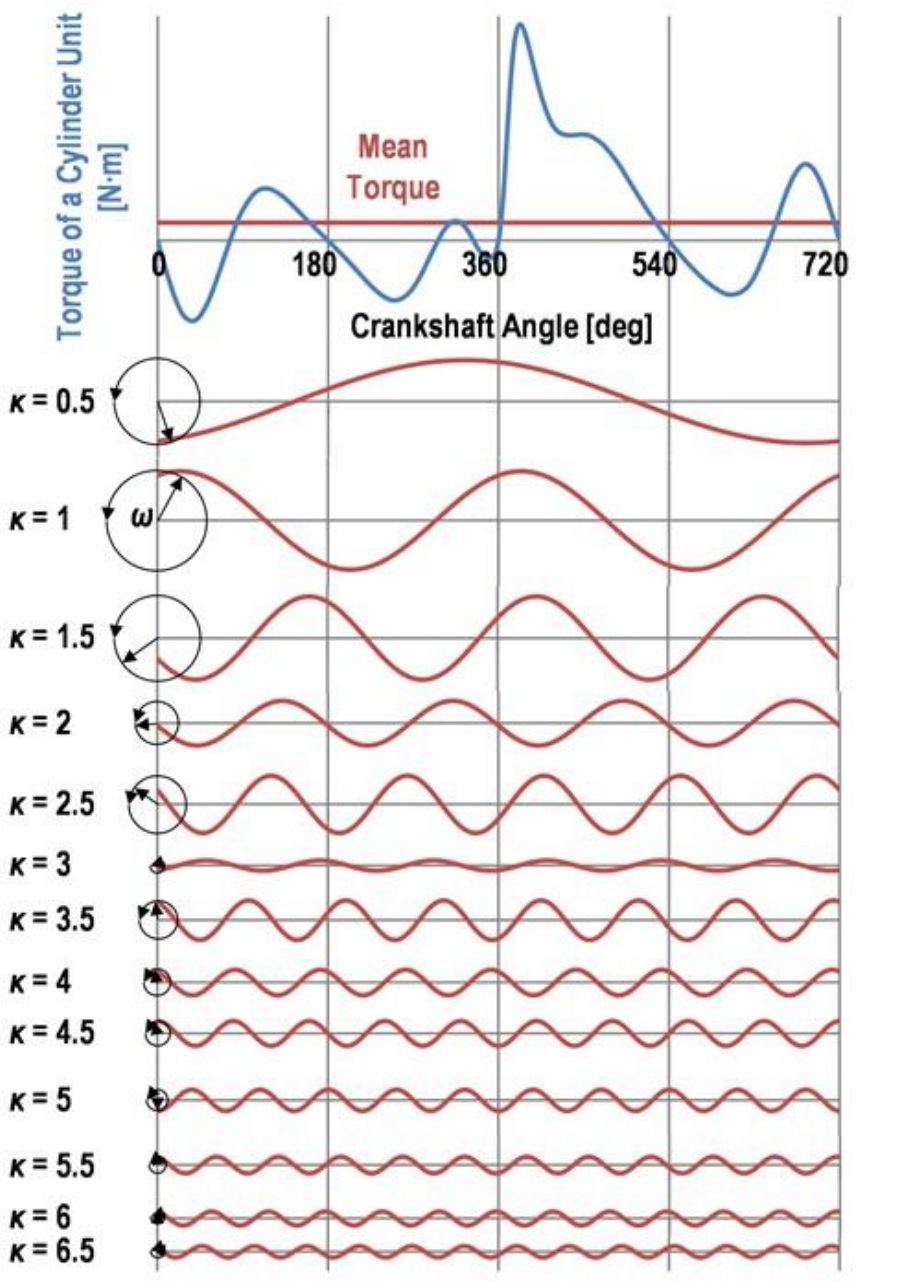

Figure 3-11: Harmonic components analysis of torque of a cylinder unit in time domain

$$\emptyset_1 = 0, \emptyset_2 = \pi, \emptyset_3 = \pi, \emptyset_2 = \pi$$

periodic force can be represented as an infinite sum of harmonic forces using Fourier series.

$$T_g = T_{g0} + \sum_{j=1}^{\infty} a_j \cos(j\theta) + \sum_{j=1}^{\infty} b_j \sin(j\theta) \tag{3-44}$$

$$T_i = \sum_{j=1}^{\infty} c_j \cos(\frac{j\theta}{m}) + \sum_{j=1}^{\infty} d_j \sin(\frac{j\theta}{m}) \tag{3-45}$$

c_j =jth cosine harmonic components du to inertia =0

d_j = sine harmonic components du to inertia which is given

d_j =0 for half order n=j/m=0.5,1.5,2.5,.....

3.9 Undamped Forced Vibration

The majority of structures can be made to resonate, i.e. to vibrate with excessive oscillatory motion. Resonant vibration is mainly caused by an interaction between the inertial and elastic properties of the materials within a structure. Today, modal analysis has become a widespread means of finding the modes of vibration of a machine

3.9.1 General Solution of MDOF

determine natural frequencies(ωi) and mode shapes {x}i from undamped free vibration. (eigen solution)use orthogonality of mode shapes to transform equations of motion into modal space. Solve n single degree of freedom problems. Use mode shapes to transform back to physical space .From the equation 4.10 and put damping coefficient [C] = 0 we obtain the following equation

3.10 Modal Space or Analysis

Original Equations of Motion:

$$[M]\{\ddot{u}\}+[C]\{\dot{u}\}+[K]\{u\}=M_t \qquad (3\text{-}46)$$

Define a new coordinate system

$$\{u\}=[X]\{q\} \qquad (3\text{-}47)$$

Where

$\{\boldsymbol{q}\}$≡ Modal Space principal coordinates (generalized coordinate vector)

[X]≡ Twist Modal Matrix

Substitute into equation of motion

$$[J][X]\{\ddot{q}\}+[C][X]\{\dot{q}\}+[K][X]\{q\}=M_t \qquad (3\text{-}48)$$

Pre-multiply by

$$[X]^T[J][X]\{\ddot{q}\}+[X]^T[C][X]\{\dot{q}\}+[X]^T[K][X]\{q\}=[X]^T M_t \qquad (3\text{-}49)$$

Modal Mass

$$[X]^T[J][X]=[\bar{J}] \qquad (3\text{-}50)$$

Modal Stiffness

$$[X]^T[K][X]=[\bar{K}] \qquad (3\text{-}51)$$

Global Modal Forces

$$[X]^T M_t=\bar{Q} \qquad (3\text{-}52)$$

Proportional or Rayleigh Damping

The damping can often be considered to be of the proportional or Rayleigh type. This exists when the damping matrix is of a form that can be diagonalized by the same real eigenvectors used to diagonalize the mass and stiffness matrices.

if [C] has the form either[C]= a[M] or b [K] then the real transformation that diagonalizes both [M] or [K] will also diagonalize[M] or [K]. Therefore [C] can be made diagonal by the real eigenvectors of the undamped system if it is of the form:

$$[C]=a[K]+b[J] \qquad (3\text{-}53)$$

where a and b are the constants

Modal Damping

$$[X]^T[C][X]=[\bar{C}] \qquad (3\text{-}54)$$

where a and b are any constants.

Then we can write the above equation

If the matrix [C] in Eq. (6.66) is written in the form of Eq. (6.67), the equations, when transformed into normal mode coordinates, become

$$[\bar{J}]\{\ddot{q}\}+[\bar{C}]\{\dot{q}\}+[\bar{K}]\{q\}=0 \qquad (3\text{-}55)$$

and all three matrices are diagonal. If a single equation, say the one representing mode j, is taken from the set, Eq. (6.68):

$$\bar{j}_{ii}\ddot{q}_i+\bar{c}_{ii}\dot{q}_i+\bar{k}_{ii}q_i=0 \qquad (3\text{-}56)$$

then c_{ii} will be given by:

$$\bar{c}_{ii}= a\bar{j}_{ii}+b\bar{k}_{ii} \qquad (3\text{-}57)$$

by using the relationship

$$\bar{k}_{ii} = \bar{j}_{ii}\omega_i^2 \qquad (3\text{-}58)$$

ω_i is the undamped natural frequency of mode i.

the non-dimensional damping coefficient for that mode, ξi , will be

$$\zeta_i = \frac{\bar{c}_{ii}}{2\bar{j}_{ii}\omega_i} = \frac{a}{\omega_i} + \frac{b\omega_i}{2} \qquad (3\text{-}59)$$

the viscous damping coefficient ξi can be made inversely proportional to the mode frequency ξi, or proportional to it, or a combination of these. Since there are only two constants in Eq. (6.71), however, truly proportional damping can only be used to set the damping coefficients for two frequencies, i.e. for two modes. The method described in Section 6.4.3 is therefore more often used in practice.

Response of multi-DOF systems by normal mode summation

We have seen that the equations of motion of a damped system in global coordinates

$$[M]\{\ddot{u}\} + [C]\{\dot{u}\} + [K]\{u\} = M_t \qquad (3\text{-}60)$$

can be transformed into normal mode coordinates using the real eigenvectors of the undamped system, provided that the damping is light, or if not light, of the proportional type, and that this covers the majority of structures, although there are some significant exceptions. The resulting equations, in modal coordinates, are then assumed to be of the form:

$$[\bar{J}]\{\ddot{q}\} + [\bar{C}]\{\dot{q}\} + [\bar{K}]\{q\} = \{Q\} \qquad (3\text{-}61)$$

where $[\bar{J}],[\bar{C}] and [\bar{K}]$ are diagonal, and the whole system consists of n completely separate single-DOF equations, each of which is of the form:

$$\bar{j}_{ii}\ddot{q}_i + \bar{c}_{ii}\dot{q}_i + \bar{k}_{ii}q_i = Q_i (i = 1, 2.....n) \qquad (3\text{-}62)$$

Provided that the system is linear, any of the methods described in Chapters 3 and 4 for finding the response of single-DOF systems can be applied to each of the equations represented by Eq. (6.78), and the results summed to produce the response of the multi-DOF system, a process known as normal mode summation.

This provides a simple, analytic method for finding the response of even quite large multi-DOF systems, to practically any input, and is therefore almost always the first method considered. It is usually found, in larger systems, that it is not necessary to use all n equations, since those having natural frequencies well above any frequencies present in the excitation will not respond, and can be omitted.

Assuming that the response of the multi-DOF system represented in global coordinates by Eq. (6.76), or in modal coordinates by Eq. (6.77), is required, the procedure is as follows:

1.The applied external forces will be known in the form of F f g in Eq. (6.76), i.e. as individual force time histories applied at the nodes or 'grid points' of the global system. These must be converted to modal forces, {Q} , using the original transformation, from global to modal forces, Eq. (6.39):

$$[X]^T M = \bar{Q} \qquad (3\text{-}63)$$

Since the transformation was to normal mode coordinates, [X] will be the modal matrix.

(2) The modal responses $\{q\},\{\dot{q}\}\{\ddot{q}\}$ are calculated from Eq. (6.78). This consists of applying the appropriate modal force to each single-DOF equation in the set represented by Eq. (6.78), using any of the methods discussed in Chapters 2 and 3.

(3) The modal responses $\{q\},\{\dot{q}\}\{\ddot{q}\}$ are converted back to actual responses $\{u\},\{\dot{u}\}\ \{\ddot{u}\}$ as required, in the global system, using the same transformation, in the form of Eq. (6.26), say, that was used to form the modal equations:

$$\{u\} = [X]\{q\} \qquad (3\text{-}64)$$

If global velocity or acceleration responses are required, Eq. (6.26) can be used in differentiated form: $\{\dot{u}\} = [X]\{\dot{q}\}$ and $\{\ddot{u}\} = [X]\{\dot{q}\}$.

The following example illustrates the normal mode summation method applied to a simple 2-DOF system.

The above equation will be solved by applying normal mode analysis method which lead to a new uncoupled equation from inertia [J] and stiffness [K] matrices of the system, the method is based on the orthogonality properties. The method utilizes the mode vectors {ʌ} as modal coordinates as one of the possible solutions for the response of the system among all other possible solutions for equation

Substitute into equation of motion 4.14 in 4.13 and multiplying all the terms by the transpose $[X]^T$ of the mode shape matrix, we have the orthogonality properties can be better visualized as a vector form than matrix form as in equation 4.15. For a given Eth modal vector $\{X_c\}$ and its transpose $\{X_c\}^{\mathrm{T}}$ and natural frequency ω_n we show the vector form in equation bellow. Note that the excitation vector $\{M\}$ is not affected by the sub index c

$$\bar{j}_{ii}\ddot{q}_i + \bar{c}_{ii}\dot{q}_i + \bar{k}_{ii}q_i = T(t) = \sum_{n=1}^{8} X_{nm}M_n \qquad (3\text{-}65)$$

$$[X]^T[J][X]\{\ddot{q}\}+[X]^T[C][X]\{\dot{q}\}+[X]^T[K][X]\{q\}=[X]^T M_t \quad (3\text{-}66)$$

Modal Mass

$$[\tilde{\bar{J}}_i]=[X_i]^T[\bar{J}][X_i] \quad (3\text{-}67)$$

Modal Stiffness

$$[\tilde{\bar{K}}_i]=[X_i]^T[\bar{K}][X_i]=\tilde{\bar{J}}_i\omega^2{}_{fi} \quad (3\text{-}68)$$

Modal Damping

$$[\tilde{\bar{C}}_i]=[X_i]^T[\bar{C}][X_i]=2\tilde{\bar{J}}_i\omega_{fi}\zeta_i \quad (3\text{-}69)$$

ζ_i =damping ratio

$$\tilde{\bar{j}}_i\ddot{q}_i+\tilde{\bar{c}}_i\dot{q}_i+\tilde{\bar{k}}_i q_i=\sum_{n=1}^{8}X_{ni}A_n+\sum_{k}^{30}\left\{\sum_{n=}^{8}X_{ni}.A_{kn}\cos(0.5kwt)+\sum_{n=1}^{8}X_{ni}.B_{kn}\sin(0.5kwt)\right\}$$

(3-70)

$$\tilde{\bar{j}}_i\ddot{q}_i+\tilde{\bar{c}}_i\dot{q}_i+\tilde{\bar{k}}_i q_i=\sum_{n=1}^{8}X_{ni}A_n+\sum_{k=1}^{30}\left[d_{ki}\cos(0.5k\omega t-\delta_{ki})\right] \quad (3\text{-}71)$$

$$\tilde{\bar{j}}_i\ddot{q}_i+\tilde{\bar{c}}_i\dot{q}_i+\tilde{\bar{k}}_i q_i=\sum_{n=1}^{8}X_{ni}A_n+\mathrm{Re}\sum_{k=1}^{30}\left[d_{ki}.e^{(0.5k\omega t-\delta_{ki})\sqrt{-1}}\right] \quad (3\text{-}72)$$

considering the solution of equation

$$q_i=\frac{\sum_{n=1}^{8}A_nX_{ni}}{\bar{k}_i}+\mathrm{Re}\sum_{k=1}^{30}\left[D_{ki}.e^{(0.5k\omega t-\delta_{ki})\sqrt{-1}}\right] \quad (3\text{-}73)$$

By differentiating twice, we find the following

$$\dot{q}_i=\mathrm{Re}\sum_{k=1}^{30}\left[m\frac{k}{2}\omega.D_{ki}.e^{(0.5k\omega t-\delta_{ki})m}\right] \quad (3\text{-}74)$$

$$\ddot{q}_i=\mathrm{Re}\sum_{k=1}^{30}\left[-\frac{k^2}{4}\omega^2.D_{ki}.e^{(0.5k\omega t-\delta_{ki})m}\right] \quad (3\text{-}75)$$

By substitute

$$\mathrm{Re}\sum_{k=1}^{30}\left[-\tilde{\bar{J}}_i\frac{k^2}{4}\omega^2.D_{ki}.e^{(\frac{k}{2}\omega t-\delta_{ki})m}+\tilde{\bar{C}}_i m\frac{k}{2}\omega.D_{ki}.e^{(\frac{k}{2}\omega t-\delta_{ki})m}+\tilde{\bar{K}}_i D_{ki}.e^{(\frac{k}{2}\omega t-\delta_{ki})m}\right]=\sum_{k=1}^{30}\left[d_{ki}.e^{(0.5k\omega t-\delta_{ki})\sqrt{-1}}\right]$$

(3-76)

$$\mathrm{Re}\sum_{k=1}^{30}\left[-\tilde{\bar{J}}_i\frac{k^2}{4}\omega^2.D_{ki}.e^{(\frac{k}{2}\omega t-\delta_{ki})m}+\tilde{\bar{C}}_i m\frac{k}{2}\omega.D_{ki}.e^{(\frac{k}{2}\omega t-\delta_{ki})m}+\tilde{\bar{K}}_i D_{ki}.e^{(\frac{k}{2}\omega t-\delta_{ki})m}\right]=\sum_{k=1}^{30}\left[d_{ki}.e^{(0.5k\omega t-\delta_{ki})\sqrt{-1}}\right]$$

3-77

$$D_{ni} = \frac{d_{ki}.e^{(\frac{k}{2}\omega t-\delta_{ki})m}}{-\tilde{\bar{J}}_i \frac{k^2}{4}\omega^2 + \tilde{\bar{C}}_i m \frac{k}{2}\omega + \tilde{\bar{K}}_i} \qquad (3\text{-}78)$$

replacing D_{ni} and equation 4.23 in equation 4.25:

$$q_{\mathrm{i}} = \frac{\sum_{n=1}^{8} A_n X_{ni}}{\bar{k}_{\mathrm{i}}} + \mathrm{Re}\sum_{k=1}^{30}\left[\frac{d_{ki}.e^{(\frac{k}{2}\omega t-\delta_{ki})m}}{-\tilde{\bar{J}}_i \frac{k^2}{4}\omega^2 + \tilde{\bar{C}}_i m \frac{k}{2}\omega + \tilde{\bar{K}}_i}\right] \qquad (3\text{-}79)$$

since we do not know the damping ratio for the system. The damping ratio could assume different values for the ith mode shape and natural frequency . This uncertain procedure could lead to many possible different responses for the modes and natural frequencies.
Using the Caughey series (Caughey, 1960) in the established 8 by 8 damping matrix [C] and with the second term of equation 4.23:

$$\tilde{\bar{C}}_i = \sum_{d}^{7} a_d \tilde{\bar{J}}_i \omega^{2.d}{}_{fi} = 2\tilde{\bar{J}}_i \omega_{fi} \zeta_i \qquad (3\text{-}80)$$

Expanding the above equation for go, ζ_i , i= 1,,.....,8 we get

$$2\zeta_i = \frac{a_1}{\omega_{fi}} + a_1\omega_{fi} + a_2\omega^3{}_{fi} + a_3\omega^5{}_{fi} + a_4\omega^7{}_{fi} + a_5\omega^9{}_{fi} + a_6\omega^{11}{}_{fi} + a_7\omega^{13}{}_{fi}$$

Replacing equation 4.23 in equation 4.26 and rearranging, we obtain one similar to equation 4.17:

$$q_{\mathrm{i}} = \frac{\sum_{n=1}^{8} A_n X_{ni}}{\bar{k}_{\mathrm{i}}} + \sum_{k}^{30} Z_{ki} H_{ki} \cos(0.5k\omega t - \delta_{ki}) \qquad (3\text{-}81)$$

$$\omega_{\mathrm{fi}} = \sqrt{\frac{\bar{J}_i}{\bar{k}_{\mathrm{i}}}} \qquad (3\text{-}82)$$

$$H_{ki} = \frac{\left(\sum_{n}^{8} X_{ni} A_{kn}\right)^2 + \left(\sum_{n}^{8} X_{ni} B_{kn}\right)^2}{\bar{J}_i \omega_{fi}{}^2} \qquad (3\text{-}83)$$

$$\delta_{ki} = \tan^{-1}\left[\frac{\sum_{n}^{8} X_{ni} B_{kn}}{\sum_{n}^{8} X_{ni} A_{kn}}\right] \qquad (3\text{-}84)$$

$$Z_{ki} = \frac{1}{1-\left(0.5k\frac{\omega}{\omega_{fi}}\right)^2} \qquad (3\text{-}85)$$

This approach is known as a mode superposition method. The simplification is permissible also where damping is not really the Rayleigh damping but is low enough. In such cases we can avoid the need to form a damping matrix based on the physical properties of individual structure elements. It is enough to know mode damping ratios i ζ .

[Any forced dynamic deflection of a structure can be represented as a weighted sum of its mode shapes. Each mode can be described by an Single Degree of Freedom (SDOF) model.

There are mainly two approaches for the study of system vibrations, analytical and experimental. The analytical starts out with knowledge about the structure geometry, boundary conditions and material characteristics (mass, stiffness and damping)](Lundkvist, 2010).

In real applications the engine dynamic twist amplitude does not reach infinity or large values because there is always some damping involved. The damping is introduced in the dynamic magnifier. Based on the research and on the experimental results, we are going to use the dynamic magnifier from equation (3.60) for our 7-DOFS:

$$Z_{ki} = \frac{3.8}{4\sqrt{H_{ki}}} \qquad (3\text{-}86)$$

This infinity or large value for the dynamic twist amplitude happens once among the 30 harmonics for each critical speed W_{nc} When the critical speed is replaced in equation 4.18, we have the dynamic magnifier W independent from its natural frequency

$$Z_{ki} = \frac{1}{1-\left(\frac{k}{s}\right)^2} \qquad (3\text{-}87)$$

CHAPTER IV RESULT AND DUSCUTIONS

4.1 Introduction

In this section torsional vibration analysis as per (Gawande *et al.*, 2010)(Nestorides, 1958) for given operating six cylinder diesel engine is carried out in details. Data required for analysis is collected from the company from available experimental set up. The following Information pertains to the four strokes, six-cylinder diesel engine.

Table 4-1: Six-Cylinder Diesel Engine Data

Engine Mass-Elastic System									
Mass		pulley	cylinder						Flywheel
			1	2	3	4	5	6	
Inertia	Kg-m^2*E6	0.09	18.64	18.64	18.64	18.64	18.64	18.64	19.21
Stiffness	MNm/rad	-	19.21	19.21	19.21	19.21	19.21	19.21	2655

Table 4-2 Engine basic data

Engine basic data	
Engine type	Deisel engine Inline six cylinder four stroke
Number of cylinder	6
Firing order	1-5-3-6-4-2
piston diameter	d = 76 mm
journal or crank radius	R0 = 35 mm
connecting rod length	L = 123 mm
total piston mass	*Mp = 0.363 kg*
total connecting rod mass	*MC = 0.096 kg*

4.2 NATURAL FREQUENCIES AND MODE SHAPES

There is a mode shape or a modal vector associated with a natural frequency. The method to compute the natural frequencies and the mode shapes is discussed in section 3.3.5. Free Vibrations of MDOF undamped System. Computation of the natural frequencies and the mode shapes is carried out by MATLAB Code see appendix B the result of calculated natural frequencies values in Table 4-3. Normal modes shapes are given in Table 4-3. And Figure 3. for the given engine to analyze the minor and major critical harmonic orders in torsional vibration analysis. It is seen that the sixth orders are the major critical orders of excitation. The corresponding critical speeds of engine operation are multiplication of fundamental frequency rpm Since the sixth order excitation of 3-node vibration mode falls within the operating range of 750 to 2200 rpm, hence the forced vibration analysis is required for this excitation frequency only.

Computation of the natural frequencies and mode shapes is performed by solving an eigenvalue problem. we solve for the eigenvalues (natural frequencies) and eigenvectors (mode shapes). Because damping is neglected in the analysis, the eigenvalues are real numbers. (The inclusion of damping makes the eigenvalues complex numbers. The solution for undamped natural frequencies and mode shapes is called real eigenvalue analysis or normal modes analysis.

Reasons to Compute Normal Modes

There are many reasons to compute the natural frequencies and mode shapes of a structure. One reason is to assess the dynamic interaction between a component and its supporting structure.

The results of the eigenvalue analysis-the natural frequencies and mode shapes-can be used in modal frequency and modal transient response analyses.

The results of the dynamic analyses are sometimes compared to the physical test results. A normal modes analysis can be used to guide the experiment. In the pretest planning stages, a normal mode analysis can be used to indicate the best location for the accelerometers. After the test, a normal modes analysis can be used as a means to correlate the test results to the analysis results.

Design changes can also be evaluated by using natural frequencies and normal modes. Does a particular design modification cause an increase in dynamic response? Normal modes analysis can often provide an indication.The physical importance of the harmonic form of the solution means that all the degrees-of-freedom of the vibrating systems move in a synchronous manner. The structural configuration does not change its basic shape during motion; only its amplitude changes.

Table 4-4 calculated natural frequencies results

rpm	2602.0	2435.1	1987.0	1529.0	993.4	390.7	0.0000

4.3 Interpretation of the Results

Once the natural frequencies are obtained from the above explained approaches, it is necessary to interpret the result and determine whether the driveline is safe from torsional resonance point of view. To avoid the torsional resonance, we must have a natural frequency of the system such that it shifts the resonance condition outside the engine operating speed. Once the natural frequencies are obtained from the above explained approaches, it is necessary to interpret the result and determine whether the engines is safe from torsional resonance point of view. This decision is arrived at based on following:

Table 4-5 Mode shape data for 7-DOFM data

Mode 1	Mode 2	Mode 3	Mode 4	Mode 5	Mode 6	Mode 7
1	1.00000	1.00000	1.00000	1.00000	1.00000	1.00000
1	-0.2476821	0.51882	- 0.24768	-1.19468	-2.10567	-2.76150
1	-1.1863357	-0.21201	-1.18634	- 0.76742	1.32819	3.86439
1	-0.6448196	0.84082	-0.64482	1.34408	0.63713	-4.04564
1	0.7012263	- 1.06505	0.70123	0.50576	- 2.03265	3.26202
1	1.1723647	-0.77679	1.17236	-1.44254	1.61032	-1.70041
1	-0.0055797	0.00966	-0.00558	0.00389	- 0.00307	0.00268

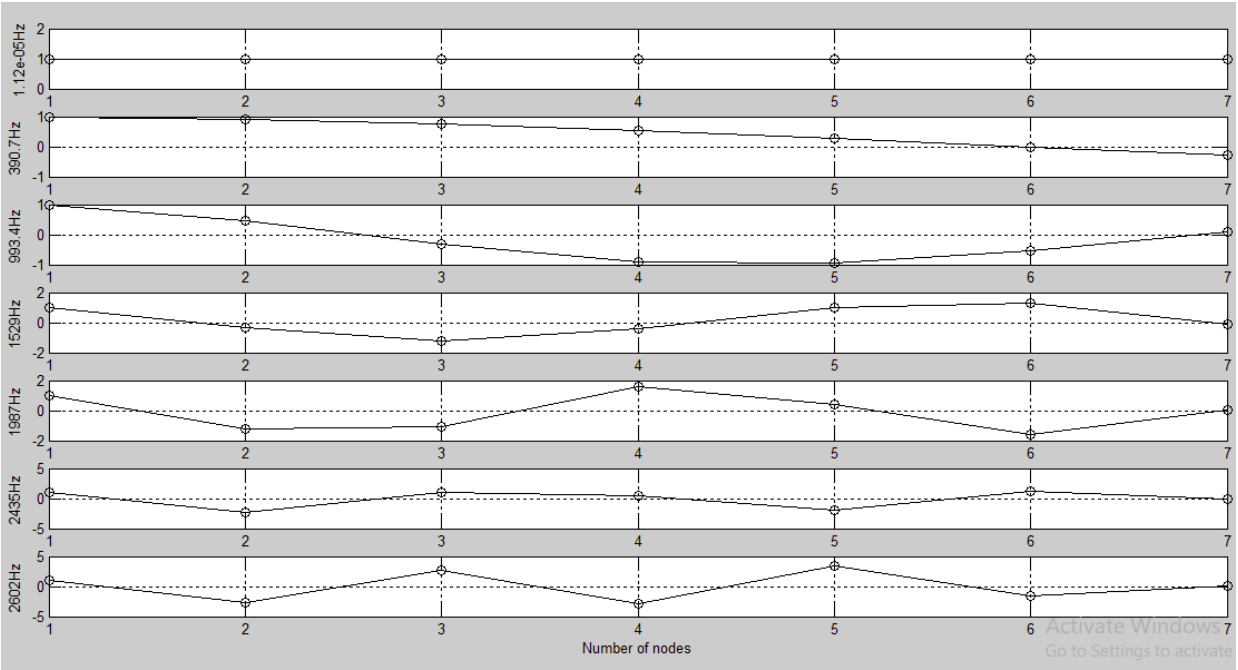

Figure 4-1:Mode Shapes

Fig. 4-1 the first mode or natural frequency contains one loop and one node. The second mode contains two loops and two nodes. The third mode contains three loops and three nodes. This pattern is repeatable at higher modes.

This elastic system has one or more modes of normal free vibration. These modes of normal vibration are distinguished by the number of nodes associated with each, nodes being points which, with respect to any particular vibration, have no motion. We may have 1 noded normal vibration, 2 noded, 8 noded, etc. In general only the first two or three forms are of practical importance. Associated with each of these normal modes of vibration is a natural frequency; the greater the number cf nodes the higher the natural frequency.

4.4 Numerical Analysis

The numerical analysis of equation 3.54 when t= 0. Note that t=0(the engine is already running),and t=0 is a selected instant to visualize the behavior of the engine for study. See Appendix D for MATLAB program.

The total engine twist amplitude $\boldsymbol{q}$ is composed of the engine static and dynamic twist. In this study, the static twist is neglected. dynamic magnifier Z_{ki}; and the critical speeds of the engine ω_c.

If we denote the above solution of system's natural frequencies and associated modes are Clearly, there are many modes of vibration: mode one ($\varphi 1$) represents rigid body mode where the centres of masses have no relative displacements, and fair enough to mention that this is of no importance; modees [X_2, X_3, X_4, X_5, X_6, X_7] represents the case where vibration amplitude is inversely proportional to inertia but opposite in phase.. Also, the point in the shaft where essentially no twisting occurs is called the node, and there is only one node or many associated with the fundamental mode. The graphical representation of mode shapes can be represented as shown in Fig. 4.3.

Table 4-6 natural frequencies

No / units	rad/s	Hz	rpm	3 order(rpm)
1	2148.6	341.9681	20517.63	6839.209
2	1959.6	311.8786	18712.81	6237.603
3	1656.8	263.6808	15821.28	5273.76
4	1257.8	200.1881	12011.11	4003.703
5	786.2	125.1336	7507.66	2502.553
6	271.7	43.245	2494.545	864.8483
7	0	0	0	0

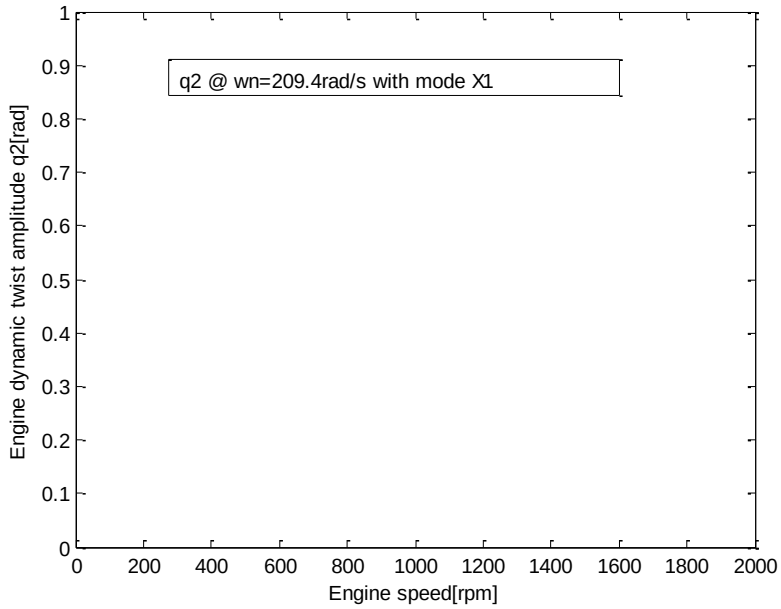

Figure 4-2: Engine dynamic twist amplitude q2 vs engine speed @ wn2=264.2 rad/s and mode {X1}.

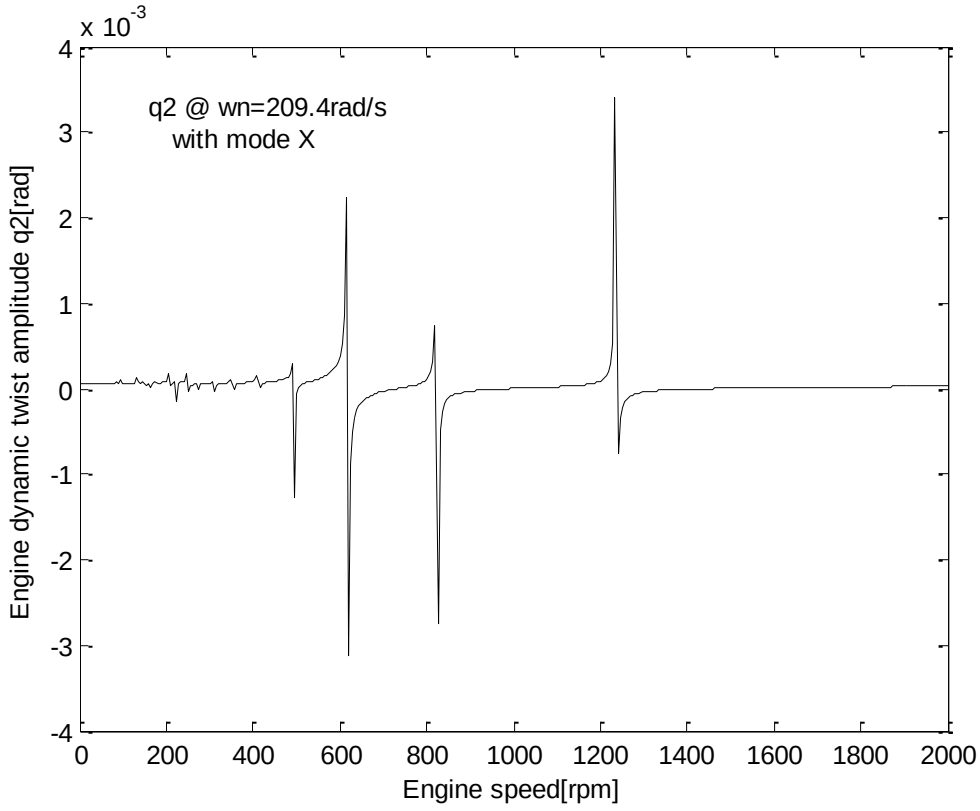

Figure 4-3 : Engine dynamic twist amplitude q2 vs engine speed ω @ wn2=264.2 rad/s and mode {X2}.

Figure 4.2 shows the plot of equation 3.54, the engine dynamic twist amplitude q_2 vs engine speed ω for its natural speed ω_{fi} = 264.2 rad / s and mode {X_2}. The 30 peaks shown in figure 4.1 correspond to the case when the dynamic magnifier M tends to infinity. This tendency happens when the engine speed ω passes by the critical speed $\omega_c = \omega_{fi}$ where s = 1, 2, 3...30. This critical speed ω_{c-1} is at the natural speed of the engine = ω_{fi}. Some of the critical speeds for ω_{fi} = 264.2 rad/ s are shown in table 4.2.

Table 4-7. Some of the critical speeds for natural speed of the engine ω_{fi} = 264.2 rad/ s

Order number	1	5	10	15	20	25	30
Critical speed rad/s	528.3	105.7	52.8	35.2	26.4	21.1	17.6

Figure 4.3 shows the plot of equation 4.17, the engine dynamic twist amplitude q_3 vs engine speed ω for its natural speed = 767.5 rad / s and mode {X3}. The 30 peaks shown in figure 4.13 correspond also when the dynamic magnifier Mic tends to infinity. Some of the critical speeds

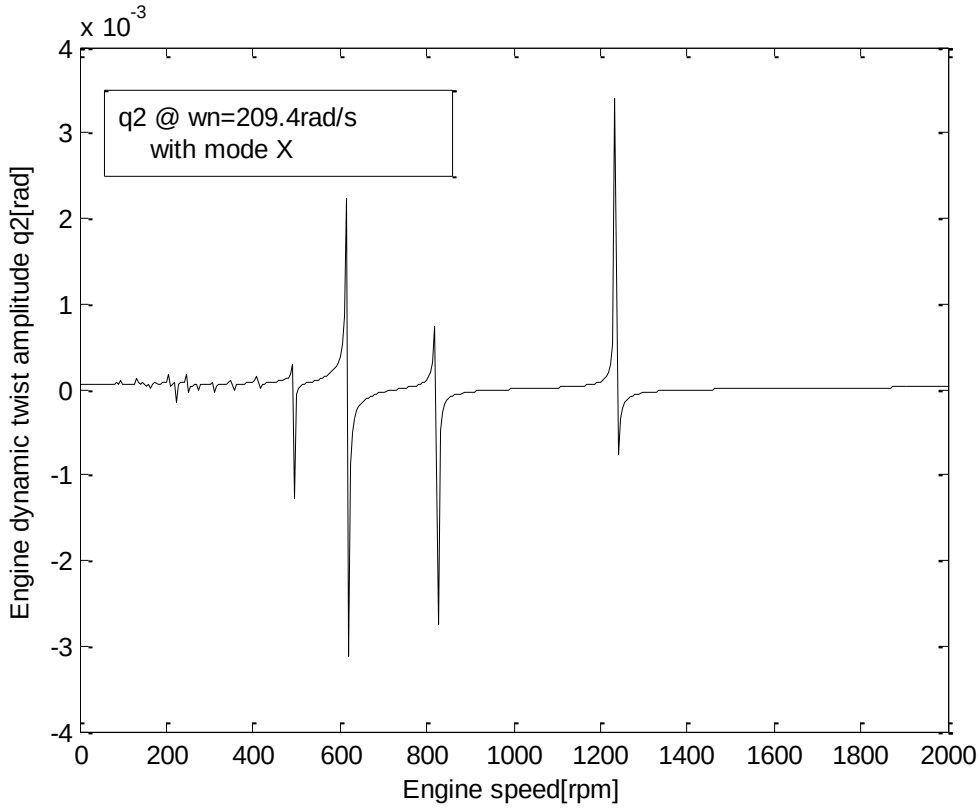

Figure 4-4Engine dynamic twist amplitude q2 vs engine speed Ω @ wn2=264.2 rad/s and mode {X3}.

Table 4-8 Some of the critical speeds for natural speed of the engine Ωc3= 767.2 rad/ s

Order number	1	5	10	15	20	25	30
Critical speed rad/s	1535	307	153.5	35.2	76.8	61.4	51.2

Figure 4.4 shows the plot of equation 4.17, the engine dynamic twist amplitude $\mathbf{q}_4$ vs Q engine speed for its natural speed wn,4= 1235.9 rad/ s and mode $\{X_4\}$. The 30 peaks shown in figure 4.4 correspond to the case when the dynamic magnifier Mis tends to infinity. Some of the critical speeds for Qn,,= 1235.9 rad/s

Table 4-9 Some of the critical speeds for natural speed of the engine Ωc3= 1235.9 rad/ s

N of order	1	5	10	15	20	25	30
Critical speed rad/s	2471.8	494.4	247.2	164.8	123.6	89.9	82.4

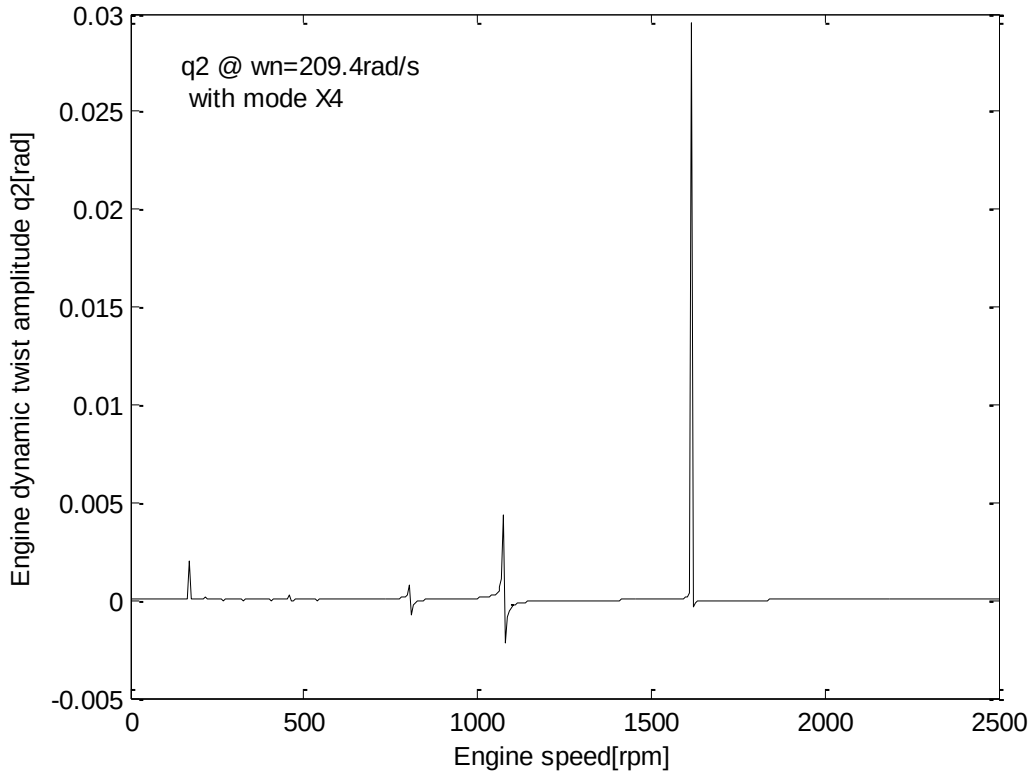

Figure 4-5: Engine dynamic twist amplitude vs engine speed for a 7-DOFS its for natural frequency w=2545 rad/s and X4

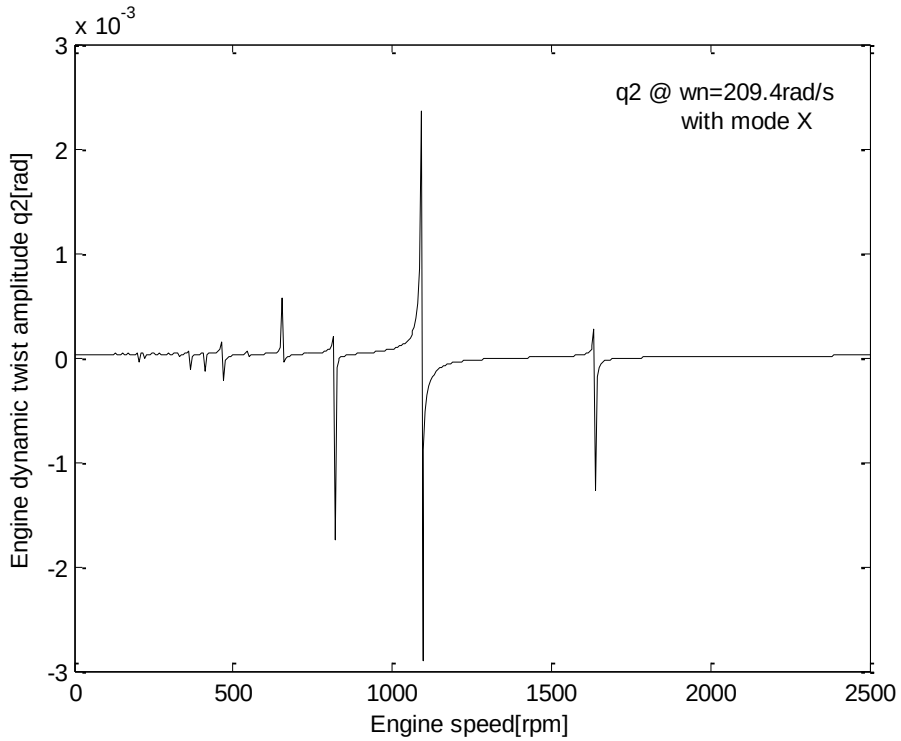

Figure 4-6: Engine dynamic twist amplitude q2 vs engine speed @ wn2=264.2 rad/s and mode {X5}.

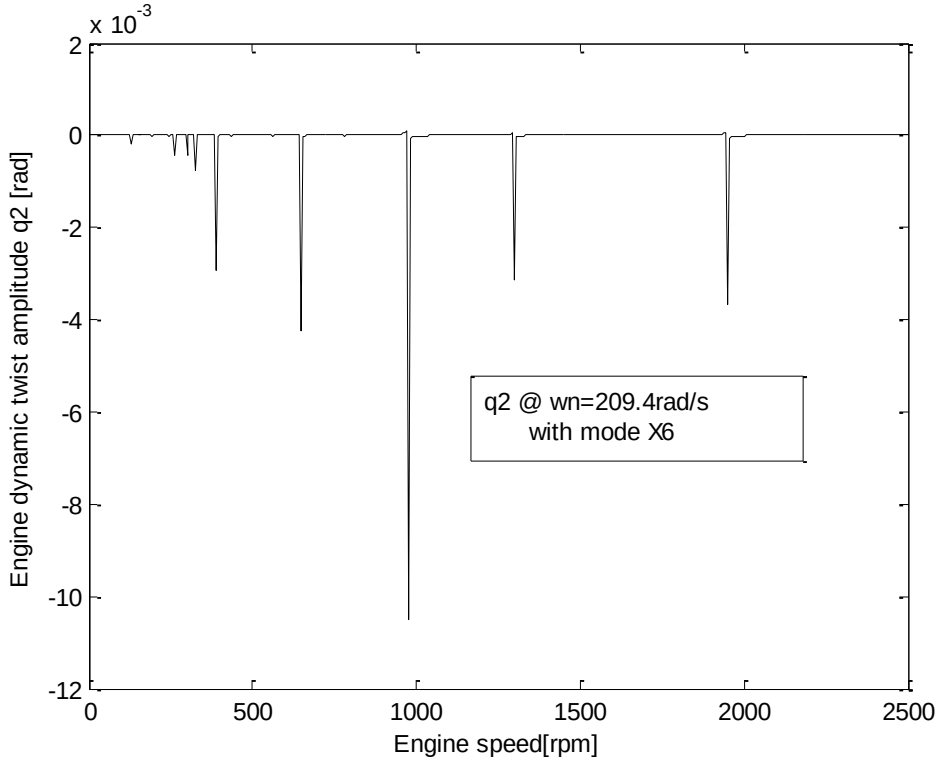

Figure 4-7: Engine dynamic twist amplitude q2 vs engine speed @ wn2=264.2 rad/s and mode {X6}.

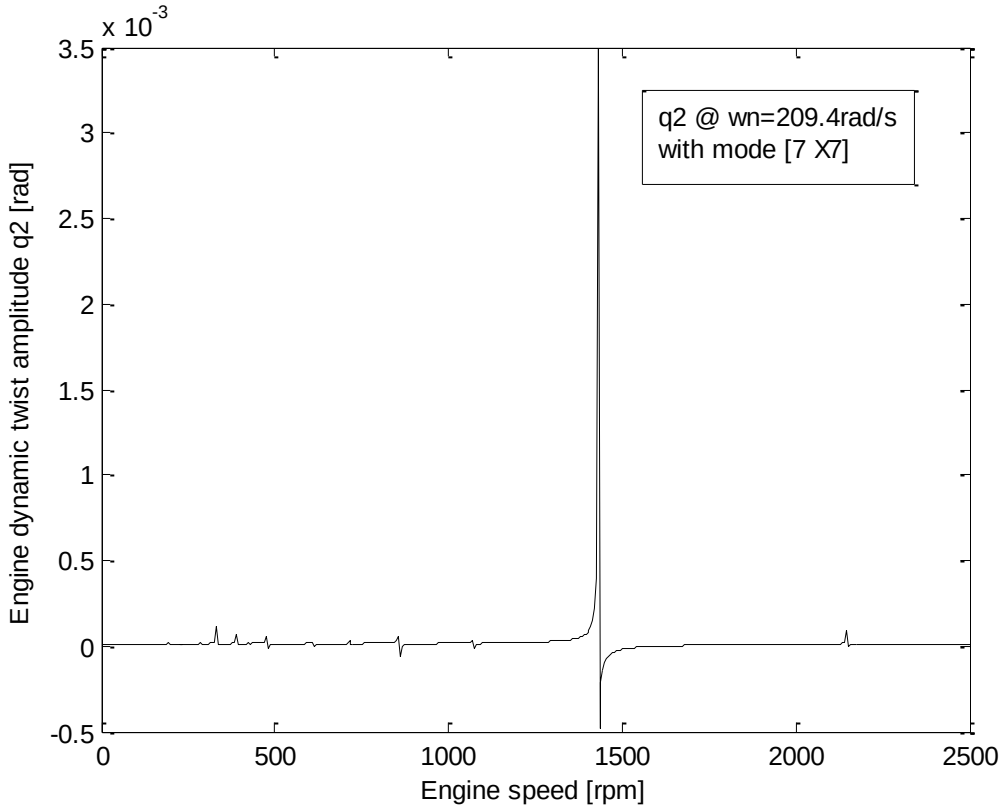

Figure 4-8: Engine dynamic twist amplitude q2 vs engine speed @ wn2=264.2 rad/s and mode {X7}.

4.5 Vibration Calculation For 8-DOFS With Damping

The 8-DOFS in this section is the 7-DOFS from section 4.4.1 with the addition of the damping device at the opposite end of the flywheel. For the damping matrix, we use the proportional damping

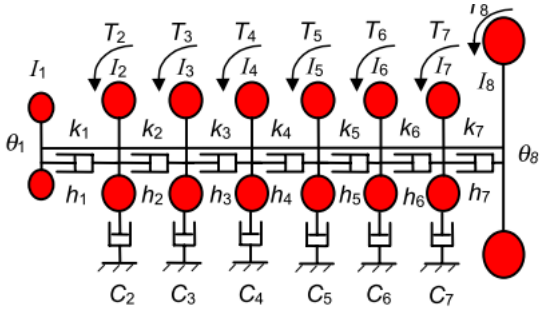

Figure 4-9: 8-DOFS equivalent system showing moments of inertia, damping and stiffness Engine(Li Jianqiu, 2000)

$$\begin{bmatrix} M_1 \\ M_2 \\ M_3 \\ M_4 \\ M_{N-1} \\ M_N \end{bmatrix} = \begin{bmatrix} 0 \\ M_1 \\ M_2 \\ M_3 \\ M_4 \\ M_5 \\ M_6 \\ M_7 \\ 0 \end{bmatrix} = \begin{matrix} 0 \\ M_2 = A_2 + \sum_{k=1}^{30} a_{k2}\cos(kwt) + b_{k2}\sin(kwt) \\ M_3 = A_3 + \sum_{k=1}^{30} A_{k3}\cos(kwt) + B_{k3}\sin(kwt) \\ M_4 = A_4 + \sum_{k=2}^{30} A_{k4}\cos(kwt) + B_{k4}\sin(kwt) \\ M_5 = A_5 + \sum_{k=2}^{30} A_{k5}\cos(kwt) + B_{k5}\sin(kwt) \\ M_6 = A_6 + \sum_{k=2}^{30} A_{k6}\cos(kwt) + B_{k6}\sin(kwt) \\ M_7 = A_7 + \sum_{k=2}^{30} A_{k7}\cos(kwt) + B_{k7}\sin(kwt) \\ 0 \end{matrix}$$

Table 4-10calculated natural frequencies results

0	135.05	286.43	1238.70	773.29	1640.55	1950.49

Table 4-11Mode shape data for 8-DOFM data

Mode 1	**Mode 2**	**Mode 3**	**Mode 4**	**Mode 5**	**Mode 6**	**Mode 7**	**Mode 8**
1	1.0000	1.0000	1.0000	1.0000	1.0000	1.0000	1.0000
1	0.1597	- 2.7801	- 26.5517	- 69.6973	- 123.0073	-174.2892	- 211.2064
1	0.1353	-2.6926	-14.3038	15.8060	144.1677	362.7336	577.7996
1	0.1089	2.4248	4.9307	81.4993	94.4038	-227.4499	-806.8768
1	0.0809	1.9945	21.7568	450475	-1628978$	-1108254	8439178
1	0.0516	1.4305	27.9561	- 47.8633	- 062.0841	350.1927	- 680.1068
1	0.0217	0.7706	20.5005	- 80.7860	175.2156	- 277.0242	354.4308
1	-0.0142	0.0745	-0.2511	0.3827	0.4723	0.5278	-0.5576

4.6 Forced Vibration {M}=0

To solve the generalized equation 4.10, we continue with the modal coordinate's method. After replacing the modal coordinate vector, equation 4.14, and multiplying the whole equation by the transpose $[X]^T$ of the mode shape matrix

$$\bar{j}_{ii}\ddot{q}_i + \bar{c}_{ii}\dot{q}_i + \bar{k}_{ii}q_i = \sum_{n=1}^{8} X_{nm}M_n \quad \text{.....(4-1)}$$

$$\bar{j}_i\ddot{q}_i + \bar{c}_i\dot{q}_i + \bar{k}_i q_i = \sum_{n=1}^{8} X_{ni}\left[A_n + \sum_{k=1}^{30}\left\{A_{kn}\cos(0.5kwt) + B_{kn}\sin(0.5kwt)\right\}\right] \quad \text{.....(4-2)}$$

Replacing equation 3.40 on the right end of the above equation, we have

The orthogonality properties can be applied in equation 4.3 for the cth modal vector {X5}, its transpose $\{X\}^T$ and natural frequency w. Note that the excitation vector {T5} is not affected by the sub index i.

The orthogonality property can also be applied to damping matrix [55] as it was »\4 f\-I applied to the stiffness [K5] and inertia [J5] matrices; in other words, the damping matrix is proportional to the stiffness and inertia matrices:

$$\text{Diag}=[\,2\tilde{\bar{J}}_1\omega_{f1}\zeta_1;\ 2\tilde{\bar{J}}_2\omega_{f2}\zeta_2\ ;\ 2\tilde{\bar{J}}_3\omega_{f3}\zeta_3\ ;2\tilde{\bar{J}}_4\omega_{f4}\zeta_4;\ 2\tilde{\bar{J}}_5\omega_{f5}\zeta_5\ \ 2\tilde{\bar{J}}_6\omega_{f6}\zeta_6\ \ 2\tilde{\bar{J}}_7\omega_{f7}\zeta_7\,]4\text{-}3$$

$$q_i = \frac{\sum_{n=1}^{8} A_n X_{ni}}{\bar{k}_i} + \sum_{k=1}^{30}\left[\frac{1}{\bar{J}_i\left[\omega_f{}^2 - (0.5k\omega)^2\right]}\left\{\sum_n^8 X_{ni}A_{kn}\cos(0.5k\omega t) + \sum_n^8 X_{ni}B_{kn}\sin(0.5k\omega t)\right\}\right] \quad (4\text{-}4)$$

$$q_i = \frac{\sum_{n=1}^{8} A_n X_{ni}}{\bar{k}_i} + \mathrm{Re}\sum_k^{30}\bar{Z}_{ki}\bar{H}_{ki}e^{(\frac{k}{2}\omega t - \delta_{ki})m} \quad \text{.....(4-5)}$$

$$\omega_{fi} = \sqrt{\frac{\tilde{\bar{J}}_i}{\tilde{\bar{k}}_i}} \quad \text{.....(4-6)}$$

$$\bar{H}_{ki} = \frac{\left(\sum_{n=1}^{8} X_{ni}A_{kn}\right)^2 + \left(\sum_{n=1}^{8} X_{ni}B_{kn}\right)^2}{\tilde{\bar{J}}_i\omega_{fi}{}^2} \quad \text{.....(4-7)}$$

$$\bar{\delta}_{ki} = \tan^{-1}\left[\frac{\sum_{n=1}^{8} X_{ni}B_{kn}}{\sum_{n=1}^{8} X_{ni}A_{kn}}\right] \quad \text{.....(4-8)}$$

$$\bar{Z}_{ki} = \frac{1}{\left[k\zeta_i \frac{\omega}{\omega_{fi}}\right]m + \left[1-\left(\frac{k}{2}\frac{\omega}{\omega_{fi}}\right)^2\right]} \quad \text{.....(4-9)}$$

4.6.1 **Numerical Analysis**

Numerical evaluation of the components of equation 4.4 when t= 0 .note that r=0 is not the time when the engine starts running. The engine is already running and t=0 is a selected instant to visualize the behavior of the engine for study. Also note the similarity of equations 4.9 and 4.29. See appendix C for the corresponding Matlab program. The total engine twist amplitude $\mathbf{q}_i$ is composed of the engine static and dynamic twist and in this study the static twist is not concidered. We focus our study on the dynamic twist: dynamic magnifier Mjc ,and the critical speeds of the engine ωc

Figure 1.6 shows the plot of equation 4.4, showing the engine dynamic twist amplitude q_2 (real) vs **ω** engine speed for its natural speed **ωfi**= 135.1 rad/s and mode $\{X_2\}$. There are 30 peaks in figure 1.6 corresponding to the dynamic magnifier $\bar{Z}_{ki}$ tending to infinity when the damping ratio ζ_i = 0. This happens when the engine speed **ω** passes the critical speed = **ωc**= ,where S =1,2, 3...28, 29, 30. This critical speed **ω**c =2***ω**fi/S is excited by the natural speed of the engine **ω**, Some of the critical speeds for **ωc** are

ωc	1	2	3	5	10	15	28	29	30
rad/s	129.6	270.2	54.0	27.0	18.0	13.5	10.8	9.0	7.0

The engine dynamic twist amplitude $\boldsymbol{q_2}$ (real+imaginary) vs engine speed ω for its natural speed ω_{f2} = 135.1 rad/s a nd mode $\{X_2\}$ is also plotted in the same figure 4.21. Note that the peaks for each critical speed have approximately the same dynamic twist amplitude for $\boldsymbol{q_2}$ (real) and $\boldsymbol{q_2}$ (real+imaginary).

The effect of damping ratio = 0.01 on the systems

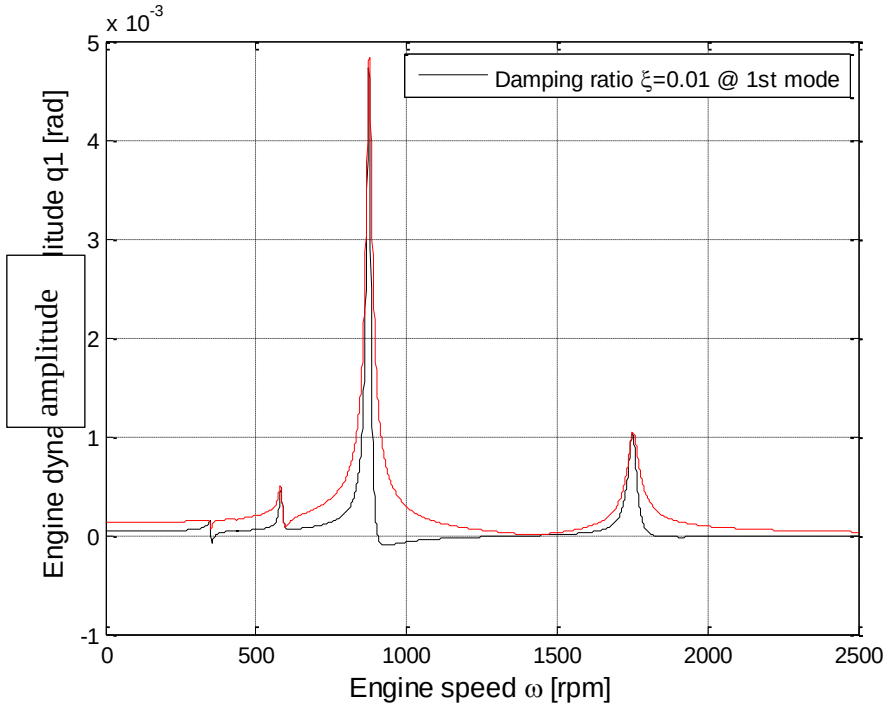

Figure 4-10 : Engine dynamic twist amplitude for an 8-DOFS (real and imganiary) damping ratio=0.01

Damping ratio 0.02

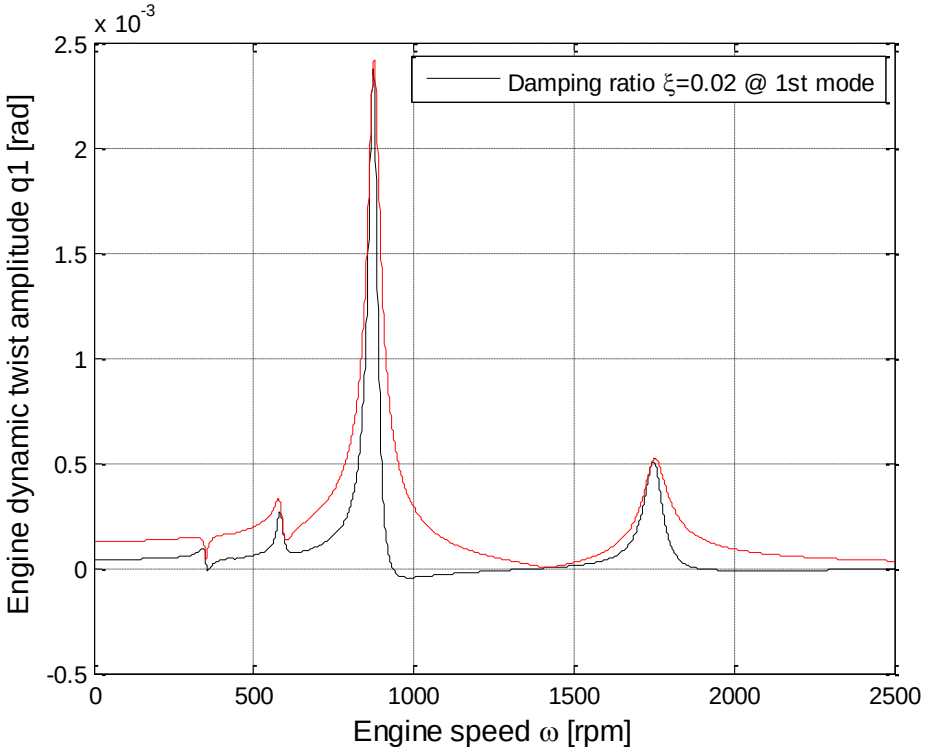

Figure 4-11:Engine dynamic twist amplitude for an 8-DOFS (real and imganiary) damping ratio=0.02

Damping ratio 0.03

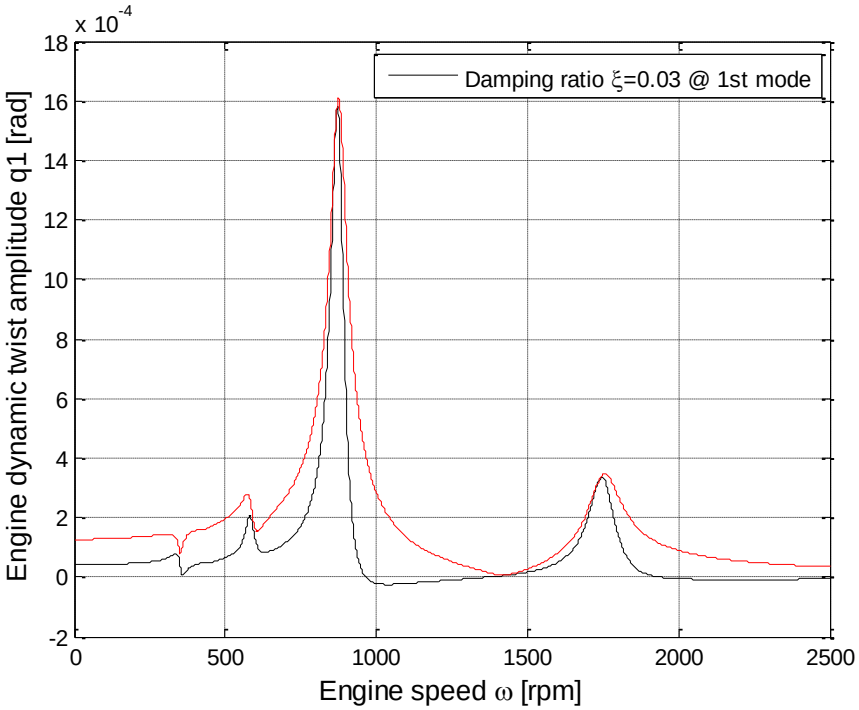

Figure 4-12 : Engine dynamic twist amplitude for an 8-DOFS (real and imganiary) damping ratio=0.03

Damping ratio =0.04

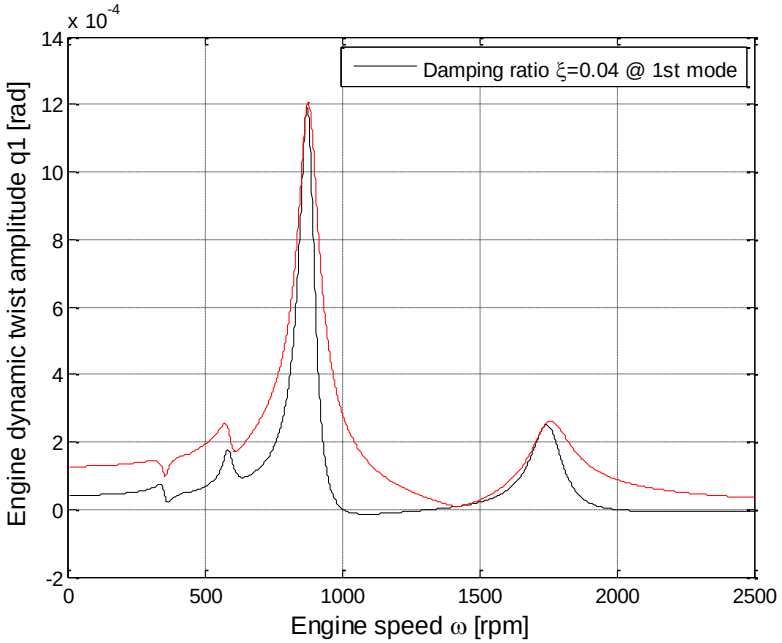

Figure 4-13Engine dynamic twist amplitude for an 8-DOFS (real and imganiary) damping ratio=0.04

Damping ratio =0.05

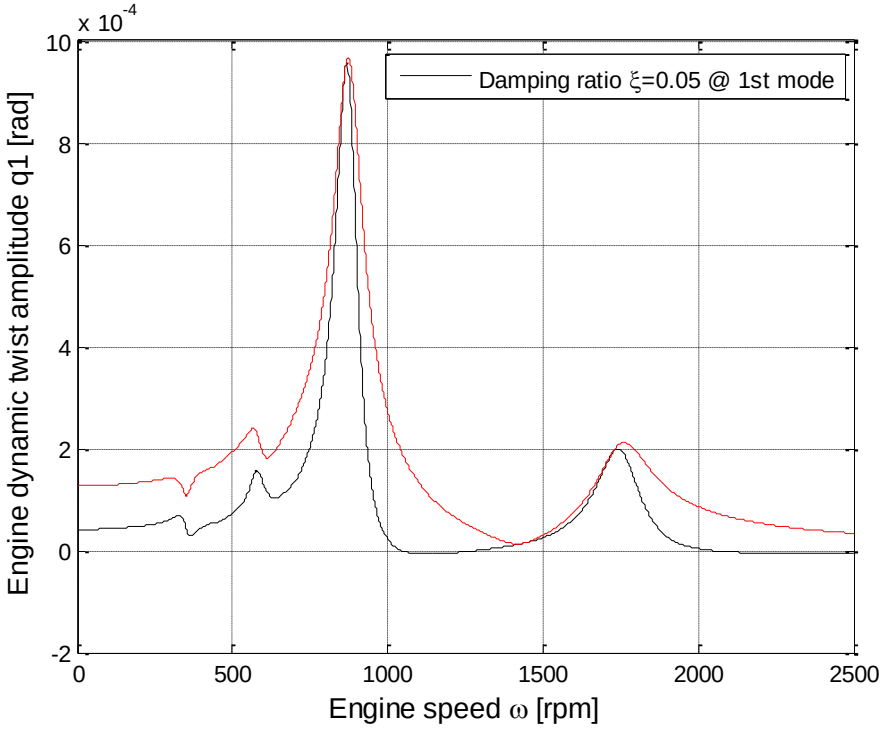

Figure 4-14 :Engine dynamic twist amplitude for an 8-DOFS (real and imganiary) damping ratio=0.05

Damping ratio =0.06

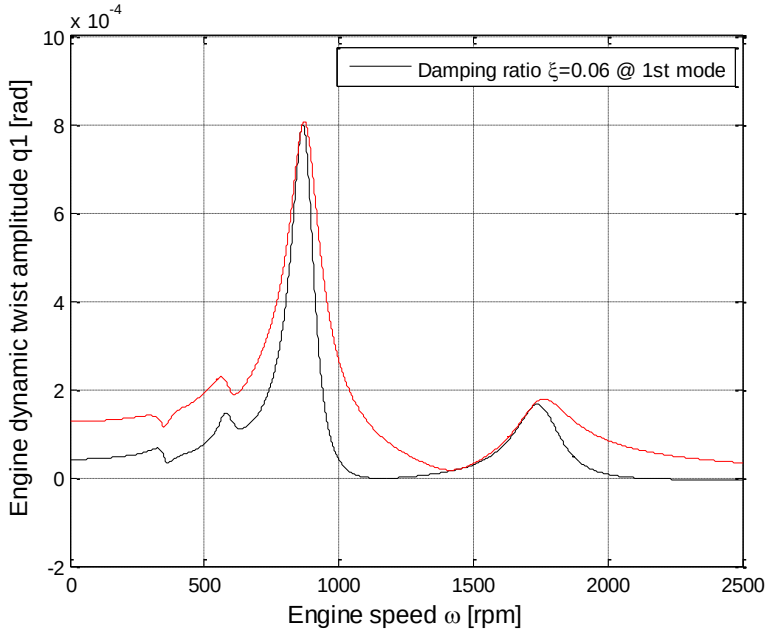

Figure 4-15:Engine dynamic twist amplitude for an 8-DOFS (real and imganiary) damping ratio=0.06

Damping ratio =0.07

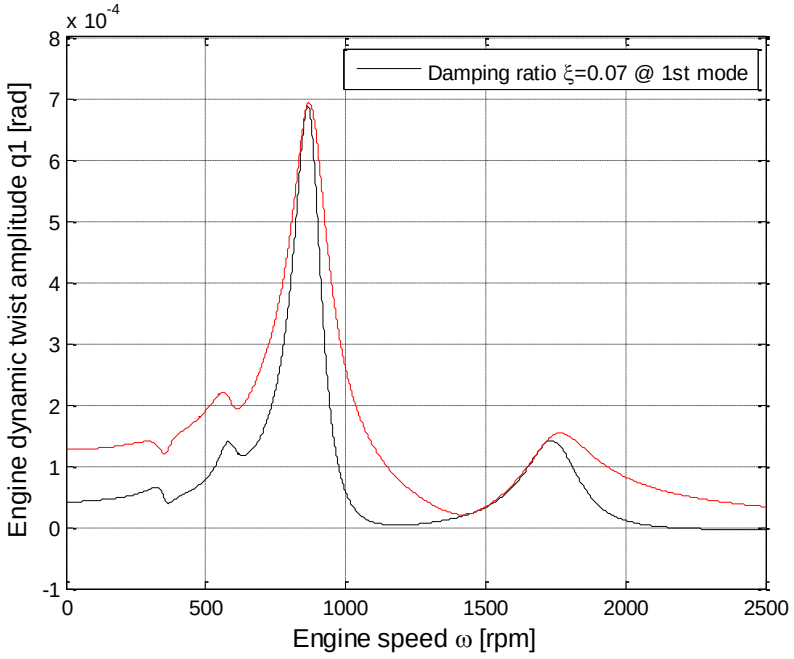

Figure 4.4-16Engine dynamic twist amplitude for an 8-DOFS (real and imganiary) damping ratio=0.07

Damping ratio =0.08

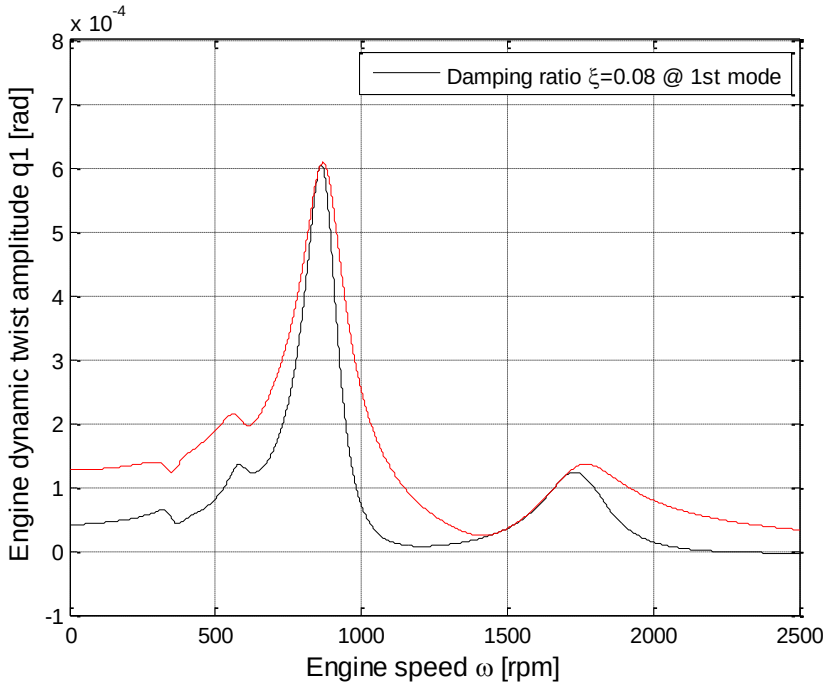

Figure 4-17: Engine dynamic twist amplitude for an 8-DOFS (real and imganiary) damping ratio=0.08

Damping ratio =0.09

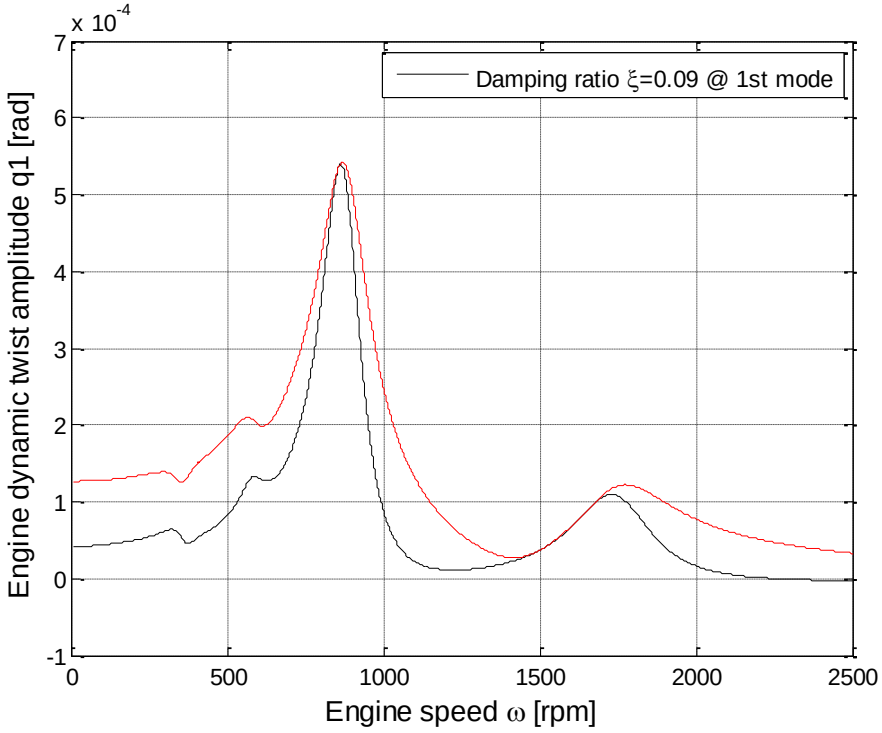

Figure 4-18: Engine dynamic twist amplitude for an 8-DOFS (real and imganiary) damping ratio=0.09

Damping ratio = 0.1

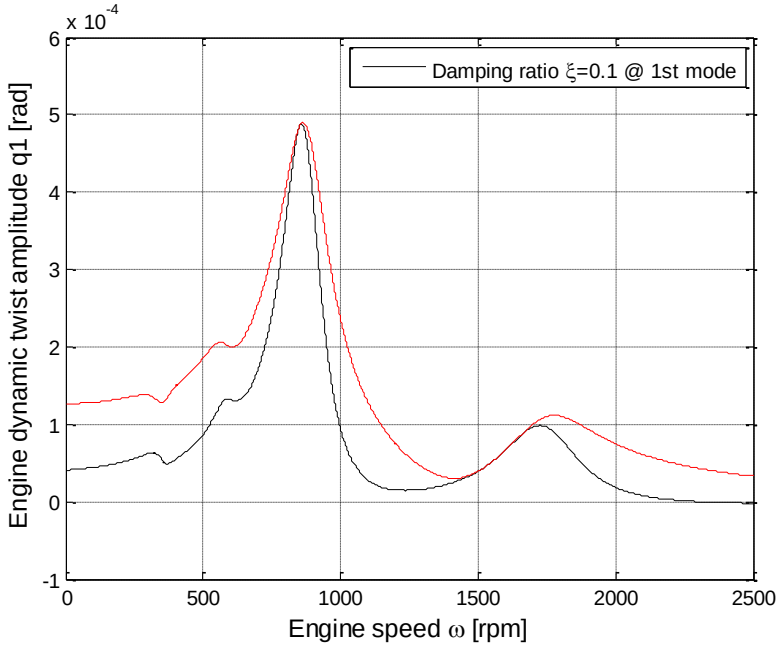

Figure 4-19Engine dynamic twist amplitude for an 8-DOFS (real and imganiary) damping ratio=0.1

Damping ratio = 0.2

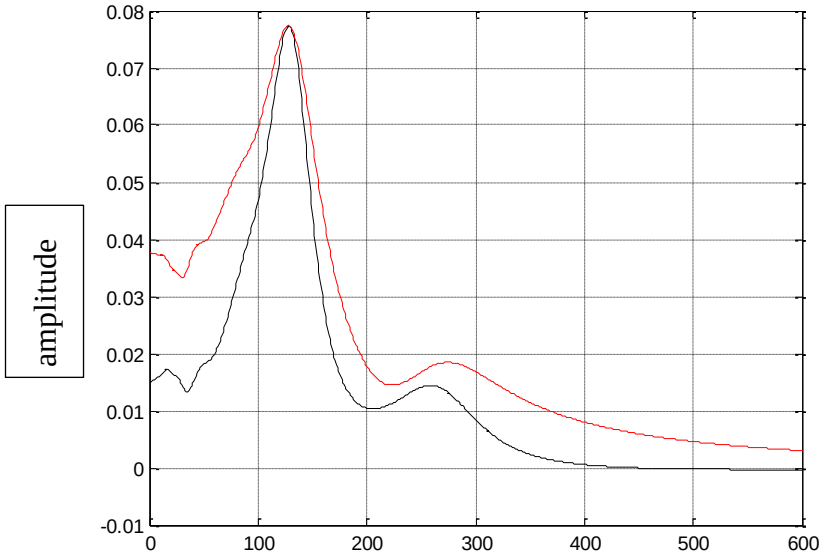

Figure 4-20Engine dynamic twist amplitude for an 8-DOFS (real and imganiary) damping ratio=0.2

Damping ratio = 0.3

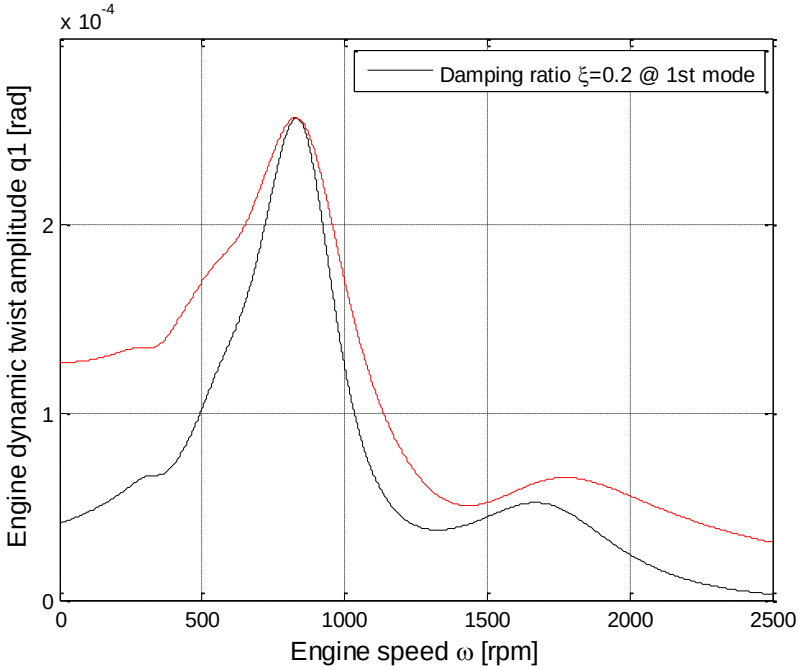

Figure 4-21Engine dynamic twist amplitude for an 8-DOFS (real and imganiary) damping ratio=0.3

Damping ratio = 0.4

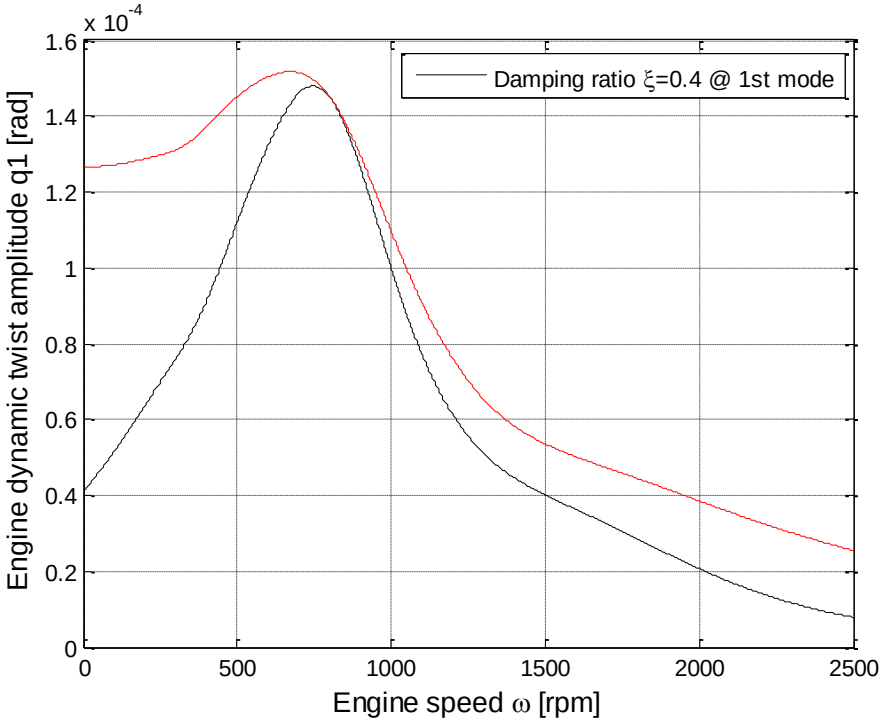

Figure 4-22Engine dynamic twist amplitude for an 8-DOFS (real and imganiary) damping ratio=0.4

Damping ratio =0.5

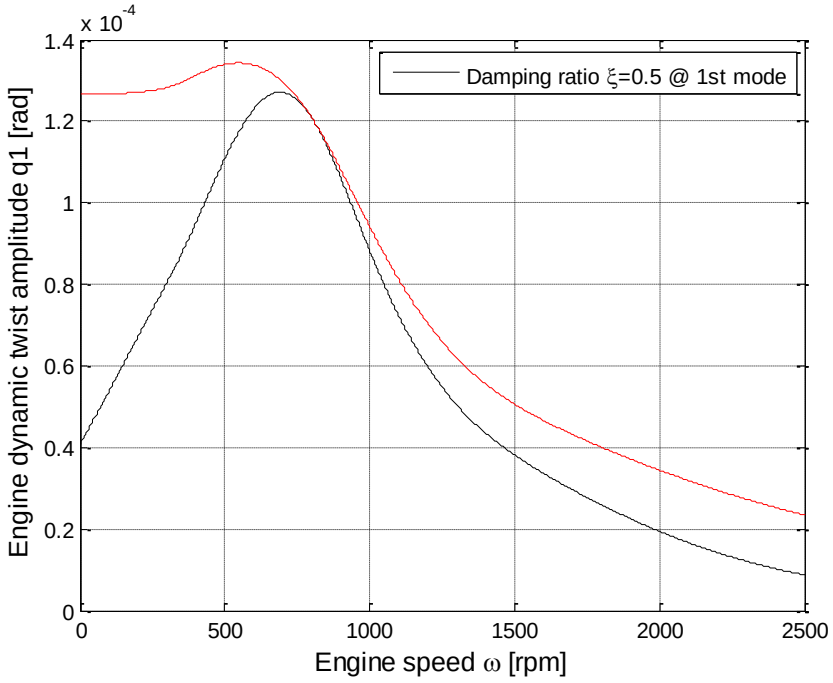

Figure 4-23Engine dynamic twist amplitude for an 8-DOFS (real and imganiary) damping ratio=0.5 for mode $\{X_4\}$.

CHAPTER V

CONCLUSIONS AND RECOMMENDATIONS

5.1 Conclusions

1. From results we found the best value of damping ratio are 0.3 ,0.4,0.5
2. It can be concluded that out of four types of vibrations like torsional, flexural, axial, coupled which affect the crankshaft, torsional vibrations are the most dangerous which can break the crankshaft.
3. Modal analysis gives the relation of frequency and the vibration characteristics of the crankshaft. The results of modal analysis are extremely important as the resonance frequency or the frequency at which the effects of vibration are maximum is provided. The modal analysis also provides the starting point for harmonic and transient analysis.
4. Critical locations on the crankshaft geometry are all located on the fillet areas because of high stress gradients in these locations which result in high stress concentration factors.
5. The model is general can describe both diesel and petrol engines, and it can with slight changes describe the behavior of an engine with an arbitrary number of cylinders.
6. The computer algorithm presented in the thesis for calculation of the frequency could be expected is proven to be useful for an arbitrary number of cylinders.

5.2 Recommendations for Future Work

Based on issues discussed in chapter four, the following Suggested future works are made for further improvement and additional studies can be done to extend the present analysis as listed in the following:

1. The study of coupled vibrations can be done.
2. The effect of the Nonlinear Torsional Vibration Analysis of Variable Inertia of the moving part in Reciprocating Engines can be included in the future study.
3. Modelling of friction in the piston ring and skirt, valve train, auxiliary and the crankshaft bearing engine can be done.
4. The estimation accuracy on the reconstructed in-cylinder pressure is evaluated by calculating the following errors.
5. The analytical results could be validated through experimental tests.

References

Akbulut, S. (2018) *Conceptual Design Analysis Of Crank Shafts Used In Heavy Vehicles*. İstanbul Technical University.

Amitpal Singh Punewale, Tushar Khobragade, Amit Chaudhari, N. M. K. (2015) 'Analysis & Optimization of Torsional Vibrations in a Four-Stroke Single Cylinder Diesel Engine Crankshaft', *International Journal of Engineering and Technical Research (IJETR)*, 3(4), pp. 87–92.

Basshuysen, R. van and , Schäfer, F. (2004) *Internal Combustion Engine Handbook Basics, Components, Systems, and Perspectives*. SAE Internationa.

Bell, J. E. (1996) *Assessment of Diesel Engine Condition Using Time Resolved Measurements and Signal Processing*. Monterey CA. Available at: .

Bibić, I. F. D. and Pecar, A. M. A. B. A. (2012) 'Preliminary Selection Of Basic Parameters Of Different Torsional Vibration Dampers Intended For Use'.

Blažević, A., Filipović, I., Bibić, D., Pikula, B., Karabegović, I., Husak, E., Stanojević, D., Lužanin, N., Vasić, M. and Stanojević, N. (2016) 'Possibilities Of Using Dynamic Torsional Vibration Dampers With Springs In Ic Engines For Road Vehicles'.

Boysal, A. and Rahnejat, H. (1997) 'Torsional vibration analysis of a multi-body single cylinder internal combustion engine model', *Applied Mathematical Modelling*. Elsevier, 21(8), pp. 481–493.

Brown T. S., N. W. S. (1992) 'Determination of Engine Cylinder Pressures from Crankshaft Speed Fluctuations.', *Society of Automotive Engineers*, p. Paper Number 920463.

Brusa, E., Delprete, C. and Genta, G. (1997) 'Torsional vibration of crankshafts: effects of non-constant moments of inertia', *Journal of sound and vibration*. Elsevier, 205(2), pp. 135–150.

C. E Beards (1983) *Structural Vibration Analysis and Damping*. Edited by Butterworth-Heinemann.

Caughey, T. K. (1960) 'Classical normal modes in damped linear systems', *Journal of Applied Mechanics*, 82, pp. 269–271.

Challen, B. and R. B. (1999) 'The theory of compression ignition engines', in *Diesel Engine Reference Book*. 2nd Editio.

Citron S. J., O'Higgins J. E., Chen L. Y., " (no date) 'Cylinder by Cylinder Engine Pressure and Pressure Torque Waveform Determination Utilizing Speed Fluctuations', *Society of Automotive Engineers*, p. Paper Number 890486, 1989.

Corbo, M. A. and Melanoski, S. B. (1996) 'Practical Design Against Torsional Vibration.', in

Proceedings of the 25th Turbomachinery Symposium. Texas A&M University. Turbomachinery Laboratories.

Desavale, R. G. and Patil, A. M. (2013) 'Theoretical and Experimental Analysis of Torsional and Bending Effect on Four Cylinders Engine Crankshafts by Using Finite Element Approach', *International Journal of Engineering Research*, 2(6), pp. 379–385.

Dondlinge, B. (2015) *Chapter 16 Cranktrain Crankshafts Connecting Rods,and Flywheel*.

Draminski, P. (1965) 'Extended treatment of secondary resonance.', *Shipbuild Marine Eng. Int*, (88), pp. 180–186.

Drápal, L. and Novotný, P. (2017) '2701 . Torsional vibration analysis of crank train with low friction losses', pp. 5691–5701. doi: 10.21595/jve.2017.17876.

Eshleman, R. L. (1988) 'Chapter 38, Torsional Vibration in Reciprocating and Rotating Machines', in *Harris' Shock and Vibration Handbook*. Fifth edit. McGraw – Hill Publication.

Eshleman, R. L. (no date) *Torsional Vibration Of Machine Systems*. Illinois.

Feese, T. and Hill, C. L. (2009) 'Prevention Of Torsional Vibration Problems In Reciprocating Machinery', in *In Proceedings of the 38th turbomachinery symposium. Texas A&M University. Turbomachinery Laboratories.*

Filipović, I. (2007) *Motori s unutarnjim izgaranjem: dinamika i oscilacije*. Mašinski fakultet.

Filipović, I. and Aleksandar Milašinović (2011) 'The Parameter Determination Of The Crankshaft Dynamical Model', 37.

FILIPOVIC, I., DOLECEK, V. and BIBIC, D. (2005) 'Modeling and the analysis of parameters in the torsional-oscillatory system equivalent to the diesel engines in heavy-duty vehicles', *Strojniški vestnik*. Strojniski vestnik, 51(12), pp. 786–797.

Frahm, H. (1911) 'Device for damping vibrations of bodies.' Google Patents.

FRANK M . LEwls, M. (1925) 'Torsional Vibration in Diesel Engine', *Society of Naval Architects and Marine Engineers New*.

Gawande, S. H., Navale, L. G., Nandgaonkar, M. R. and Butala, D. (2010) 'Torsional frequency analysis of multi-cylinder inline diesel engine generator system', in *Proc. of The 2010 International Conference on Mechanical, Industrial, and Manufacturing Technologies*, pp.519–524.

George Nerubenko and Vitaliy Krupenin (2008) 'Radical Reduction Of Crankshaft Torsional'.

Gerhardt, F., Fechler, C., Lehmann, S. and Langeneckert, H. (2002) 'Internal Crankshaft Damper', in *7th LuK Symposium*, pp. 41–49.

Griffin, T. R. (1998) *Computer-Aided Design Software for Torsional Analysis*. Blacksburg,

Virginia Keywords:

Harris, C. M. (2002) *Shock And Vibration Handbook*. Edited by C. M. H. and And.

Den Hartog, J. P. (1985) *Mechanical vibrations*. New York: Dover Publications.

Hestermann, D. C. and Stone, B. J. (1994) 'Secondary inertia effects in the torsional vibration of reciprocating engines – a literature review', *Proc. Instn Mech. Engrs, Part C Journal of Mechanical Engineering Science*, pp. 11–15.

Homik, W. and Ph, D. (2011) 'Damping of torsional vibrations of ship engine crankshafts – general selection methods of viscous vibration damper', 18(3), pp. 43–47.

Homik W. (2012) 'The Effect of liquid temperature ande viscosity on the amplitude-frequency characteristics of a viscotic torsion damper', *Polish Maritime Research*, 19, pp. 71–77.

Honda, Y. and Saito, T. (1987) 'Dynamic characteristics of torsional rubber dampers and their optimum tuning', *SAE technical paper 870580*.

Hudson, J. W. (1997) *Development And Calibration Of A_ - Torsional Engine Model For A Three-Cylinder, Two-Stroke Diesel Engine*.

Iwamoto, S. and Wakabayashi, K. A. (1985) 'study on the damping characteristics of torsional vibration in diesel engines (Part I)', *J. Marine Eng. Soc.*, 19, pp. 34–39.

J.C. (Buddy) Wachel, F. R. S. (1993) 'Analysis Of Torsional Vibrations In Rotating Machinery', in *Proceedings of22nd Turbomachinery Symposium.* San Antonio, Texas.

Johnston, P. R. and Shusto, L. M. (1987) 'Analysis of diesel engine crankshaft torsional vibrations', *SAE Spec. Pub., presented at SAE Government/Industry Meeting and Exposition, Washington, DC, USA*, pp. 21–26.

Kabele, D. F. (1984) 'A New Approach in the Simulation of Crankshaft Torsional Vibration', *Society ofAutomotive Engineers*, p. Paper Number 844140,.

Klaus Mollenhauer and Helmut Tschoeke (2010) *Handbook of Diesel Engines*. fifth. Newyork: springer.

Kroll, J., Kooy, A. and Seebacher, R. (2010) 'Torsional vibration damping for future engines', in *9th Schaeffler Symposium*.

Kushwaha, M., Gupta, S., Kelly, P. and Rahnejat, H. (2002) 'Elasto-multi-body dynamics of a multicylinder internal combustion engine', *Proceedings of the Institution of Mechanical Engineers, Part K: Journal of Multi-body Dynamics*. SAGE Publications Sage UK: London, England, 216(4), pp. 281–293.

Lee, D.C., Lee, B.W., Park, Y.N. and Park, B. . (1992) 'A Study on the Dynamic Characteristics and Performance of Geislinger Type Torsional Vibration Damper for Two stroke Low Speed

Diesel Engines', *Journal of the Korean Society of Marine Engineering*, 16(5), pp. 329–340.

Li Jianqiu, Y. M. (2000) 'Analysis of the Influence of Crankshaft Vibration Upon the Instantaneous Flywheel Speed', *Seoul 2000 FISITA World Automotive Congress*.

Lundkvist, A. (2010) 'Modal Analysis Project'.

Magazinović, G. (1998) 'Shafting Vibration Primer', *On Torsional Vibrations of the Propulsion Plant Shafting*, pp. 11–14.

Malanoski, M. A. C. and S. B. (no date) 'Practical design against torsional vibration.'

Maragonis, I. E. (1992) 'The torsional vibrations of marine diesel engines under fault operation of its cylinders', *Forschung im Ingenieurwesen – Eng. Res.*, 58, pp. 13–25.

Mathias Pfabe and Christoph Woernle (2009) 'Reduction of Periodic Torsional Vibration using Centrifugal Pendulum.pdf', in *Appl. Math. Mech*.

Meirelles, P. S. et al. (2007) 'Mathematical Model for Torsional Vibration Analysis in Internal Combustion Engines', *12 th IFToMM World Congress12 th IFToMM World Congress*.

Montazersadgh. F. H., F. A. (2008) 'Optimization of a Forged Steel Crankshaft Subject to Dynamic Loading', *SAE Paper*.

Nestorides, E. J. (1958) 'A Handbook on Torsional Vibration', *British Internal Combustion Engine Research Association, Cambridge University Press*.

Norton, R. L. and Worcester (1999) *Design of Machinery, An Introduction to Synthesis and Analysis of Mechanisms of Machines.pdf*. six editio. 1bomas Casson.

Okamura H, et al (1983) 'Experiments on the coupling and Transmission Behavior of Crankshaft Torsional, Bending and longitudinal vibrations in high Speed Engines', in *Proc. of 2nd Int. pacific Conf. on Automotive Engine*. Tokyo, pp. 205–218.

P. S. Meirelles, D. E. Zampieri, A. S. M. (2007) 'Experimental Validation of Methodology for Torsional Vibration Analysis in Internal Combustion Engines', *12 th IFToMM World Congress Besancon (France)*.

Pasricha, M. S. (2001) 'Effect of the gas forces on parametrically excited torsional vibrations of reciprocating engines', *J. Ship Res.*, 4(45), pp. 262–268.

Piotr Deuszkiewicz, J. P. (2015) 'Nonlinear model of rubber torsional vibration damper', *JVE International Ltd*, 6, pp. 13–17.

POLÁČEK, B. M. (2011) *Modal Properties Of 6-Cylinder Tractor Engine Powertrain*. Institute Of Automotive Engineering.

Rao, S. S. (2004) *Mechanical Vibrations*. Fifth Edit. Prentice Hall.

Rizzoni, G. (1989) 'Diagnosis of Individual Cylinder Misfires by Signature Analysis of Crankshaft

Speed Fluctuations', *Society of Automotive Engineers*, (Paper Number 89088).

Sobel J. R., Jeremiasson J., W. C. (1AD) 'Instantaneous Crankshaft Torque Measurement in Cars', *Society ofAutomotive Engineers*, (Paper Number 960040).

Song, X. G., Song, T. X., Xue, D. X. and Li, B. Z. (1991) 'Progressive torsional-axial continued vibrations in crankshaft systems: A phenomenon of coupled vibration', *Trans. ASME, Rotating Mach. Vehicle Dyn*, 35, pp. 319–323.

Spångberg, N. (2012) *Damping of vibrations in asingle-cylinder engine test bed*. Stockholm.

Tomoanki Kodama, Katsuhiko Wakabayashi and Yasuhiro Honda, S. I. (2001) 'Dynamic Characteristics of viscous friction Dampers by Simultaneous Vibration Displacement Measurement at Two Points', *SAE 2001-01-0281 World Congress Detroit, Michigan*.

V.R.Navale, C. L. D. (2015) 'Torsional Vibration In Engine and use of viscous damper.', *IJARIIE*, volume 1(5).

Wang, Y. and Lim, T. C. (2000) 'Prediction of torsional damping coefficients in reciprocating engine', *J. Sound Vibr.*, 238(4), pp. 710–719.

Weaver Jr, William and Timoshenko, Stephen P and Young, D. H. (no date) *Vibration problems in engineering*.

William J. Bottega (2011) *Engineering Vibrations*. New York A: Taylor & Francis Group.

Wilson, W. K. (1956) *Practical Solution of Torsional Vibration' Problems Revised*. Third Edit. John Wiley & Sons Inc.

Wilson, W. K. (1968) *Pratical Solution of Torsional Vibration Problems: Devices for Controlling Vibration*. Chapman & Hall.

Wladyslaw Mitianiec, K. B. (no date) 'Torsional Vibration Analysis of Crankshaft in Heavy Duty Six Cylinder Inline Engine'.

Wojciech Homik (2011) 'Damping of torsional vibrations of ship engine crankshafts-general selection methods of viscous vibration damper', *Polish research*, 18, pp. 43–471.

Xingyu, L., Gequn, S., Lihui, D., Bin, W. and Kang, Y. (2011) 'Progress and Recent Trends in the Torsional Vibration of Internal Combustion Engine', in *Advances in Vibration Analysis Research*. IntechOpen.

Appendices

Appendix A Matlab Code: Stiffness And Inertia Calculation

```
%input('Enter G: '); %shear modulus of rigidity
input('Enter L: ');  %the connecting rod length
input('Enter a: ');  %the distances from the con-rod mass center to piston pin
input('Enter mp: '); % piston mass
input('Enter c: ');  %the distances from the con-rod mass center to crankpin geometric centers
input('Enter R: ');  % crank radius(Crank throw)
input('Enter r: ');  % fly wheel radius
input('Enter Mfly: '); %fly wheel mass
input('Enter n: ');  % no of cylinder
input('Enter mcn: '); %connecting rod mass
%input('Enter mpin: ');  %crank pin mass
%input('Enter mweb: ');  %crank web mass
mcnrot = mcn*c/L;  %rotary part mass of the connecting rod
mcnrec = mcn* a/L;%reciprocating part mass of the connecting rod
%Mcn = mcnrec + mcnrot; %total mass of connecting rod
%Mrot = mpin+mweb+ mcnrot; %rotaing mass
Mrec = mp + mcnrec; %total mass reciprocating parts
for i=1:1:n;
Jcyl(i)=Mrot*R^2+0.5*Mrec*R^2; %second polar moments of inertia
end
JF =Mfly* r^2; %second polar moments of inertia
```

Appendix B :Matlab Code For Calculation Of Mode Shape An Natural Frequencies

```
v=[0.00551 0.00489  0.00602 0.00602 0.00489 0.00625 0.06753];
J=diag(v);
K=1000*[392 -392 0 0 0 0 0
-392 784 -392 0 0 0 0
  0 -392 784 -392 0 0 0
  0 0  -392 784 -392 0 0
  0 0 0  -392 784 -392 0
  0 0 0 0  -392 847 -455
     0 0 0 0 0 -455 455];
ws = eig(K/J);;
w = sqrt(ws); % (rad/sec) natura1 frequencies
whz = w/(2*pi) % (Hz) natura1 frequencies
for i = 1 :7;
   kj = K-J*w(i)^2;
   A(1,i) = 1;
   A(2,i) = -A(1,i)*kj(1,1)/kj(1,2);
A(3,i) = (-A(1,i)*kj(2,1)-A(2,i)*kj(2,2))/kj(2,3);
A(4,i) = (-A(2,i)*kj(3,2)-A(3,i)*kj(3,3))/kj(3,4);
A(5,i) = (-A(3,i)*kj(4,3)-A(4,i)*kj(4,4))/kj(4,5);
A(6,i) = (-A(4,i)*kj(5,4)-A(5,i)*kj(5,5))/kj(5,6);
A(7,i) = (-A(5,i)*kj(6,5)-A(6,i)*kj(6,6))/kj(6,7);
% A(8,i) = (-A(6,i)*kj(7,6)-A(7,i)*kj(7,7))/kj(7,8);
end
[whz,I] = sort(abs(whz));
A;
 figure (1)
for i = 1:7
subplot(7,1,i)
plot(A(:,I(i)),'k');grid;hold on
plot(A(:,I(i)),'ko')
ylabel ([num2str(whz(i),4),'Hz'])
end
tit1e ([Mode num2str(i,7)]);
% J= diag[0.09; 0.039; 0.038 0.038 0.038 0.039 0.611];
% K=[6545000 -6545000 0 0 0 0 0 0
%  -6545000 7568000 -1203000 0 0 0 0 0
% 0 -1203000 2406000 -1203000 0 0 0 0
% 0 0 -1203000 3279000 -1356000 0 0 0
% 0 0 0 -1356000 2750000 -1400000 0 0
% 0 0 0 0 -1400000 2423000 -1023000 0
% 0 0 0 0 0 -1023000 3486000 -2463000
% 0 0 0 0 0 0 -2463000 2463000];
c12=0.01;  c23=0.01; c34=0.01;  c45=0.01; % c56=0.01;  c2=0.013; c3=0.013; c4=0.013;1b*in*sec/rad
%%%%%%%%%%%%%%%%%%%%%%%%%%%%%%%%%%%%%%%%%%%%%%%%%%%%%%%%% - —
```

```
ws = eig(K/J);
w = sqrt(ws); % (rad/sec) natura1 frequencies
whz = w/(2*pi) % (Hz) natura1 frequencies
for i = 1 :13;
 kj = K-J*w(i)^2;
 A(1,i) = 1;
 A(2,i) = -A(1,i)*kj(1,1)/kj(1,2);
A(3,i) = (-A(1,i)*kj(2,1)-A(2,i)*kj(2,2))/kj(2,3);
A(4,i) = (-A(2,i)*kj(3,2)-A(3,i)*kj(3,3))/kj(3,4);
A(5,i) = (-A(3,i)*kj(4,3)-A(4,i)*kj(4,4))/kj(4,5);
A(6,i) = (-A(4,i)*kj(5,4)-A(5,i)*kj(5,5))/kj(5,6);
A(7,i) = (-A(5,i)*kj(6,5)-A(6,i)*kj(6,6))/kj(6,7);
A(8,i) = (-A(6,i)*kj(7,6)-A(7,i)*kj(7,7))/kj(7,8);
end
[whz,I] = sort(abs(whz));
A;
 figure (1)
for i = 1:8
% subplot(8,1,i)
plot(A(:,I(1)),'k');grid;
figure (2)
plot(A(:,I(2)),'k');grid;
figure (3)
plot(A(:,I(3)),'k');grid;
figure (4)
plot(A(:,I(4)),'k');grid;
figure (5)
plot(A(:,I(5)),'k');grid;
figure (6)
plot(A(:,I(6)),'k');grid;
figure (7)
plot(A(:,I(7)),'k');grid;
figure (8)
plot(A(:,I(8)),'k');grid;
% hold on
% plot(A(:,I(i)),'ko')
ylabel ([num2str(whz(i),4),'Hz'])
end
tit1e ([Mode num2str(i,8)]);
```

Appendix C : Program For Pressure Vs Crank Angle ,Total Torque And Harmonic Coefficients

```
Ti = 300; % inlet temperature, K
Pi = 50; %P1=0.1 MPa inlet pressure, kPa
Pe = 100; % exhaust pressure, kPa
CR = 17.5; % compression ratio
K1 = 1.4; % ideal gas specific heat ratio
K2=1.3;
% b=0.120;
gam=(K1 -1)/K1;
% s = 0.1207;% stroke (m)
% a=s/2;
% len= 0.150; %connecting rod length (m)
s = 0.07;% stroke (m)
len=0.123;% in mm, conrod length
lamda=s/(2*len);
w=800*(2*pi/60); %rps
a=0.035;% in mm, crankshaft radius
b=0.76;%in mm, piston diameter
% A=pi*d^2/4;% in mm‘2, piston area
W=800; %rotating speed of engine in rad/sec
% Mp=0.363; % kg, total piston mass
% Mc=0.096; % kg, total connecting rod mass
% a=(Ro/L)^2;
% theta=-180:1:180; %crankangle theta vector
A_piston = pi/4*b^2; % Crossectional Area of Piston
Vd = s*A_piston; % Displacement Volume
Vc = Vd/(CR-1); % Cylinder Clearence Volume
Vt1=Vd+Vc;
m4=.022;
m3a=.02*.4;
m3b=.02*.6;
m2a=.3*.06;
mb=m3b+m4;
ma=m2a+m3a;
% ak=0;bk=0;a0=0;ftm=0;
% for m=1:1:720
% for i=1:1:30
for j= 1:1:720
%  X=(theta*pi/180)
%  V=Vc+A_piston(( l + a -a*cos(X)-(s^2-a^2*(sin(X))^2)^0.5))
% Piston displacement
PD(j)= (1 + a - sqrt(1^2-a^2*(sind(j))^2) - (a*cosd(j)) );
V(j) = (Vd/(CR-1))+ (A_piston * (PD(j))); % VOLUME
if j<=180
 P(j)=Pi;
elseif j<=360
 P(j)=Pi*(Vt1/V(j))^K1;
elseif j<=410
 P(j)=P(360);
elseif j<=540
 P(j)=P(360)*(V(410)/V(j))^K2;
elseif j<=720
```

```
 P(j)=Pe;
end
%Gas torque
Fg(j)=P(j)*A_piston;
Tg(j)=(Fg(j)*a)*sind(j)*(1+(a/len)*cosd(j));
%Inertia Force
xb=-a*w^2*(cosd(j)+(a/len)*cosd(2*j));
Aa=-a*w^2*cosd(j)-a*w^2*sind(j);
Fi(j)=(-ma*Aa-mb*xb)+(-ma*Aa);
Ti(j)=(0.5*mb*a^2*w^2)*((a/2*len)*sind(j)-sind(j)-((3*a)/(2*len)).*sind(3*j));
Tt(j)=Tg(j)+Ti(j);
end
ak=0;bk=0;a0=0;ftm=0;ph=360;
for m=1:1:720
for i=1:1:30
for j=1:1:720
akk(j)=2/(4*pi)*Tt(j)*cosd(i*j-ph);
bkk(j)=2/(4*pi)*Tt(j)*sind(i*j-ph);
a00(j)=2/(4*pi)*Tt(j);
ak=ak+akk(j);
bk=bk+bkk(j);
a0=a0+a00(j);
end
akkk(i)=ak;
bkkk(i)=bk;
ftm=ftm+akkk(i)*cosd(i*m-ph)+bkkk(i)*sind(i*m-ph);
ak=0;bk=0;
end
ft(m)=a0+ftm;
end
 figure(1)
 for i=1:1:720;
 plot(i,V(i),'-')
 ylabel('PRESSURE (KPa)')
  %  set(h'FontName','Times','FontSize',12)
 hold on
 end
 figure(2)
 for i=1:1:720;
 plot(i,P(i),'-r')
 hold on
 end
 figure(3)
 for i=1:1:720;
 plot(V(i),P(i),'-k')
 hold on
 end
 figure(4)
 for i=1:1:720;
 plot(i,Tg(i),'-r')
 hold on
 end
 figure(5)
 for i=1:1:720;
```

```
 plot(i,Ti(i),'-k')
 hold on
 end
 figure(6)
 for i=1:1:720;
 plot(i,Tt(i),'-r')
 hold on
 end
 figure(7)
  for i=1:1:720;
  plot(i,ft(i),'--')
%  set(h'FontName','Times','FontSize',12)
  hold on
 end
% for i = 1 : 1 : 179
% P1=Pi;
```

Appendix D : Program For 7-DOFS Engine Dynamic Twist 7 Vs Engine Speed

```
coeficients=xlsread('harcoflast.xlsx'); %/N.m
coeficients=coeficients*100; %N.m
Aji2=coeficients(:,1);
Bji2=coeficients(:,2);
Aji3=coeficients(:,3);
Bji3=coeficients(:,4);
Aji4=coeficients(:,5);
Bji4=coeficients(:,6);
Aji5=coeficients(:,7);
Bji5=coeficients(:,8);
Aji6=coeficients(:,9);
Bji6=coeficients(:,10);
Aji7=coeficients(:,11);
Bji7=coeficients(:,12);
delta=[0,0,480,240,600,120,360,0];
Gic=[1.000000000,
0.15966499569224,
0.13529774698925,
0.10891490329351,
0.08090950239633,
0.05169875409666,
0.02171782482792,
-0.01428155083981];
K1=5.9712e5;K2= 22.82e6; K3= 22.82e6; K4= 22.82e6; K5= 22.82e6; K6= 22.82e6; K7= 19.21e6;
J1=27.5126;J2=18.64;J3=18.64;J4=18.64;J5=18.64;J6=18.64;J7=18.64;J8=2655; %kg.m”2 flywheel
JE=diga[J1;0,J2;0,0,J3;J4;;J5;J6;J7;J8];
KE=[K1, -K1,0,0,0,0,0,0;
-K1, K1+K2, -K2,0,0,0,0,0;
0,-K2, K2+K3, -K3,0,0,0,0;
0,0,-K3, K3+K4, -K4,0,0,0;
0,0,0,-K4, K4+K5, -K5,0,0;
0,0,0,0,-K5, K5+K6, -K6,0;
0,0,0,0,0,-K6, K6+K7, -K7;
0,0,0,0,0,0,-K7, K7];
Jpc=Gic'*JE*Gic;
```

```
Kpc=Gic'*KE*Gic;
wnc=sqrt(Kpc/Jpc);
damping_ratio=0.01; %.01;
for damping_ratio=0.01:0.02:0.1
Cpc=2*Jpc*wnc*damping_ratio;
t=0;
c_w=0;
for w=0:1:300
c_w=c_w+1;
for j=1:1:30
aji2(j)=(Aji2(j)*cosd(j*delta(2)/2)-Bji2(j)*sind(j*delta(2)/2));
bji2(j)=(Aji2(j)*sind(j*delta(2)/2)+Bji2(j)*cosd(j*delta(2)/2));
aji3(j)=(Aji3(j)*cosd(j*delta(3)/2)-Bji3(j)*sind(j*delta(3)/2));
bji3(j)=(Aji3(j)*sind(j*delta(3)/2)+Bji3(j)*cosd(j*delta(3)/2));
aji4(j)=(Aji4(j)*cosd(j*delta(4)/2)-Bji4(j)*sind(j*delta(4)/2));
bji4(j)=(Aji4(j)*sind(j*delta(4)/2)+Bji4(j)*cosd(j*delta(4)/2));
aji5(j)=(Aji5(j)*cosd(j*delta(5)/2)-Bji5(j)*sind(j*delta(5)/2));
bji5(j)=(Aji5(j)*sind(j*delta(5)/2)+Bji5(j)*cosd(j*delta(5)/2));
aji6(j)=(Aji6(j)*cosd(j*delta(6)/2)-Bji6(j)*sind(j*delta(6)/2));
bji6(j)=(Aji6(j)*sind(j*delta(6)/2)+Bji6(j)*cosd(j*delta(6)/2));
aji7(j)=(Aji7(j)*cosd(j*delta(7)/2)-Bji7(j)*sind(j*delta(7)/2));
bji7(j)=(Aji7(j)*sind(j*delta(7)/2)+Bji7(j)*cosd(j*delta(7)/2));
sumGic_aji(j)=Gic(2)*aji2(j)+Gic(3)*aji3(j)+Gic(4)*aji4(j)+Gic(5)*aji5(j)+Gic(6)*aji6(j)+Gic(7)*aji7(j)
sumGic_bji(j)=Gic(2)*bji2(j)+Gic(3)*bji3(j)+Gic(4)*bji4(j)+Gic(5)*bji5(j)+Gic(6)*bji6(j)+Gic(7)*bji7(j)
Qjc(j)=sqrt(sumGic_aji(j)^2+sumGic_bji(j)^2)/Jpc/wnc^2;
eta_jc(j)=atan(sumGic_bji(j)/sumGic_aji(j));
Mjc(j)=1/((1-(j*w/2/wnc)^2)+(j*damping_ratio*w/wnc)*i);
exponential(j)=exp((j*w*t/2-eta_jc(j))*i);
end
%sum_gamc=Ao;
sum_gamc_real=0;
sum_gamc_abs=0;
for h=1:1:30
sum_gamc_real=sum_gamc_real+real(Mjc(h)*Qjc(h)*exponential(h));
sum_gamc_abs=sum_gamc_abs+(Mjc(h)*Qjc(h)*exponential(h));
end
```

```
gamc_real(c_w)=sum_gamc_real;%in radians
gamc_abs(c_w)=abs(sum_gamc_abs);%in radians
omega(c_w)=w;%in rad/sec
clear sum_gamc_real sum_gamc_abs
end
plot(omega,gamc_real,'-k');
hold on
plot(omega,gamc_abs,'-r');
grid on
% axis([5 1000 -0.001 10])
%legend('Gama_c real','Gama_c abs')
gama_c_real(:,1)=omega';
gama_c_real(:,2)=gamc_real';
% xlswrite('points_gama_omega_eq_4_24~real_2.xls',gamc_real);
gama_c_abs(:,1)=omega';
gama_c_abs(:,2)=gamc_abs';
% xlswrite('points_gama_omega_eq_4_24_abs_2.xls',gama_c_abs);
end
xlsxwrite('points_gama_omega_eq_4_24_abs_2.xlsx',gama_c_abs);
% coeficients=xlsread('Harmonic_coeficients 400.xlsx'); %/N mm
```

Appendix E: matlab Code For 8-DOFS Engine Dynamic Twist X Vs Engine Speed

```
coeficients=xlsread('harcoflast.xlsx'); %/N.m
coeficients=coeficients*100; %N.m
Aji2=coeficients(:,1);
Bji2=coeficients(:,2);
Aji3=coeficients(:,3);
Bji3=coeficients(:,4);
Aji4=coeficients(:,5);
Bji4=coeficients(:,6);
Aji5=coeficients(:,7);
Bji5=coeficients(:,8);
Aji6=coeficients(:,9);
Bji6=coeficients(:,10);
Aji7=coeficients(:,11);
Bji7=coeficients(:,12);
delta=[0,0,480,240,600,120,360,0];
Gic=[1.000000000,
0.15966499569224,
0.13529774698925,
0.10891490329351,
0.08090950239633,
0.05169875409666,
0.02171782482792,
-0.01428155083981];
K1=5.9712e5; K2= 22.82e6; K3= 22.82e6;K4= 22.82e6; K5= 22.82e6;K6= 22.82e6;K7= 19.21e6;
J1=27.5126;J2=18.64;J3=18.64;J4=18.64;J5=18.64;J6=18.64;J7=18.64;J8=2655; %kg.m”2 flywheel
JE=[J1;J2; J3; J4; J5; J6; J7; J8];
KE=[K1, -K1,0,0,0,0,0,0;
-K1, K1+K2, -K2,0,0,0,0,0;
0,-K2, K2+K3, -K3,0,0,0,0;
0,0,-K3, K3+K4, -K4,0,0,0;
0,0,0,-K4, K4+K5, -K5,0,0;
0,0,0,0,-K5, K5+K6, -K6,0;
0,0,0,0,0,-K6, K6+K7, -K7;
0,0,0,0,0,0,-K7, K7];
Jpc=Gic'*JE*Gic;
Kpc=Gic'*KE*Gic;
wnc=sqrt(Kpc/Jpc);
damping_ratio=0.01; %.01;
for damping_ratio=0.01:0.02:0.1
Cpc=2*Jpc*wnc*damping_ratio;
t=0;
c_w=0;
for w=0:1:300
c_w=c_w+1;
for j=1:1:30
aji2(j)=(Aji2(j)*cosd(j*delta(2)/2)-Bji2(j)*sind(j*delta(2)/2));
bji2(j)=(Aji2(j)*sind(j*delta(2)/2)+Bji2(j)*cosd(j*delta(2)/2));
aji3(j)=(Aji3(j)*cosd(j*delta(3)/2)-Bji3(j)*sind(j*delta(3)/2));
bji3(j)=(Aji3(j)*sind(j*delta(3)/2)+Bji3(j)*cosd(j*delta(3)/2));
aji4(j)=(Aji4(j)*cosd(j*delta(4)/2)-Bji4(j)*sind(j*delta(4)/2));
bji4(j)=(Aji4(j)*sind(j*delta(4)/2)+Bji4(j)*cosd(j*delta(4)/2));
```

```
aji5(j)=(Aji5(j)*cosd(j*delta(5)/2)-Bji5(j)*sind(j*delta(5)/2));
bji5(j)=(Aji5(j)*sind(j*delta(5)/2)+Bji5(j)*cosd(j*delta(5)/2));
aji6(j)=(Aji6(j)*cosd(j*delta(6)/2)-Bji6(j)*sind(j*delta(6)/2));
bji6(j)=(Aji6(j)*sind(j*delta(6)/2)+Bji6(j)*cosd(j*delta(6)/2));
aji7(j)=(Aji7(j)*cosd(j*delta(7)/2)-Bji7(j)*sind(j*delta(7)/2));
bji7(j)=(Aji7(j)*sind(j*delta(7)/2)+Bji7(j)*cosd(j*delta(7)/2));
sumGic_aji(j)=Gic(2)*aji2(j)+Gic(3)*aji3(j)+Gic(4)*aji4(j)+Gic(5)*aji5(j)+Gic(6)*aji6(j)+Gic(7)*aji7(j);

sumGic_bji(j)=Gic(2)*bji2(j)+Gic(3)*bji3(j)+Gic(4)*bji4(j)+Gic(5)*bji5(j)+Gic(6)*bji6(j)+Gic(7)*bji7(j);

Qjc(j)=sqrt(sumGic_aji(j)^2+sumGic_bji(j)^2)/Jpc/wnc^2;
eta_jc(j)=atan(sumGic_bji(j)/sumGic_aji(j));
Mjc(j)=1/((1-(j*w/2/wnc)^2)+(j*damping_ratio*w/wnc)*i);
exponential(j)=exp((j*w*t/2-eta_jc(j))*i);
end
%sum_gamc=Ao;
sum_gamc_real=0;
sum_gamc_abs=0;
for h=1:1:30
sum_gamc_real=sum_gamc_real+real(Mjc(h)*Qjc(h)*exponential(h));
sum_gamc_abs=sum_gamc_abs+(Mjc(h)*Qjc(h)*exponential(h));
end
gamc_real(c_w)=sum_gamc_real;%in radians
gamc_abs(c_w)=abs(sum_gamc_abs);%in radians
omega(c_w)=w;%in rad/sec
clear sum_gamc_real sum_gamc_abs
end
plot(omega,gamc_real,'-k');
hold on
plot(omega,gamc_abs,'-r');
grid on
% axis([5 1000 -0.001 10])
%legend('Gama_c real','Gama_c abs')
gama_c_real(:,1)=omega';
gama_c_real(:,2)=gamc_real';
% xlswrite('points_gama_omega_eq_4_24~real_2.xls',gamc_real);
gama_c_abs(:,1)=omega';
gama_c_abs(:,2)=gamc_abs';
% xlswrite('points_gama_omega_eq_4_24_abs_2.xls',gama_c_abs);
end
xlsxwrite('points_gama_omega_eq_4_24_abs_2.xlsx',gama_c_abs);
% coeficients=xlsread('Harmonic_coeficients 400.xlsx'); %/N mm
```

EUROPEAN ACADEMIC RESEARCH
ISSN 2286-4822
www.euacademic.org

EUROPEAN ACADEMIC RESEARCH
Vol. VI, Issue 12/ March 2019

Impact Factor: 3.4546 (UIF)
DRJI Value: 5.9 (B+)

Cylinder Pressure Variation Modeling inside a Diesel Engine

SABIR ABUSHOUSHA AHMED
Assistant Professor, Mechanical Engineering Department
Faculty of Engineering, Eldaien University
TAGELSSIR HASSAN HUSSAN
Associate Professor, Mechanical Engineering Department
Faculty of Engineering Sciences, Omdurman Islamic University
OMER MUSA
Assistant Professor, Mechanical Engineering Department
Faculty of Engineering Sciences, Omdurman Islamic University

Abstract

The in-cylinder pressure is the key of an internal combustion engine. Since direct measurement is not feasible, effort has been taken to find it find theoretical approach. Engine parameters studying by experimentation time consumes and efforts. Simulation the engine to find the performance output leads to resource saving. In this study a four-stroke diesel engine has been modeled to calculate the pressure inside the combustion chamber, gas and inertia forces instead of experimental data taken from real engine. The paper investigates the pressure variation inside a diesel engine during a complete cycle with respect to the crank angle at a constant speed, without considering properties change with temperature by proximate the real processes. In this work a simple method is proposed to estimate the in-cylinder pressure. The proposed method incorporates a combustion model. The model results have been compared to real data measured from a 6-cylinder compression engine. The results demonstrate the method's capability to update the model parameters, such that accurate in-cylinder pressure estimations are possible even under the influence of unknown disturbances.

Key Words: in- Cylinder pressure, Engine Model, diesel engine.

INTRODUCTION

In-cylinder pressure always has been a significant experimental diagnostic due to its direct relation to the combustion and work producing processes during internal combustion engine analysis. The in-cylinder pressure reflects the combustion process involving piston work produced on the gas due to changes in cylinder volume. Thus, for accurate knowledge of how the combustion process propagates through combustion chamber is required and each of these processes must be related to cylinder pressure Richard Stone [1999], and [1] [1998], Usually a table is created according to the engine data from experiment test data.

There is no measurement available to validate the ability of the engine model to describe a diesel engine. J. Scarpati et al. in 2007, however used the same model to describe the cylinder pressure in straight 6-cylinder diesel engine, [5]. the comparison between the model output and measured cylinder pressure is done for three different engine speeds. There are different approaches and ways of modeling ranging from easy to compound method and may vary in both structure and correctness. Several approaches of recording engine data are possible. In conventional applications data is logged with a fixed acquisition rate, whereby the time interval between two following recordings is fixed. However, because an engine runs in a cycle dictated by a set of mechanical mechanisms slider-crank, poppet valves, etc. – and because these mechanisms have fundamental consequences to how combustion takes place, it is necessary to record data at known crank angle intervals.

Physical equations hypothetically describing the system is the common method since it makes a general model working

for many working areas. Its weaknesses it is difficult to describe reality appropriately in theory. Also, it is often resource consuming.

Another approach is to base the model entirely on measurements. The measured data is kept as a table of two or more dimensions in a so-called black box and then fetched when needed depending on one or more input signals. This method often delivers an accurate outcome since it is based directly on empiricism, however it is only defined for a restricted region. A combination of both methods, where the main basis of the model rests on physical equations and black boxes are used to model certain complexities, is also common.

An engine model therefore is either single-zone or multi-zone. In a single-zone model the gas blend inside the cylinder is considered to be consistent for each sample. It is also supposed to be made of perfect gases. In a multi-zone model, the gases are also ideal. However, the homogenous method has been replaced by a heterogeneous one. Here the cylinder is also divided into two zones, one containing injected fuel and the other surrounding air. Each zone itself is homogenous and no heat transfer arises between the two sectors. The simplicity of the single-zone model makes it fast and applicable in real time systems. The multi-zone model is more complicated and more accurate and frequently wanted for combustion chamber design. a single-zone model is good enough, for most using.There are two main approaches firstly to model all cylinders as one, describing the entire engine torque as a mean value over one or more engine cycles. Method is called Mean Value Engine Model. An alternative method is a model describing the in-cycle variation torque. It describes each cylinder individually and generates a torque signal with each combustion pulse present. The objective of this study is to model in cylinder-pressure diesel engine. The model should focus on the torque generation and, in order to keep the model

complexity as well as the calculation time should be kept to a minimum. Article structure

Reciprocating internal combustion engine working principle

With the intake valve open, the piston makes an intake stroke to draw a fresh charge into the cylinder. Next, with both valves closed, the piston undergoes a compression stroke raising the temperature and pressure of the charge. A combustion stroke is then initiated, resulting in a high-pressure, high-temperature gas mixture. A power stroke follows the compression stroke, during which the gas mixture expands and work is done on the piston. The piston then executes an exhaust stroke in which the burned gases are purged from the cylinder through the open exhaust valve. The processes in the air-standard Diesel cycle are

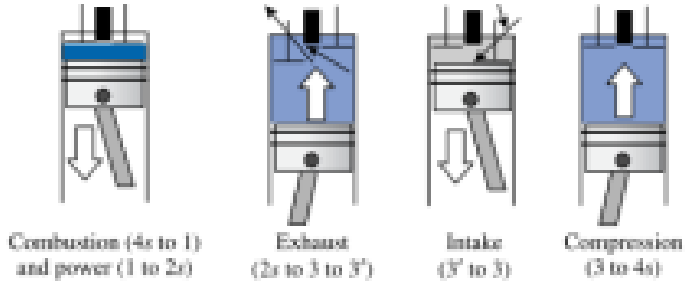

Fig.1. the operation of a four stroke Diesel cycle engine[8]

Air-Standard Dual Cycle

Pressure–volume diagrams of actual internal combustion engines are designated by dual cycle as shown in Fig.2 Process 1–2 is an isentropic compression starting with the piston at bottom dead center. The heat addition occurs in two steps Process 2–3 and 3–4 are a constant-volume+ pressure heat addition; Process 3–4 also makes up the first part of the power stroke. Expansion occurs is entropically from state 4 to state 5 is the remainder of the power stroke. The cycle is completed by a constant-volume heat rejection process, Process 5–1.

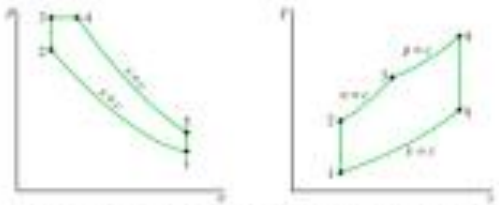

Fig. 2. p–v & T–s diagrams of the air-standard dual cycle

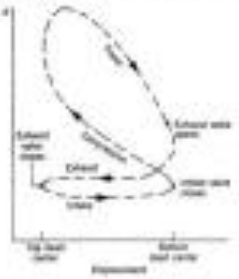

Fig.3. p–V indicator diagram (actual cycle)

Pressure calculation

Crank Mechanism Kinematics

The pressure generated in the cylinder is depend on angular movement of piston

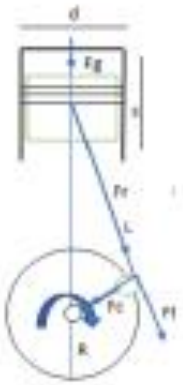

Fig. 4 dynamics of the crank mechanism

The above schematic drawing shows the crank mechanism. It consists of the piston, connecting rod and the crankshaft.

TDC = top dead center,

DC = bottom dead center

d = bore diameter,

L = connecting rod length

R = crank radius

$R = \frac{S}{2}$

X = piston displacement, relative to TDC

θ = crank angle, clockwise relative to TDC

ω =the rotational speed of the crankshaft.

$n = \frac{R}{L}$ crank radius connecting rod ratio

$V_c = 2.R.\frac{\pi d^2}{4}$ displacement volume

V_c= clearance volume

$CR = \frac{V_c + V_d}{V_c}$=compression ratio

Using these geometry parameters, the displacement of the piston (relative to TDC) can be estimated. From this expression the piston speed and acceleration can be derived [MOOG00]:

$$V(\theta) = V_c + \frac{\pi d^2}{4} * X(\theta)$$

$$V(\theta) = \frac{\pi . R . d^2}{4} * \left[\frac{2}{CR-1} + (1 - \cos(\theta)) + \frac{1}{n} * \left(1 - \sqrt{1 - n^2 \sin^2\theta}\right)\right]$$

This expression for the volume contains only cylinder geometry parameters, which are known.

Where the angle dependent cylinder volume and angular velocity and acceleration can be found as shown below [PISC89]:

The in-cylinder pressure was calculated based on the thermodynamics properties (Heywood, 1988) as given in the equations (5) and (6).

In the suction stroke the pressure is equivalent to atmospheric pressure so it can be approximated by

$$V_{t1} = V_d + V_c$$

The angular velocity

$$\omega = \frac{2.N.\pi}{60}$$

The crank angle range for one cycle

$$\theta = 1:720$$

$$\theta = \omega . t$$

1. Intake stroke: θ =0-180

$$\theta \leq 180$$

$$p_{in} = p_{atm}$$

2. Compression stroke: θ =180– 360

$$\theta \leq 360$$

$$p_{comp} = p_{int}\left(\frac{V_{11}}{V_\theta}\right)^K$$

3. Heat addition at constant pressure

$\theta \leq 410$

$$p_{comp} = p_{360}$$

4. The expansion stroke: θ =360– 540

$$\theta \leq 540$$

$$p_{comp} = p_{360}\left(\frac{V_{410}}{V_\theta}\right)^K$$

5. The exhaust stroke: θ =540– 720

$$\theta \leq 720$$

$$p_{EX} = p_E$$

RESULTS AND DISCUSSION

The graphs obtained by the ideal system and actual systems have been given below in figure 2 The graphics showed more clearly the difference between two systems.

Serious differences are seen in compression region of the both graph the theoretical one and actual cycle this is due to we don't add the effect of combustion in cycle analysis

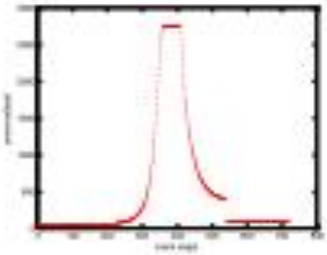

Fig. 2 Crank Angle vs Pressure [kpa]

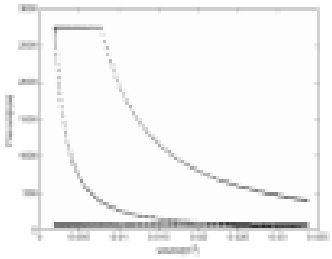

Fig. 3 Volume vs Pressure [kpa]

CONCLUSION

In-cylinder diesel engine model describing the engine torque has been derived and validated. The engine torque produced is the summation of all individual cylinder torques. Each cylinder torque is composed of gas pressure torque and inertia torque working on the crankshaft. The model constructed is neither computationally complex nor does it require any special efforts in order to be parameterized.

The model is general in the sense that it can describe both diesel and petrol engines. It could also be concluded that the algorithm presented in the paper could be expected is proven to be useful for an arbitrary number of cylinders.

The model is tested and evaluated for different scenarios, and the results are then compared to measurements made with a test vehicle in order to determine the accuracy

The gas torque during expansion stroke is more difficult to predict due to the unknown gas composition and initial gas condition at end of the combustion process. Therefore, the expansion period (mostly the crank angle after TDC) was avoided in the final implementation of this method.

The adiabatic process model Eq.12 is used to predict the gas pressure during the compression stroke.

REFERENCES

1. HEYWOOD, J. B. *Internal Combustion Engine Fundamentals*. (McGraw- Hill, 1988).
2. Challen, B. and R. B. in *Diesel Engine Reference Book* (1999).
3. Burghardt, M. D. and J. A. H. *Engineering Thermodynamics*. (Harper Collins College Publishers, 1993).
4. Robert T. Balmer. *Modern Engineering Thermodynamics*. (Elsevier Inc, 2011).
5. Moran, M. J. *Engineering Thermodynamics*. (John Wiley & Sons Inc., 2006).
6. Hill Book Company, International edition, 1988.
7. J. Karlsson and J. Fredriksson. Cylinder-by-cylinder engine models vs mean value engine models for use in powertrain control systems. Technical Report 99P-174, Society of Automotive Engineers, 1998. Chalmers University of Technology, Sweden.
8. J.I. Ramos. Internal Combustion Engine Modeling. Hemisphere Publishing Corporation, 1989.
9. Stefan Sinsel. Echtzeit simulation von Nutzfahrzeug-Diesel motoren mit Turbolader zur Entwicklung von Motor management systemen. Dissertation.